DOE/ET/28393-16

REPORT OF INVESTIGATION
UTAH GEOLOGICAL AND MINERAL SURVEY

NO. 139

GEOTHERMAL INVESTIGATIONS AT CRYSTAL HOT SPRINGS SALT LAKE COUNTY, UTAH

by
Peter J. Murphy, Geologist
J. Wallace Gwynn, Research Geologist
Research Geology Section
October, 1979

Prepared for
Department of Energy/Division of Geothermal Energy
Under Contract DE-AS07-77ET28393

NOTICE

This report was prepared to document work sponsored by the United States Government. Neither the United States nor its agent, the United States Department of Energy, nor any Federal employees, nor any of their contractors, subcontractors or their employees, makes any warranty, express or implied, or assumes any legal liability or responsibility for the accuracy, completeness, or usefulness of any information, apparatus, product or process disclosed, or represents that its use would not infringe privately owned rights.

NOTICE

Reference to a company or product name does not imply approval or recommendation of the product by the Utah Geological and Mineral Survey or the U.S. Department of Energy to the exclusion of others that may be suitable.

TABLE OF CONTENTS

LIST OF ILLUSTRATIONS

TABLES

GEOTHERMAL INVESTIGATIONS
AT
CRYSTAL HOT SPRINGS
SALT LAKE COUNTY, UTAH

by
Peter J. Murphy, Geologist
J. Wallace Gwynn, Research Geologist
Research Geology Section
November, 1979

ABSTRACT

The Crystal Hot Springs geothermal system is located in southern Salt Lake County, Utah 22.5 km (14 miles) south of Salt Lake City near the town of Draper. The system is immediately west of the Wasatch Mountains at the easternmost edge of the Basin and Range physiographic province within an active seismic zone referred to as the Intermountain Seismic Belt. The springs are located north of an east-west trending horst known as the Traverse Range. The range is intermediate in elevation between the Wasatch Range to the east and the valley grabens to the north and south. A series of northeast striking normal faults with a combined displacement of at least 900 m (3,000 ft.) separate the horst from the Jordan Valley graben to the north. The spring system is located between two closely spaced range-front faults where the faults are interesected by a north-northeast striking fault. The fractured Paleozoic quartzite bedrock 25 m (80 ft.) beneath the surface leaks thermal water into the overlying unconsolidated material and the springs issue along zones of weaknesses in the relatively impermeable confining zone that parallel the bedrock faults. Meteoric water from the Wasatch Range is warmed in the normal geothermal gradient of the province (approximately 32° C/km) as the water circulates to a minimum depth of approximately 2.5 km (1.55 miles) via an undetermined path through aquifers and faults. Data collected at the Crystal Hot Springs system under the DOE state coupled program is presented for use by individuals interested in the system.

INTRODUCTION

Under contract with the U. S. Department of Energy/Division of Geothermal Energy (DOE/DGE), the Utah Geological and Mineral Survey (UGMS) has been conducting research to advance the utilization of low temperature geothermal heat in the state of Utah. Activities related to the contract (originally EG-77-S-07-1679 but later changed to DE-AS07-77ET28393) began on July 1, 1977 and will continue into 1980.

To date, UGMS has concentrated its investigations along the Wasatch Front from Utah Valley on the south to the Utah-Idaho state line on the north (figures 1 and 2). The reasons for the

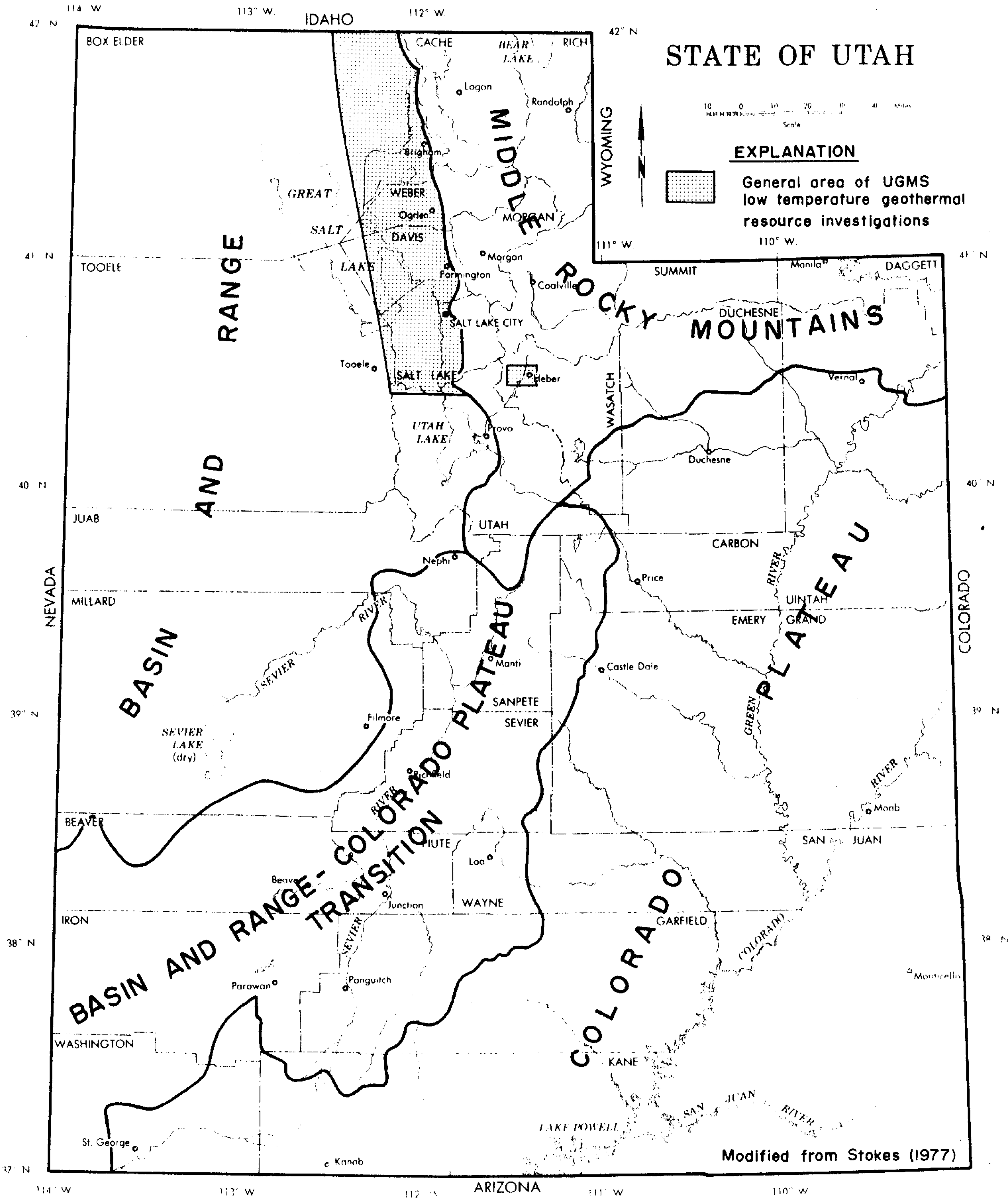

Index map showing major physiographic provinces of Utah

Figure 1

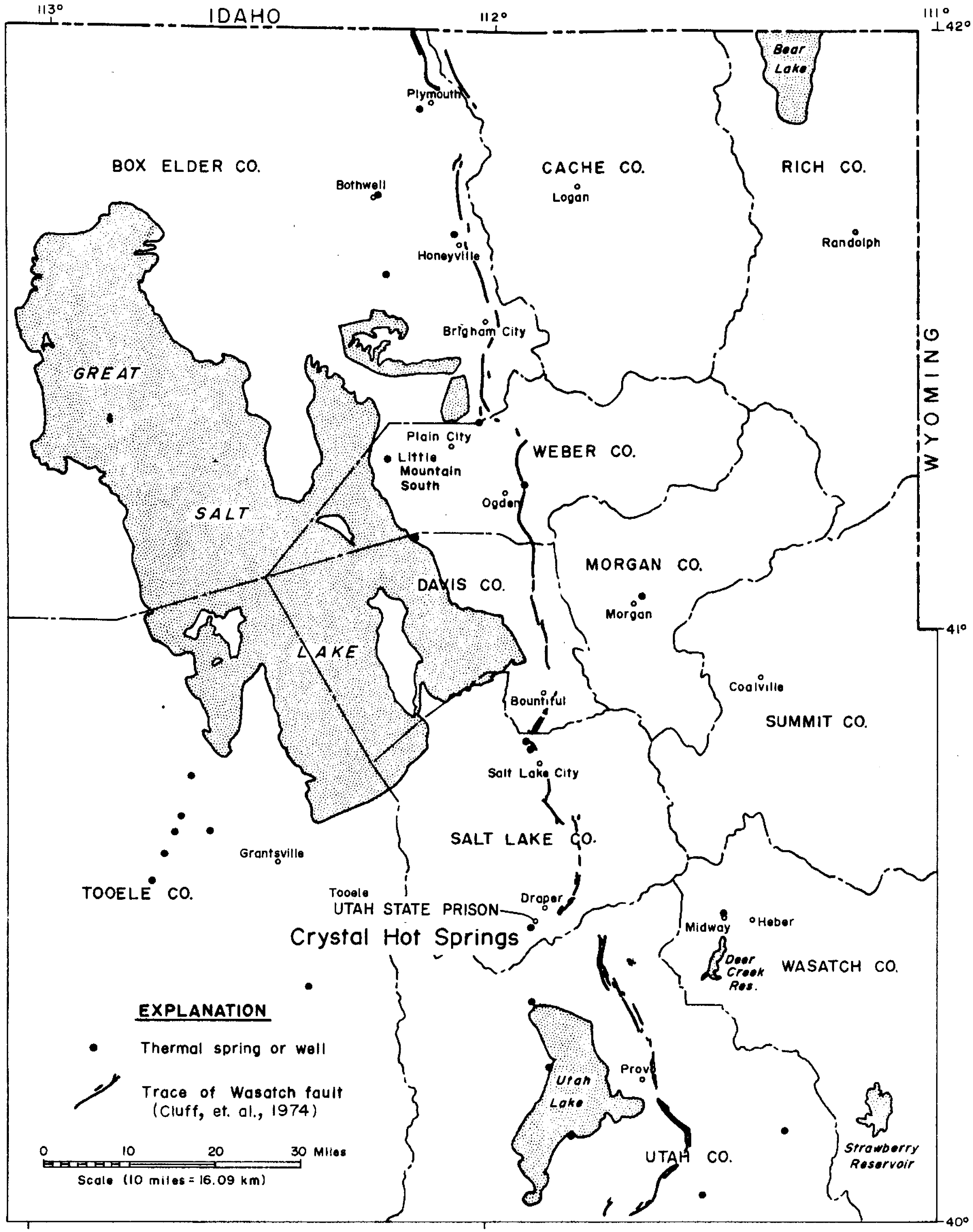

Index map of northern Utah with the locations of Crystal Hot Springs and other major thermal springs of the Wasatch Front.

Figure 2

concentration of effort in this area of the state are as follows: 1) the concentration of apparent geothermal resources in this area and 2) the three major population centers of the state: (north to south) Ogden, Salt Lake City, and Provo lie within the region. The co-location of low temperature geothermal resources and potential users increases the possibility of timely resource development. Therefore, resource definition in populated areas should encourage the development of low temperature resources for direct heat applications by providing a data base from which potential users can make informed decisions. At the same time, investigations of the Basin and Range Province geothermal systems of the Wasatch Front will provide data for models that will be applicable to other Basin and Range geothermal systems.

In addition to the reasons sited above, the investigation of the Crystal Hot Springs geothermal system in southern Salt Lake County (figure 2) was initiated because of the apparent high quality of the resource. The maximum measured temperature of the system (86°C) and the geothermal fluids containing approximately 1500 mg/l TDS, combine to make this geothermal system attractive from the standpoint of use and disposal. Should the quality resource prove to be more wide spread at depths of 305 m (1,000 ft.) or less than presently indicated by the existing surface expression of the hot spring system, a wide variety of uses might be made of the geothermal fluids.

The following report of investigation represents the present state of knowledge of the Crystal Hot Springs geothermal system and the surrounding area. Additional investigations are planned for this resource area under the DOE/DGE state coupled program and a P.O.N. (project opportunity notice) award to the State of Utah by DOE/DGE for the State Prison facilities at Point of the Mountain. Reports on future investigations will be made available as progress continues.

REGIONAL GEOLOGIC AND STRUCTURAL SETTING

The Salt Lake area lies at the intersection of three major tectonic elements: 1) the Uinta Arch (figures 3 and 4), 2) the Thrust Belt (figures 3 and 4), and 3) the Intermountain Seismic Zone (figure 6).

Uinta Arch

The Uinta Arch, a broad anticlinal structure, is a westward continuation of the anticlinal structure of the Uinta Mountains. The axis of the fold in the Wasatch Mountains strikes N60°E, dips 30°E, and is exposed along the Wasatch Front just north of the mouth of Little Cottonwood Canyon. North of the Uinta Arch axis is a broad syncline referred to as the Parleys Canyon synclinorium (figure 4), a multiple fold structure containing two smaller synclines and a tight anticline. The axis of the

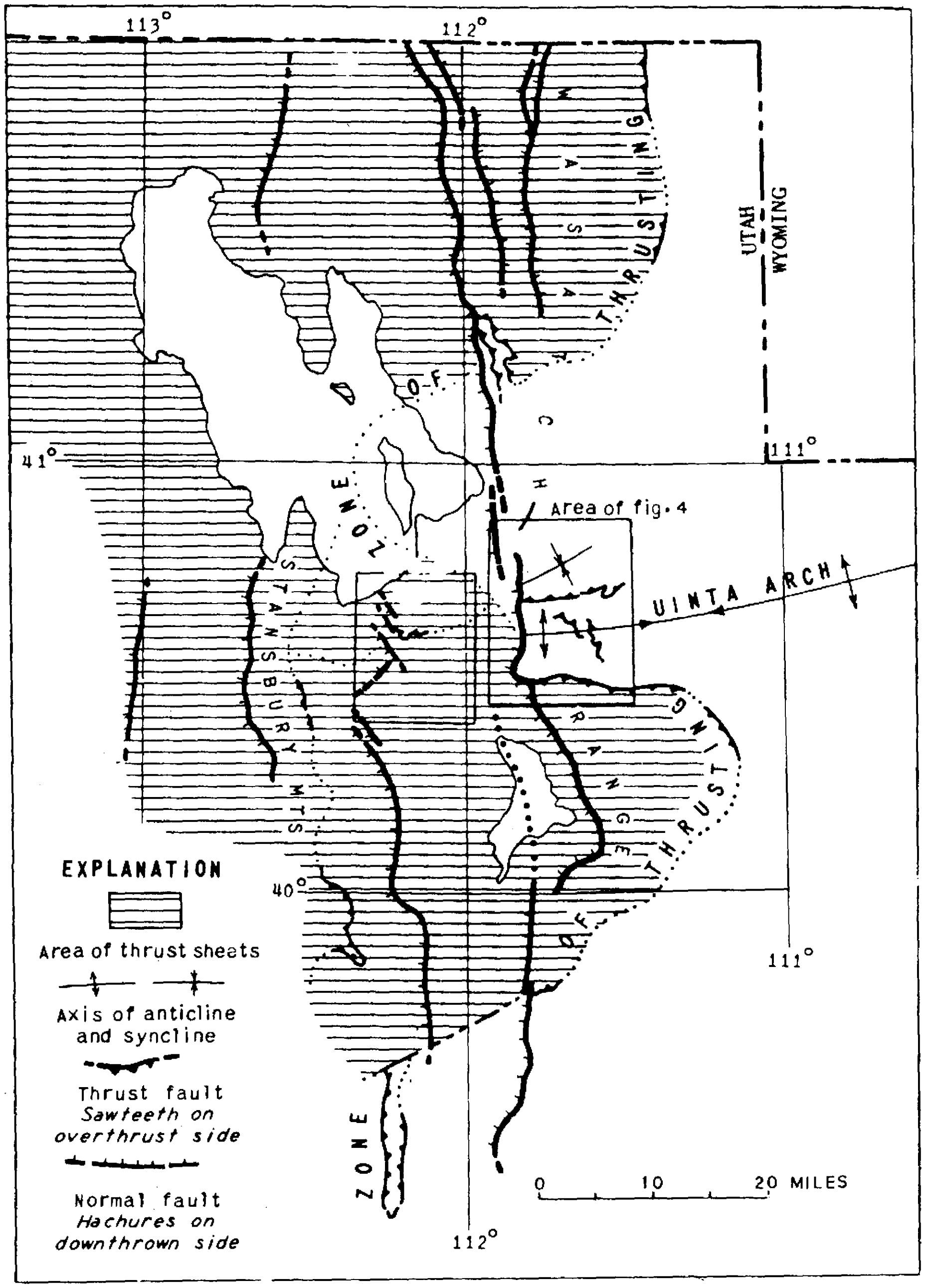

Figure 3. Structural setting of Salt Lake area (Modified from Crittenden, 1964)

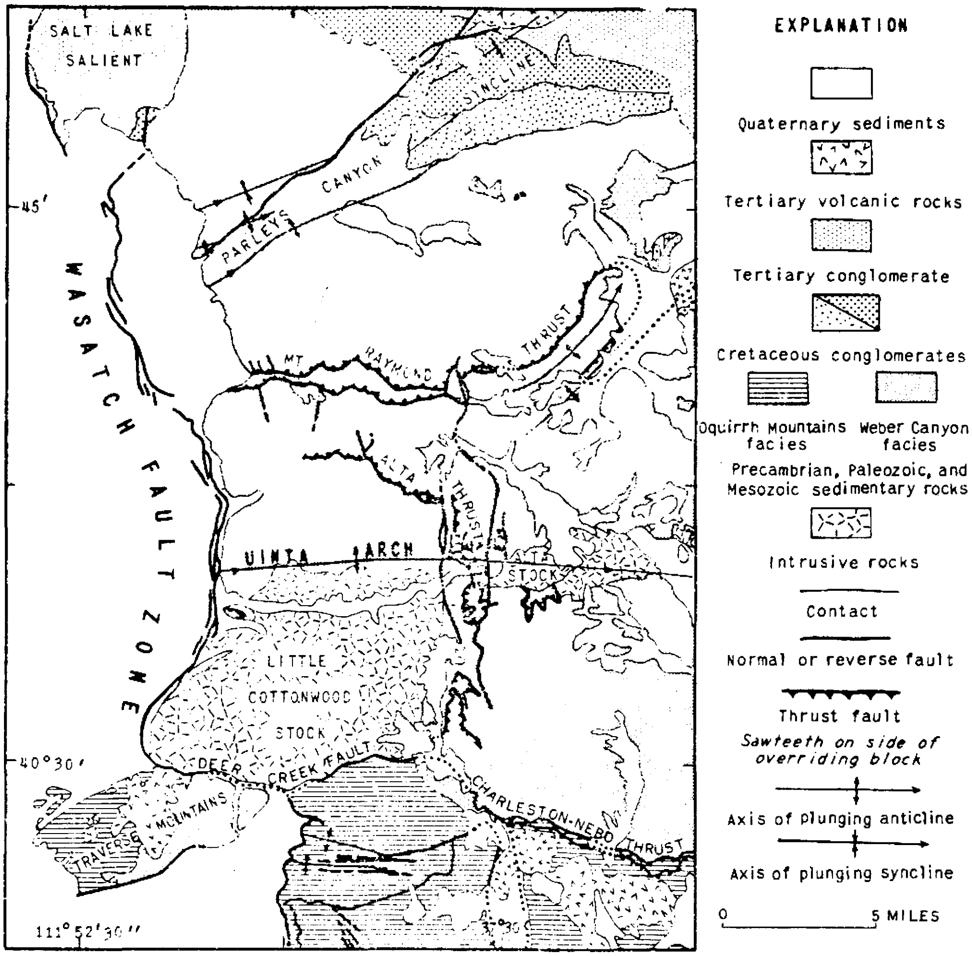

Figure 4. Internal structure of the Wasatch Range east of Salt Lake County, Utah (from Crittenden, 1964).

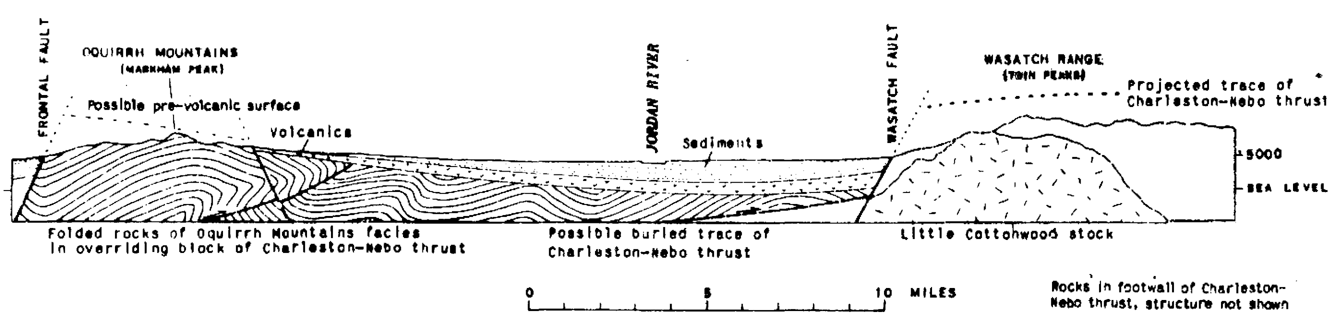

Figure 5. Generalized cross section from Markham Peak in Oquirrh Mountains through Twin Peaks in Wasatch Range. (Modified from Crittenden, 1964).

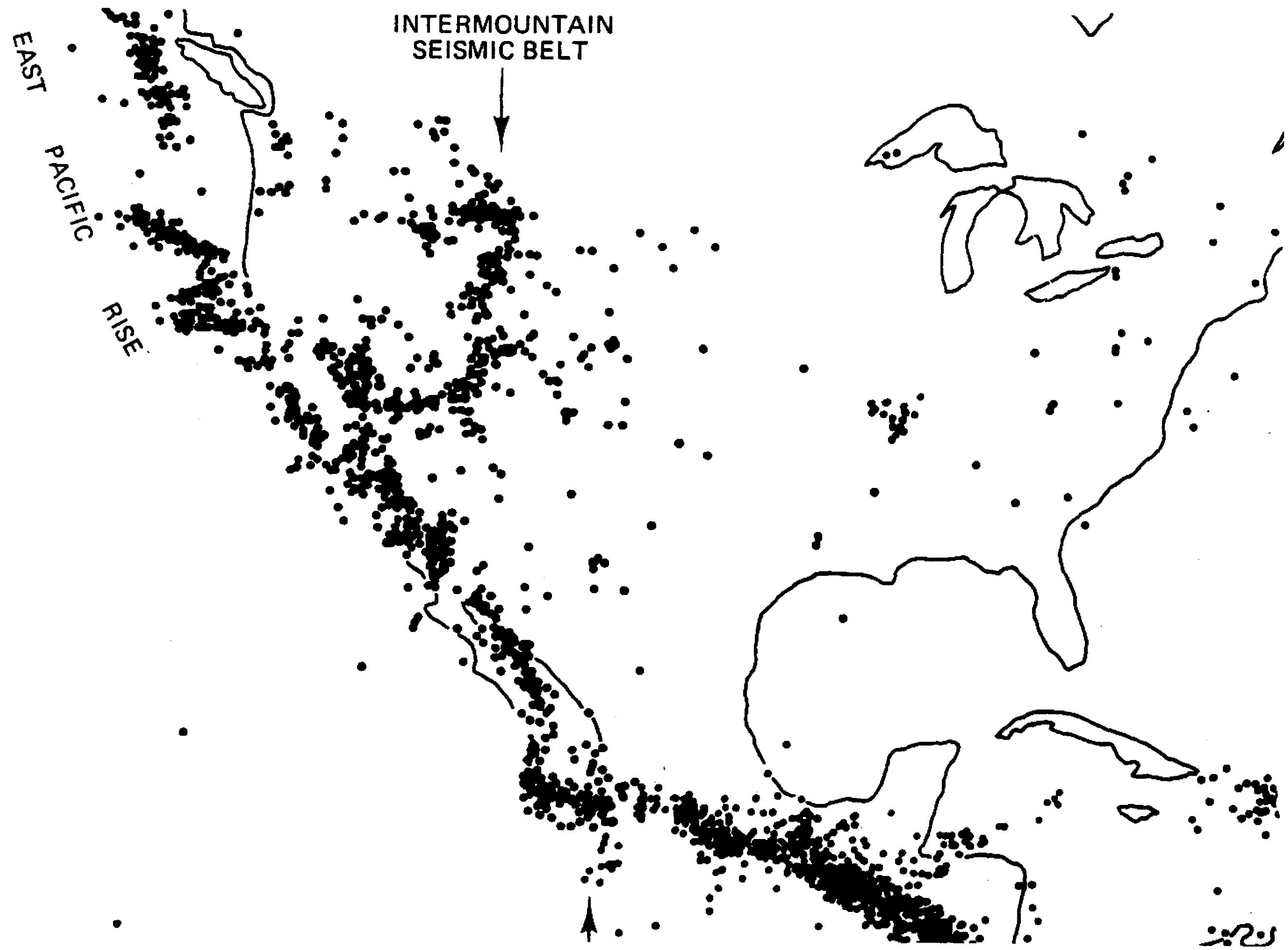

Figure 6. Earthquake epicenters in United States and adjacent regions during 1961-67. Note northward-trending Intermountain Seismic Belt extending through central Utah (Cook, 1971).

Parleys Canyon synclinorium is sub parallel to the axis of the Uinta Arch. Precambrian to Jurassic rocks are present in the folds. Uplift and deformation of the Parleys Canyon syncline occurred in three pulses: 85-90, 75, and 60-70 million years ago (Crittenden, 1964).

Thrust Belt

East to west thrusting occurred during the Laramide orogeny and is represented in the Salt Lake area by three recognized thrust sheets (figure 4). The Alta and Mount Raymond thrusts are present to the east and north of the Little Cottonwood stock and are approximately 125 and 85-90 million years old respectively (Crittenden, 1964). The Charleston-Nebo thrust fault (figures 3 and 4) has a total displacement of 64 km (40 miles) or more, and is the youngest thrust identified in the Salt Lake area at 75-80 million years old (Crittenden, 1964). Evidence for the Charleston-Nebo thrust is present in the Wasatch Mountains (figure 4), but the inferred trace of the fault has been extended westward through the Wasatch, between the East Traverse Range and the Little Cottonwood stock. The fault also extends north and west of the area between the Oquirrh Mountains and Antelope Island to be linked with the Willard thrust east of Ogden (figure 3). This interpretation of thrusting in the Salt Lake area places both the Traverse Ranges and the Oquirrh Mountains on the thrust plate, and explains the differences in geology between the Wasatch and Oquirrh Ranges. The thrust plane of the Charleston-Nebo thrust dips westward (figure 5) and may be as deep as 3.2-8.0 km (2 to 5 miles) beneath the Oquirrh Mountains. Northwest striking folds present in the southern Oquirrh Mountains and the West Traverse Range may have been formed during thrusting, as wrinkles on the upper plate. (Crittenden, 1964).

Intermountain Seismic Belt

The Intermountain Seismic Belt is a 100 km wide zone of relatively high seismicity, extending from northern Arizona to northwestern Montana (figure 6) and locally coincident with the Wasatch Front. This zone parallels the eastern margin of the Basin and Range physiographic province; seismic studies by Smith and Sbar (1970), and Shur and Barazongi (1970) suggest the zone is an active rift system with the tensional axis orientated in an east west direction. The tensional forces are those that, over the past 20 to 25 million years, have produced the fault block mountains of the Basin and Range province.

THE TRAVERSE MOUNTAINS

Geology

In greatly simplified terms, the Traverse Ranges can be described as folded and fractured Paleozoic limestones and quartzites, mantled in places by Tertiary volcanics, and Quaternary sediments of

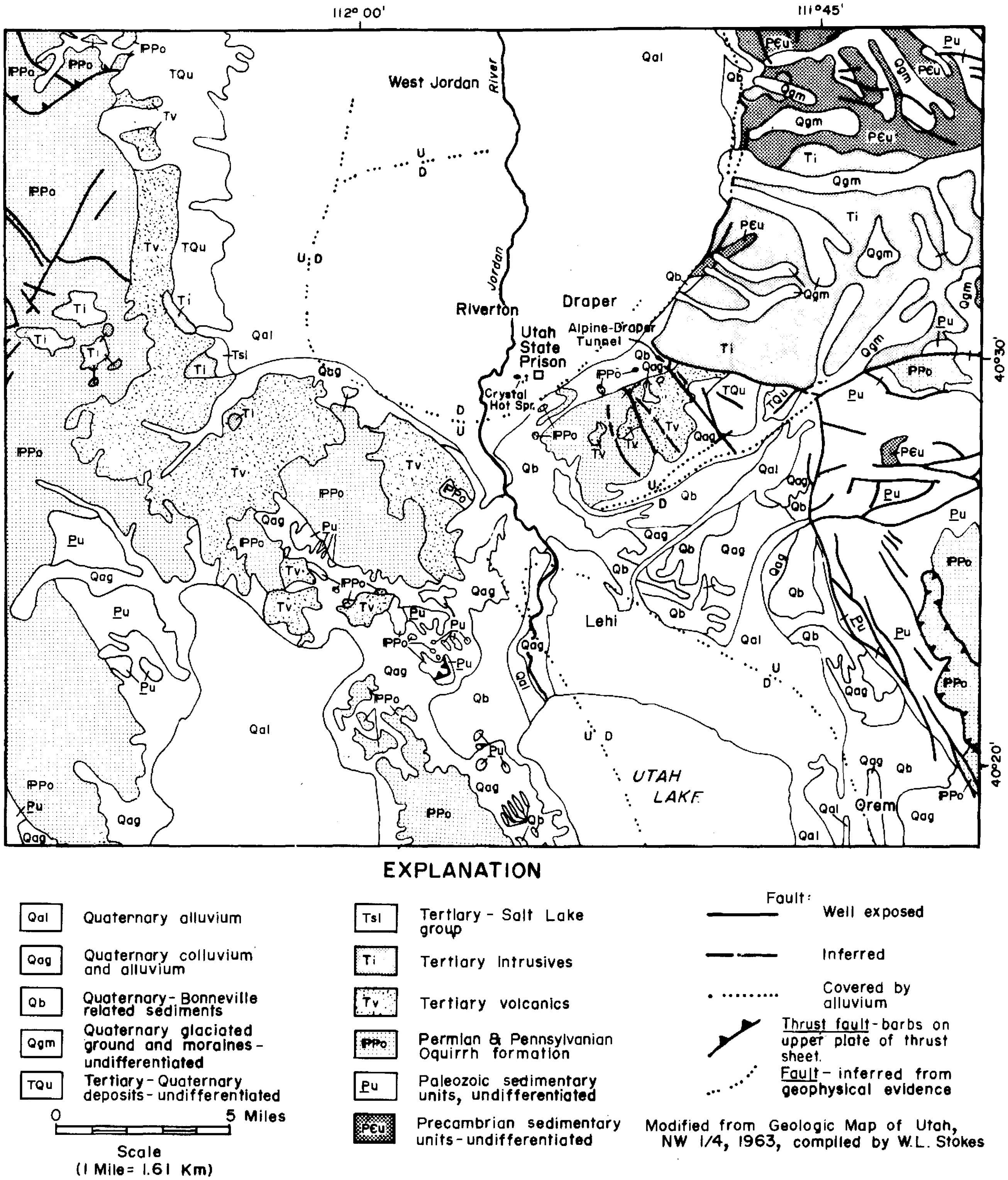

Geology of the Traverse Mountain Region, Utah

Figure 7

varying origins. The following is a brief description of the rocks of the Traverse Ranges.

Paleozoic System

The Paleozoic rocks of the Traverse Ranges are predominately Pennsylvanian rocks of the Oquirrh Formation (Marsell, 1932) (figure 7). Manning Canyon shale of Mississippian-Pennsylvanian age, and Mississippian Great Blue limestone are present on the south flank of the West Traverse range, but are only exposed in relatively small areas (Pitcher, 1957). Bullock (1958) assigned a total thickness of 1,524 m (5,000 feet) to the Oquirrh Formation in the Lehi quadrangle, and Pitcher (1957) reported the Oquirrh Formation in the Jordan Narrows quadrangle to be approximately 1,128 m (3,700 feet) thick. Pitcher's (1957) stratigraphic column has been reproduced here in figure 8, where the lithologies of the Marrowan, Attokean, and Desmoines series of the Oquirrh Formation are described. Marsell (1932) indicates that the most abundant rock type in the ranges is quartzite, and less often limèstone and sandstone can be found. Pitcher (1957) mapped large areas of the Desmoines series in the Jordan Narrows quadrangle.

The Paleozoic rocks are present through the Traverse ranges, even where Tertiary volcanics and Quaternary deposits are present at the surface (figure 7).

Tertiary System

Sedimentary Rock: Slentz (1955) noted and described four units of the Salt Lake group in the vicinity of the Jordan Narrows. In order of decreasing age, the units are: 1) the Jordan Narrow unit consisting of marlstones, 2) the Camp Williams unit consisting of poorly consolidated mudstones and siltstones, 3) the Travertine unit that, in places, resembles tufa, and 4) the Harkers fanglomerate displaying torrential bedding and cut-and-fill structures.

The Travertine unit: ". . . varies from dense, massive flinty travertine to coarse, crustiform, or even cavernous, limestone, often resembling tufa" (Marsell, 1932) contains lenses of manganese ore, and was deposited by hot spring activity. The age of the unit has been established as late Pliocene by identification of a jaw bone and teeth found in the travertine by Marsell (Slentz, 1955). Slentz (1955) shows three locations where the Travertine unit is present, the northern and westernmost of the three exposures are on strike with the westward extension of the Steep Mountain fault line scarp (figure 21a).

Volcanics: Tertiary volcanics in the Traverse ranges (figure 7) are primarily andesitic lava flows that vary in composition. Marsell (1932) described the volcanic rocks in some detail and found that in the East Traverse mountains the lavas were principally andesite porphyries and augite-andesite prophyries. In the West Traverse mountains the composition varied from sub-basic augite prophyry to augite latities; four sets of flows were identified.

The lavas were extruded during the late Oligocene or early Miocene through vents at South Mountain and Step Mountain in the West Traverse range. No such vents were found in the East Traverse range. The first lavas were extruded on to a deeply eroded surface, and weathered surfaces on some flows indicate that eruptive events were separated by time.

The scattered distribution of lava flow remnants throughout the Traverse ranges (figure 7), is an indication that the flows were at one time more extensive than at the present and may have covered adjacent portions of the Oquirrh and Wasatch mountains (Marsell, 1932). At the present time the volcanics flank the eastern edge of the Oquirrh Mountains south of Copperton; extending south and southeast to cover a large area of the western West Traverse range. A second major area of volcanics covers the northeast corner of the western range, while small patches of volcanics dot the southern flank of the range. About one third of the bedrock surface in the Eastern Traverse range is covered by volcanics, though exposures are limited to the eastern portion of the range (figure 7).

Intrusives: Two areas containing large igneous intrusions are present in the vicinity of the Traverse ranges (figure 7): the Little Cottonwood-Alta stock, and the Bingham Canyon area. The granitic intrusions of the Little Cottonwood area were emplaced between 41 - 24 million years ago with the Little Cottonwood stock being emplaced 24 -31 million years ago (Crittenden, et. al, 1973). The quartz monzonite intrusions in the Bingham area were emplaced during the late Eocene or early Oligocene (Bray, et. al., 1975).

In the West Traverse Mountains near their junction with the Oquirrh Mountains are four volcanic plugs or necks and one small stock (Marsell, 1932). Marsell describes the stock at Shaggy Peak as a ". . . rounded hill of rhyolite porphyry, surrounded on all sides of flows of andesite breccia and latite". According to Marsell, Step Mountain is a volcanic neck, and South Mountain is a group of three volcanic necks. The rock in all four of the necks is mica-andesite prophyry.

Quaternary System

Deposits of Quaternary age that have been recognized in the Traverse Ranges include: 1) Pre-Lake Bonneville fans, 2) the Lake Bonneville group consisting of the Alpine and Bonneville and Provo formations, and 3) post-Provo deposits. The prominent spit at the western end of the East Traverse range is a portión of the Bonneville Formation, as are the discontinuous beach deposits along the north flank of the range.

	Formation	Thickness	Description
QUAT.			Gravel, sand and silt.
TERT.	Salt Lake group	600 +	Marlstone, siltstone, limestone, tuff and conglomerate.
PENNSYLVANIAN	Oquirrh formation	1,000+	Desmoines series Light brown to tan quartzite with some medium gray orthoquartzite interbedded with a few light to medium gray beds of limestone.
		1,913±	Atokan series Medium to dark gray, sandy limestone that weathers light gray, interbedded with light brown to tan cross-bedded orthoquartzite.
		854	Morrowan series Limestone; medium to dark gray, medium to thick bedded, fetid in part, sandy, with some cherty beds.
PENNSYLVANIAN / MISSISSIPPIAN	Manning Canyon shale	1,200 ±	Shale; light brown to black with some quartzite and limestone beds. Springeran probably begins at the bottom of the prominant bed of scintillating quartzite.
MISSISSIPPIAN	Great Blue limestone	800 +	Limestone; medium gray, weathering light gray, mediumto thick bedded and platy in places, sandy.

Section

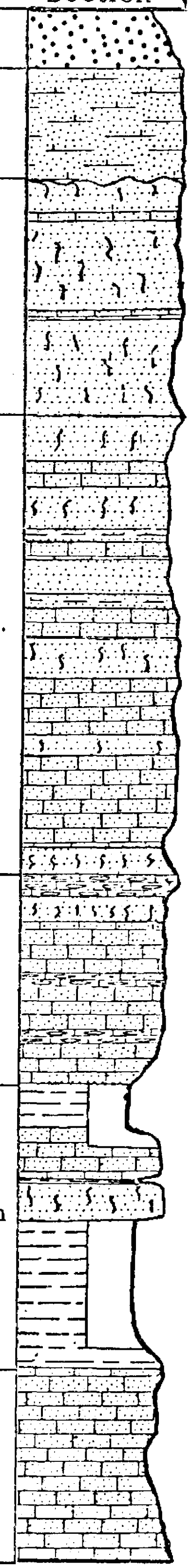

Figure 8. Stratigraphy of the Jordan Narrows quadrangle (Modified from Pitcher, 1957).

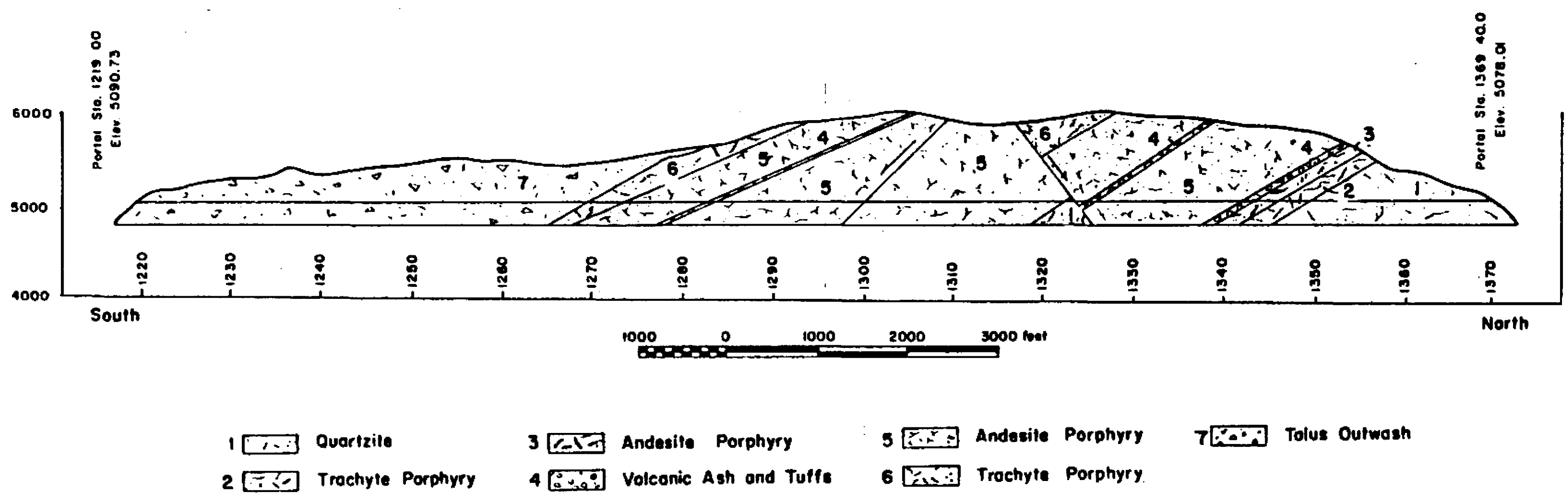

Figure 9. Structural section along Alpine-Draper Tunnel after J. N. Murdock September 1941.
Cross-section from (Bullock, 1958).

Structures Bounding the Traverse Mountains

The Traverse Ranges trend east-west in a region where the prevailing structural trends are north-south (figure 7), and as a result, the structural detail is complex. The northern edge of the Traverse Ranges is bounded by a series of normal faults that separate the ranges from the Jordan Valley graben (figure 7) to the north (Cook and Berg, 1961). Striking almost east-west and dipping southward, the main branch of the Wasatch fault separates the eastern end of the East Traverse mountains from the Little Cottonwood stock (figure 7). Although no fault has been found on the southern flank of the Western Traverse range, a series of normal faults similar to those on the north flank separate the East Traverse range from the Utah Valley graben to the south (Cook and Berg, 1961). Marsell (1932) reports that the folds of the Oquirrh Mountains could be traced into the West Traverse range, and the ranges were not separated by Basin and Range faulting.

Internal Structures of the Traverse Ranges

Marsell (1932) describes the Western Traverse Range as ". . . a homoclinal succession with a general east-west strike, and a north dip which averages 35°. As a junction of the range with the Oquirrh Mountains is approached, the strike swings more to the northwest, in conformity with the trend of the east limb of the Tickville Gulch anticline in the latter range".

Marsell (1932) viewed the East Traverse mountains as a "steeply pitching anticlinal nose, which, in the vicinity of the Jordan Narrows, appears to merge with the homocline of the West Traverse mountains". As evidence for the anticlinal nose structure, Marsell sites the "general" dip of the rocks on the north flank to the north, the south flank to the south, and the rocks near the Jordan Narrows to the west; measured strikes and dips are not given. Bullock (1958) presents a cross-section, shown here in figure 9, through the East Traverse mountains that was prepared along the Alpine-Draper Tunnel by J. N. Murdock (1941). The location of the cross-section near the eastern end of the range is indicated in figure 7. The apparent dips of the rocks, as observed in the cross-section, are all southward at approximately 23°. Neither Pitcher (1957) nor Bullock make any suggestions concerning the overall structure of the ranges, however there is considerable doubt that Marsells interpretation of the internal structure of the East Traverse range is correct.

One of the difficulties encountered when working in the Traverse Ranges is the highly fractured nature of the rocks. The intense fracturing along with the well developed soil cover are undoubtedly the reason for the lack of good geologic and structural information. Marsell (1932) was, however, able to identify a series of north-northwest trending faults in the East Traverse Ranges (figure 7) that were determined to be older than the Tertiary volcanics that once covered the range. Marsell suggests these faults were formed at the time of the anticlinal folding, and notes how the faults have the same trends as the large scale folding in the Oquirrh Mountains.

DESCRIPTION OF CRYSTAL HOT SPRINGS

The surface expression of the geothermal resource at the Point of the Mountain is restricted to a group of springs known as Crystal Hot Springs, which are found within an area of approximately 70 acres bounded by the Utah State Prison farm on the north, the Utah State Prison minimum security buildings on the east, the Bluffdale Road on the south, and by a number of small farms on the west. No surface expressions of the Crystal Hot Spring system have been found outside of this area.

There are large number of spring orifices associated with the Crystal Hot Spring system (figure 10). Some of these orifices are beneath the surfaces of the small ponds located near the eastern edge of the system, and a few are present at the bottom of the large western lake. The remainder of the orifices are found in the bottoms of relatively small circular depressions near the southern boundary of the area and north of the large western lake.

Although water at the surface of the eastern ponds feels only warm to the touch, temperatures as great as 84°C have been measured at spring orifices within the lake muds. The water from the springs drain northward through a series of channels connecting individual ponds. The total flow from the eastern lakes is diverted westward through a drainage ditch to the large western lake, (figure 10).

The western lake is at least 15 meters deep, and is divided into two basins by a ridge that almost reaches the surface of the lake. The owner of the spring has indicated that at one time a heavy weight was lowered into one of the orifices and no bottom was encountered; he estimated the total depth of the lake to be approximately 90 meters (300 feet). Divers who have been in the lake on a number of occasions, however, found the maximum depth of the lake to be approximately 15 meters (50 ft.). Bottom mud temperatures as great as 82°C have been measured in this lake.

Taylor and Leggette (1949) report the results of a pump test in which the western basin of the large western lake was pumped at a rate of 8.6 feet^3/sec. for 26 hours. Important results of this test are as follows:

1) The pumping exposed several small orifices of the eastern edge of the lake that remained several inches above the fluctuating level of the lake.

2) After removing a total 9.86 acre-feet of water, the lake refilled at a rate that decreased from

1.30 feet^3/sec. to 1.12 feet^3/sec. as the lake returned to pre-test levels.

3) The springs in the western portion of the lake produce water at a rate of approximately 1.13 feet^3/sec.

4) Water levels in auger holes to the north and south of the lake did not fluctuate as the lake level decreased.

5) Drawdown in the western lake did not induce drawdown in the eastern ponds.

Further details of this test are given in the reference cited above and the same account is reproduced in Goode (1978).

Most of the combined spring outflow drains out the western end of the lake through a pipe and into a drainage ditch. However, a tropical fish hatchery and a beaver farm divert some of the water for heating purposes before discharging this water into the same ditch. The water eventually drains into the Jordan River.

In addition to the hot spring orifices that are associated with the western lakes and eastern ponds, there are two areas where springs and seeps occupy the bottoms of small circular depressions. In the bottoms of some of the depressions only damp soil is present, while in others standing water less than 1 meter deep is found. In both areas, there is little or no flow away from the springs.Ten to twenty of these orifices are found in an east-west trending zone that begins south of the eastern ponds and ends south of the western lake. Just north of the western lake are about 5 depressions measuring from one to five meters across and containing up to several meters of standing water.

Water level information in the vicinity of Crystal Hot Springs is presented in figure 11. Contours in this figure represent the water surface level of ponds without outlets in the spring system, relative to the pond which is located to the northwest of the large western lake. The water surface in the area conforms to the topography of the spring site. The approximate elevations to which water rises in water wells within the area is also indicated. Depth-to-water in each hole was measured when access to the hole was obtained; measurements span a period of one year. The regional flow of groundwater is to the north and west away from the springs.

Other Occurrences of Warm Water

Although Crystal Hot Springs is the only source of water above 30°C in the southern Jordan Valley, additional occurrences of warm water have been reported. In the Jordan Narrows, the Camp Williams warm spring (C-4-1) 23 bcb issues in the vicinity of Tertiary tufa deposits at a temperature

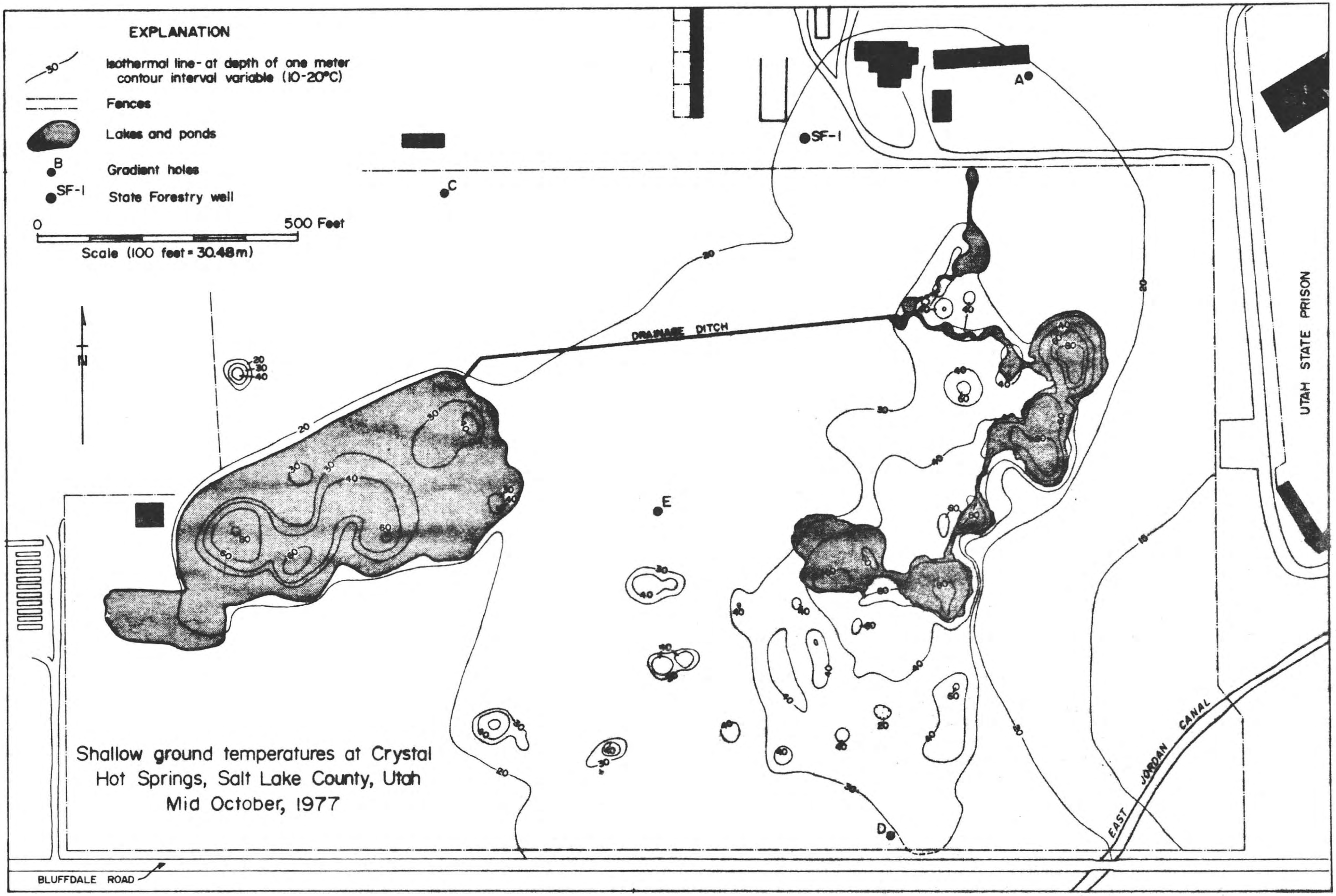

EXPLANATION
Isothermal line - at depth of one meter contour interval variable (10-20°C)
Fences
Lakes and ponds
Gradient holes
State Forestry well
0
500 Feet
Scale (100 feet = 30.48 m)
N
DRAINAGE DITCH
UTAH STATE PRISON
EAST JORDAN CANAL
BLUFFDALE ROAD
SF-1
A
B
C
D
E
Shallow ground temperatures at Crystal Hot Springs, Salt Lake County, Utah
Mid October, 1977

Figure 10

of approximately 23°C (figure 21). Further south in the Jordan Narrows, Milligan, et. al. (1966) reported the presence of 27°C water 6 feet below the surface where the Provo Reservoir Canal crosses the Jordan River (C-4-1) caa (figure 21). Warm water (21-25.5°C) at depths of less than 180 m has also been reported in Draper area, (D-3-1) 29, water wells.

Ten miles due south of Crystal Hot Springs in Utah Valley are two hot springs. Saratoga Hot Spring, (C-5-1) 25 cd, on the northwest shore of Utah Lake flows to the surface at 38 to 44°C. One mile east-northeast of Saratoga, in Utah Lake, is Crater Hot Spring with reported temperatures ranging from 42-44°C.

SHALLOW GROUND TEMPERATURE SURVEY

Techniques

A detailed shallow ground temperature survey was conducted in the immediate vicinity of the Crystal Hot Spring system to determine if the temperature of the ground at a depth of approximately one meter could yield information on the distribution of hot water in the subsurface. To conduct the survey, shallow holes, approximately one meter deep, were augered with a small hand-held power auger, at numerous locations throughout the spring area. The hole locations were marked, and after sufficient time had passed for the soil to dissipate the temperature effects induced by drilling, the sites were revisited and temperature measurements made. Additional measurements were taken in and around the lakes and spring orifices by pushing a long, thin temperature probe into the bottom muds and grass mat to a depth of approximately 1 meter. All of the temperature measurements were taken within a three day period during September of 1977.

The measurements were made with a thermistor device built at UGMS in which the resistance across the thermistor is read directly as temperature (°C) on a liquid crystal display, to within .1°C. The thermistor is mounted on the end of the probe which is about 2 meters long.

Results

The results of the shallow ground temperature survey, shown in figure 10, were very useful, and a number of assumptions that had been made on the basis of these data were later confirmed by the drilling of 75-meter (250 ft.) gradient holes. The main features to be noted in figure 10 are:

1. A distinct north-northeast trending zone of high temperatures that is coincident with the the eastern zones. The temperatures reach a maximum of 86°C near the southern end of the zone, but temperatures of 80 to 85°C were measured at other orifices in that zone.

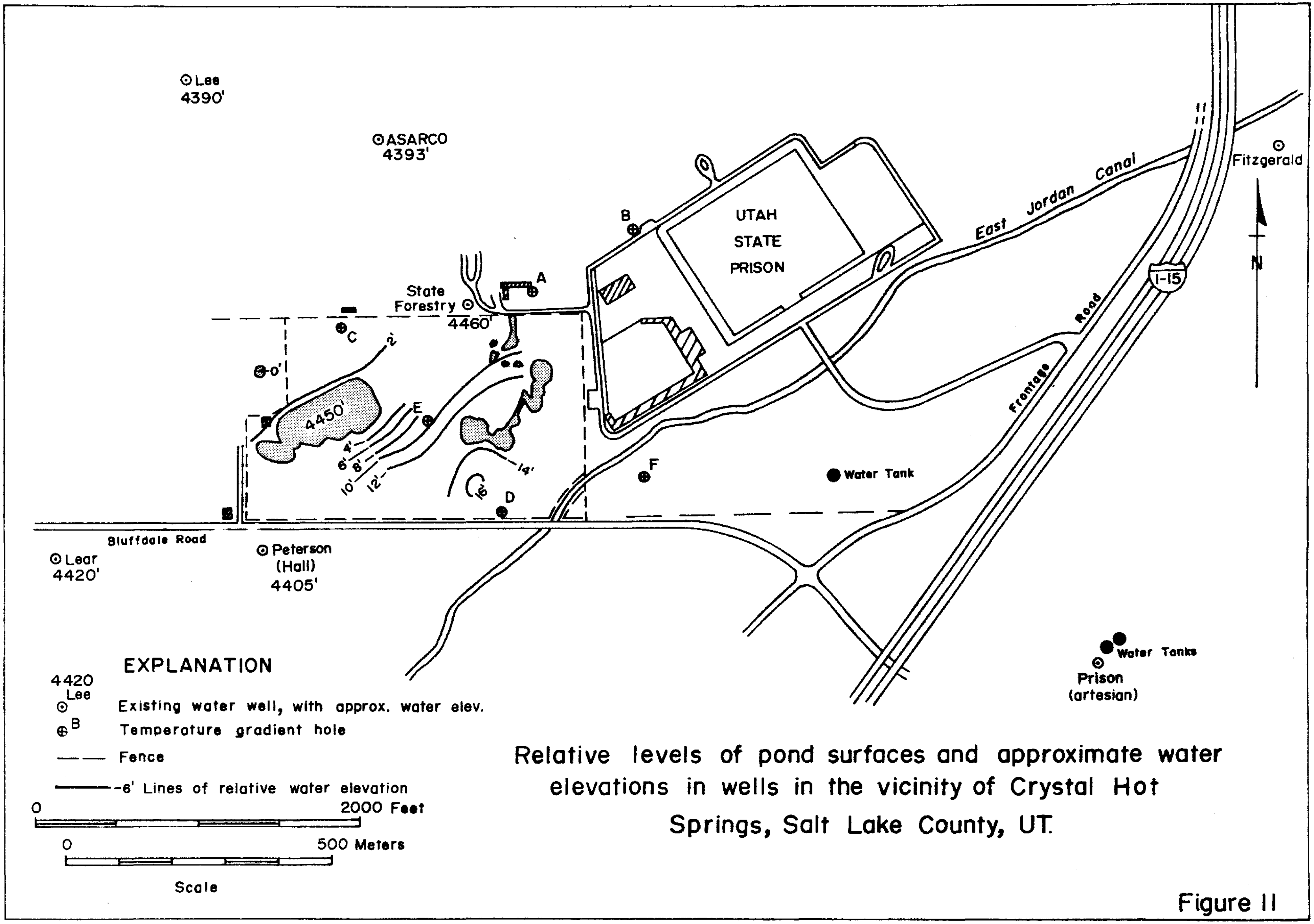

Relative levels of pond surfaces and approximate water elevations in wells in the vicinity of Crystal Hot Springs, Salt Lake County, UT.

Figure 11

2. A rapid decrease in temperature with distance to the east of the high temperature zone. The temperatures decrease from 80 to 85°C to less than 20°C over distances commonly less than 100 meters distance from the high temperature zone. The coolest temperatures measured were approximately 12 and 13°C in the southeasternmost corner of the study area.

3. A gradual decrease in ground temperature to the west of the high temperature zone. The 20°C isotherm is commonly 200 to 300 meters west of the high temperature zone.

4. The presence of warm water in numerous spring orifices southwest of the eastern lakes. Temperatures taken in most of these orifices were between 50 and 60°C, but in those that had outlets and flowed, temperatures were as high as 75°C. The majority of these orifices are in a zone that trends east-northeast in the south-central portion of the area.

5. The presence of a number of hot water spring orifices in the large western lake. At least three major orifices exist and others may be present. Their detection, however, was difficult because water depths exceeded 15 m (50 feet) in several portions of the eastern half of the lake.

6. Relatively cool ground temperatures that lie to the north and south of the large western lake. Temperatures in these areas are commonly 17 to 18°C.

Water Chemistry

Analyses from a number of locations in the vicinity of the hot springs are presented in table 1. Temperature pH, conductivity and HCO_3 determinations were done by UGMS personnel in the field. The remaining parameters were determined by the State Health Department laboratory on unacidified samples. All samples were filtered in the field, but the strict sampling procedures outlined by the U.S.G.S. (Presser and Barns, 1974) were not followed when the samples were collected. The analyses in table 1 should be used as indicators of general water chemistry only, and are not suitable for use in geothermometry calculations.

The chemical quality of the thermal water of Crystal Hot Springs is excellent when compared with other low temperature thermal waters along the Wasatch Front. The total dissolved solids content has been used to rank the general water quality of Wasatch Front springs as presented in table 2.

The factors contributing to the anomolously good quality of the thermal waters at Crystal Hot Springs are not fully understood, however, a number of factors could possibly contribute to the observed water chemistry. First, the water recharging the system is snow melt and low in total dissolved solids. Second, the water may move rapidly through the system thereby decreasing the time available for the dissolution of soluble components along the flow path. Third, the material through which the water flows is not readily soluble. Fourth, the thermal water has not been contaminated with non-thermal brines

LINEAMENTS

The most prominent linear feature on the north flank of the East Traverse range is the base of Steep Mountain (see figure 21 A). Gilbert (1890) and Marsell (1932) did not recognize the plane of Steep Mountain as a fault line scarp, but referred to the feature as a great sea cliff. Slentz (1955), Dolan (1957), and Bullock (1957) present evidence that supports the theory that the north face of Steep Mountain is a fault line scarp. Bullock (1957) also suggests that a second scarp coincides with the Provo shoreline at an elevation of 1463 m (4,800 feet).

Structures buried under Quaternary valley fill often have subtle expressions at the surface of the valley fill. In figure 12 two sets of lineament data taken from aerial photography are portrayed: 1) lineaments reported by Cliff, et. al. (1970), and 2) leached soil lineations observed by UGMS personnel.

Cliff, et. al. (1970) used low sun angle photography to identify scarps and tilled ground surfaces related to faulting or ground movements. Lineaments were divided into three classes based on the level of certainty that the lineaments were controlled by faulting as follows:

CLASS I -	Prominent or obvious fault, or very fresh fault related feature
CLASS II -	Probable fault or rupture, or fault showing a lack of recent activity.
CLASS III -	Possible fault or rupture.

Class I and II lineaments in figure 12 are beyond the area covered by the special low sun angle photography used for the investigation but the scarps are visible on standard aerial photography as vertical displacements and linear features in alluvium in the vicinity of the Jordan River channel. These scarps strike at N40°E, roughly paralleling the mountain front below an elevation of 1402 m (4600 feet). Above 1402 m (4600 feet) there are a great number of class III lineaments that closely parallel the Provo and Bonneville shorelines. There are two sets of class III lineaments in figure 12: 1) those striking northeast that are related to the main range front structural trend; and 2) a group of short lineaments that, as a unit, strike north-northeast and are possibly related to north-northeast striking features present in the subsurface.

The soil lineaments in figure 12 can be seen on standard areal photography as light colored soil patches having a very straight, well defined northern edge and irregular boundaries on the south. Soil within the light patches is enriched with calcium carbonate with respect to the surrounding soil.

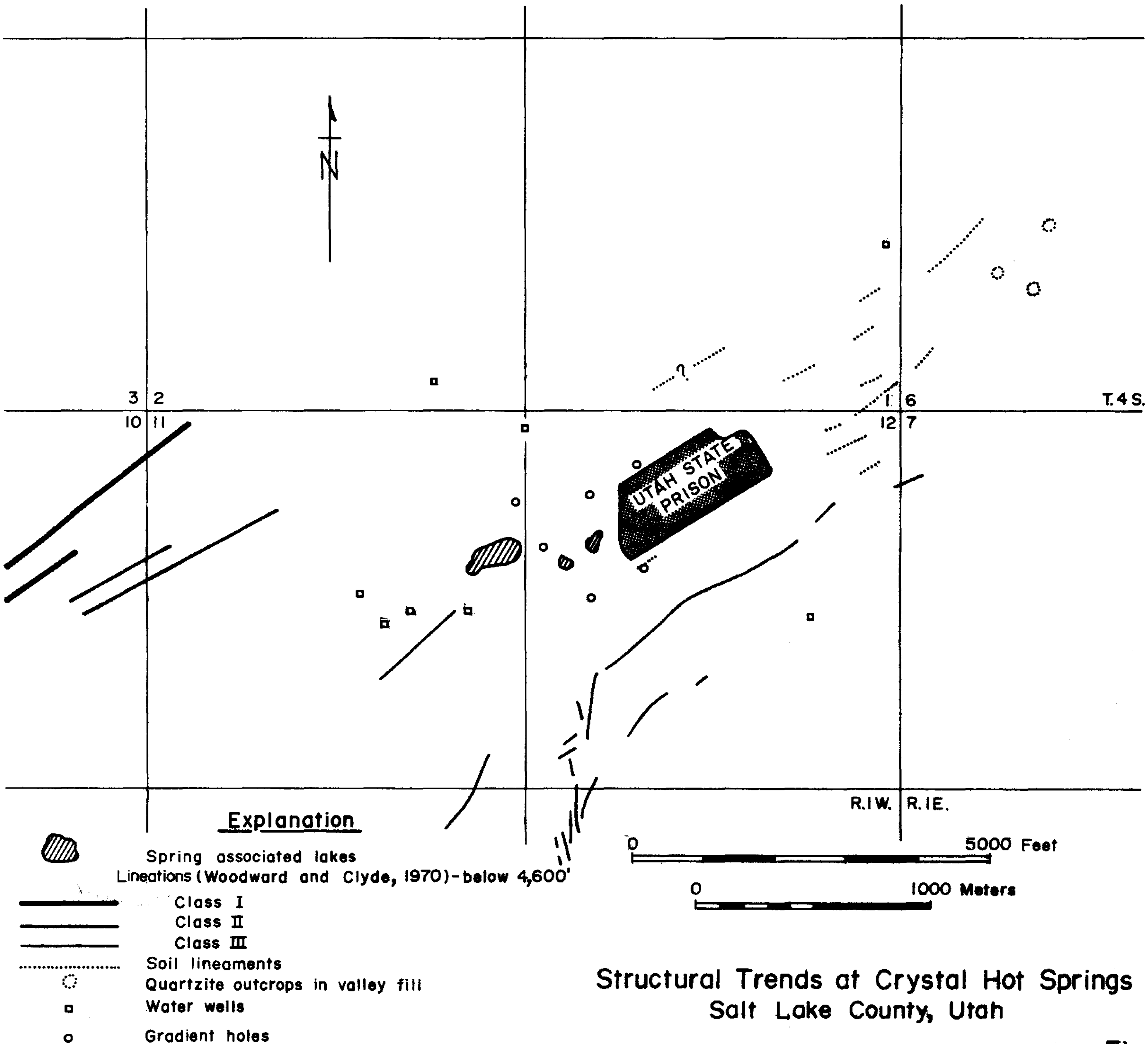

Structural Trends at Crystal Hot Springs
Salt Lake County, Utah

Figure 12

Table 1. Water analyses of well and spring water in the vicinity of Crystal Hot Springs

Owner or Name	Temp.	Depth	Date of Collection	SiO_2	Ca	Mg	Na	K	HCO_3	SO_4	Cl	TDS	Cond. mmho	pH
				mg/l										
Crystal Hot Springs eastern ponds	61.6°C		6/22/78	66	128	34	325	70	230	74	590	1,462	2.4×10^3	5.9
State Forestry Test Well	62.°C	280	6/21/78	59	136	39	380	70	260	71	685	1,660	3.0×10^3	6.25
Water Well Hall	39.°C	236	6/21/78	30	132	34	220	45	260	52	530	1,304	2.7×10^3	6.4
Water Well -Lear	18.°C	200	6/22/78	26	88	49	115	8	210	200	160	842	1.36×10^3	6.8
Water Well Fitzgerald	16.1°C	167	6/29/78	45	82	55	150	20	210	280	210	1,052	1.65×10^3	7.16
Water Well USP	16.2°C	800	6/29/78	20	45	23	22	2	150	29	36	288	5.1×10^2	7.3
Camp Williams Warm Spring	23.5°C		6/30/78	24	54	29	25	5	170	41	58	372	5.6×10^2	7.45

Table 2. Approximate total dissolved solids and maximum reported temperatures at selected Wasatch Front thermal springs.

Spring	Approximate TDS (mg/1)*	Maximum reported Temperature
Crystal	1,500	86°C (187°F)
Saratoga	1,500	44°C (111°F)
Udy	7,900	54°C (121°F)
Wasatch	8,600	42°C (108°F)
Beck	13,700	55°C (132°F)
Utah	29,200	62°C (144°F)
Crystal (Madsen)	42,900	57°C (135°F)

*From Mundorff (1970)

Although the origin of the lineations is still in question, a tentative hypothesis is that the light soil patches are concentrations of calcium carbonate deposited in small sag ponds associated with buried range front structures. Minor topographic lows were not noted to occur with the light soil patches, but years of farming may have masked the very slight depressions.

The quartzite mounds in figure 12 are along the major structural trend, and are anomalous in that they are totally surrounded by valley fill. The water well 457 m (1500 feet) north-northwest of the westernmost outcrop encountered quartzite at a depth of 91 m (300 feet).

Geophysical Investigations

Magnetic Surveys

Two types of ground magnetic surveys were undertaken at the Crystal Hot Spring resource using an E. J. Sharpe, Fluxgate vertical field magnetometer (Model no. MF-1T-100). First, a detailed survey in the vicinity of the springs was made in which most of the shallow ground temperature grid stations were occupied with the magnetometer. Readings at any given station were quite variable due to problems with the magnetometer, and any minor magnetic variations were not identifiable. Second, two one-mile traverses X-X′ and Y-Y′ shown in figure 13 were run to determine the position of the magnetic high shown on the state magnetic map (Zietz, et.al. 1976) relative to the hot spring system. As the profiles are not tied into a magnetic base station of known value, the readings are only relative, and diurnal magnetic variations have not been removed. The most prominent feature in profile X-X′ is the large magnetic anomaly at the northern end of the area. The anomaly is very steep on the southern flank, increasing sharply over a very low background value, to the south. The profile is interpreted as indicating that material of high magnetic susceptibility in the subsurface is positioned adjacent to material of very low magnetic susceptibility. The north end of profile Y-Y′ has a similar but less intensive anomaly and the slope of the southern flank is not as steep nor the anomaly as intense as that seen in profile no 1. The anomaly at the south end of profile Y-Y′ is presently unexplained, but may represent a small patch of volcanic material on the Oquirrh Formation.

Aeromagnetic Survey: A total intensity aeromagnetic map flown by the U. S. G. S., but contoured by ASARCO (1954), was provided to the UGMS by ASARCO after profiles X-X′ and Y-Y′ had been run. A portion of the ASARCO map is reproduced in figure 14.

The anomaly, as depicted on figure 14, is elongated in an east-west direction, and roughly parallels the northern flank of the East Traverse Mountains. The most intense portion of the anomaly is roughly triangular in shape and is bounded by the 1,400 gamma contour. The springs and the State Prison are located on the southern flank of the anomaly. Within the area of the anomaly defined by

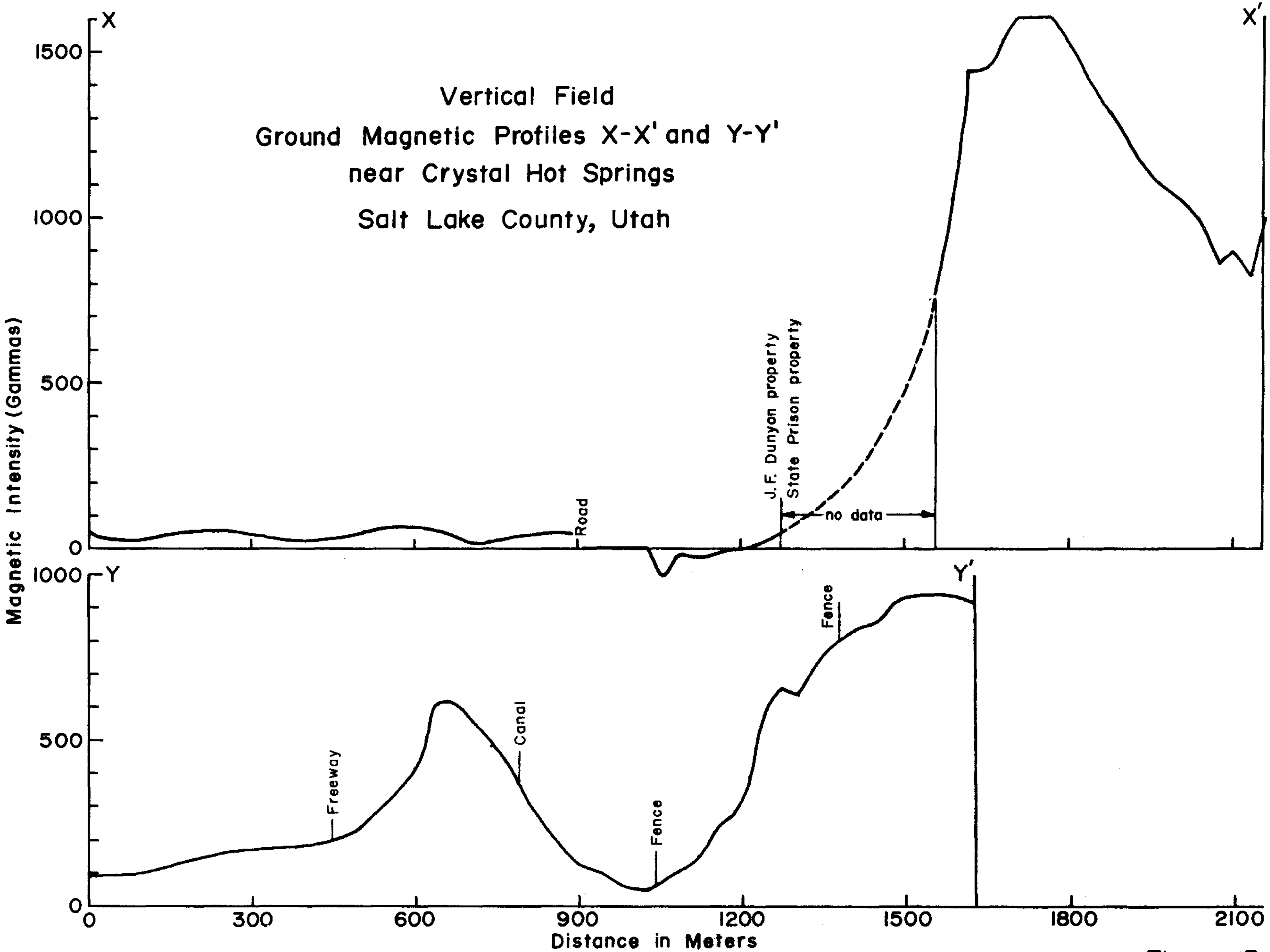

Vertical Field
Ground Magnetic Profiles X-X' and Y-Y'
near Crystal Hot Springs
Salt Lake County, Utah
X
X'
Y
Y'
Magnetic Intensity (Gammas)
1500
1000
500
0
1000
500
0
Road
J.F. Dunyon property
State Prison property
no data
Freeway
Canal
Fence
Fence
0
300
600
900
1200
1500
1800
2100
Distance in Meters

Figure 13

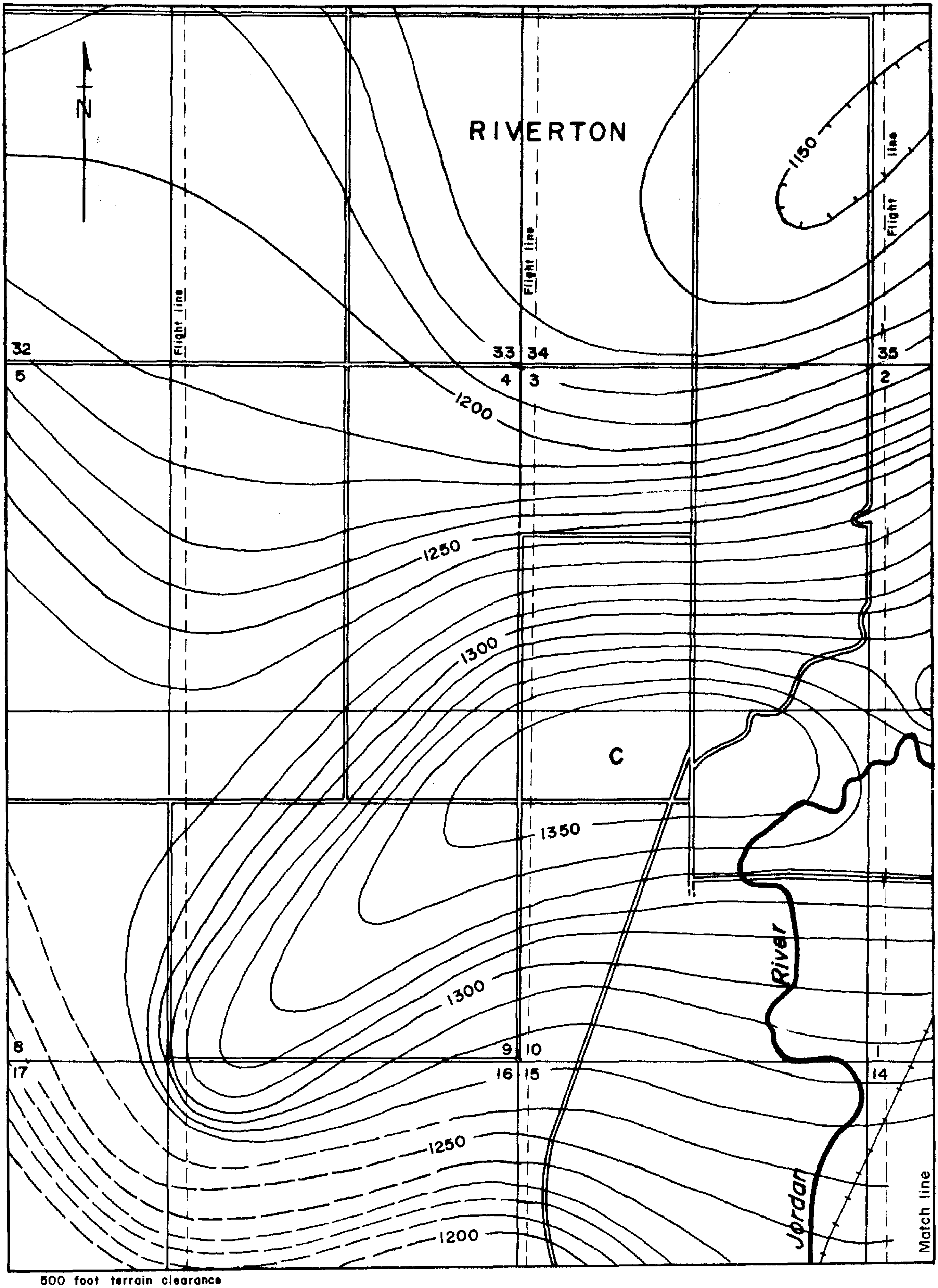

Aeromagnetics in Vicinity of Crystal Hot Springs

Figure 14a

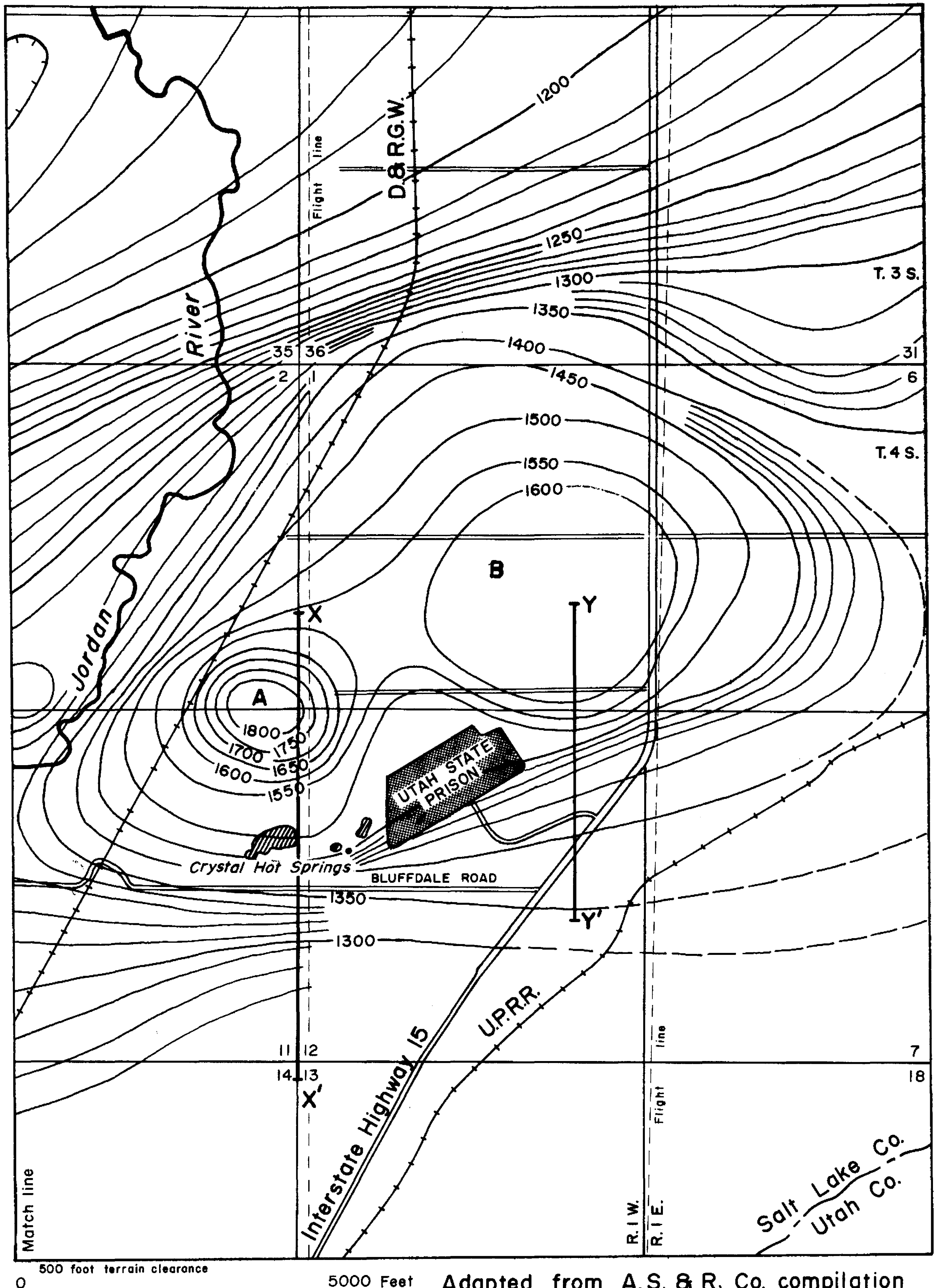

Adapted from A.S. & R. Co. compilation of U.S.G.S. data, A.S. & R. Co. (1954)

Figure 14b

the 1,400 gamma contour are two roughly circular areas. The western portion ("A" in figure 14) is intense, and relatively sharp as compared to the less intense and broad eastern portion ("B" in figure 14). Just west of the Jordan River is a less intense portion of the total anomaly ("C" in figure 14) with closure at 1,340 gammas. This portion is separated from the magnetic high to the north of the springs by a slight depression in the intensity. The western edge of the anomaly is steep and linear.

ASARCO targeted and drilled the "A" portion of the anomaly to determine if the buried body responsible for the anomaly was mineralized. The location of the drill hole is plotted in figure 16; the log of the hole is presented in Appendix A. At a depth of 113 m (370 feet), an andesite porphyry containing approximately 2% magnetite was encountered; the hole continued in andesite prophyry to a total depth of 287 m (940 feet), mineralization of commercial value was not found.

Magnetics Summary: Magnetic surveys have provided valuable information on the distribution of magnetic materials in the subsurface, and the location of subsurface structures. In the study area, an andesite porphyry with high magnetic susceptibility is present on the downthrown side of normal faults just north of the spring system, and has been faulted against materials of low magnetic susceptibility. Additionally, normal faults in the material of high magnetic susceptibility, having vertical displacement, are also discernable. The differences in the shape and intensity of magnetic anomalies A, B, and C are likely to be attributed to vertical displacement of the andesite porphyry to varying depths across normal faults.

Gravity Surveys

The only gravity data available for the Traverse Mountains area are those published by Cook and Berg (1961). The Traverse Mountains are coincident with a regional gravity high that separates the Jordan Valley graben to the north from the Utah Valley graben to the south (figure 15). Although only a few gravity stations are present in the immediate vicinity of the springs, the isobars are shifted valleyward in the vicinity of the hot springs, thus putting the hot springs on the local gravity high, on the southern flank of the Jordan Valley graben.

DRILL HOLE DATA

Holes of Opportunity

A number of water wells exist in the vicinity of the hot springs, and have provided data in areas where gradient holes were not drilled by UGMS. The holes referred to as Lee, Hall and U. S. P. (figure 16), (Utah State Prison) were open at the beginning of the investigation. The ASARCO exploration hole was cleaned to a depth of 42 m by UGMS at the time the gradient holes were drilled. The Lear hole was drilled as a water well at the time gradient hole drilling was proceeding, but independent of the UGMS project. Lithologic information for water wells, when available, is taken from driller logs, and is presentedin Appendix A.

Gradient Holes

The information presented in previous sections was used to site six geothermal gradient holes in and around the Crystal Hot Spring system. The drilling was done by K. O. Burt, of Springville, Utah, who began drilling on February 17, 1978, and finished on March 21, 1978. Drilling was done with a rotary rig, and holes were completed to depths that range from 61 m to 85 m (200 to 280 feet). Each hole was spudded with air then advanced to the desired depth using mud. Upon completion of the drill ing, a one inch black iron pipe, capped at the bottom, was run to the total depth of the hole. The hole was then back-filled with cuttings, where possible, and the top 3 m (10 feet) filled with concrete. When artesian conditions were encountered, the holes were grouted from total depth to the surface.

The six gradient holes were sited to yield a maximum of information pertaining to the spring system and to test the hypotheses made after conducting the shallow ground temperature survey. Holes (C, D, E) were drilled across the surface expression of the springs along a line that strikes to the northwest (figure 16). Holes (B, F) were drilled to the east of the springs where ground temperatures had been found to decrease rapidly with distance from the eastern lakes. Hole (A) was drilled near what was believed to be the possible intersection of two faults. A number of existing water wells (holes of opportunity) to the south and west of the system were used to fill in data on geology and temperatures present in those areas. Subsequent to gradient hole drilling by UGMS, the Division of State Forestry drilled a geothermal production well for the purpose of space heating a greenhouse. The Forestry well was drilled between gradient holes A and D, and is referred to as SF-1.

The gradient holes were logged and the cuttings sampled as drilling proceeded. The samples were divided into two portions, one portion was dried and preserved as it was taken, and the second portion was washed and saved for analysis. These samples are stored in the UGMS sample library. Lithologic logs of the holes are presented in Appendix A.

The gradient hole drilling program has provided subsurface geologic, hydrologic, and temperature information unatainable by any indirect method. The nature, thickness, and lateral extent of unconsolidated material; as well as the nature, distribution and depth to consolidated material are a number of geologic parameters that have been determined from the drilling program.

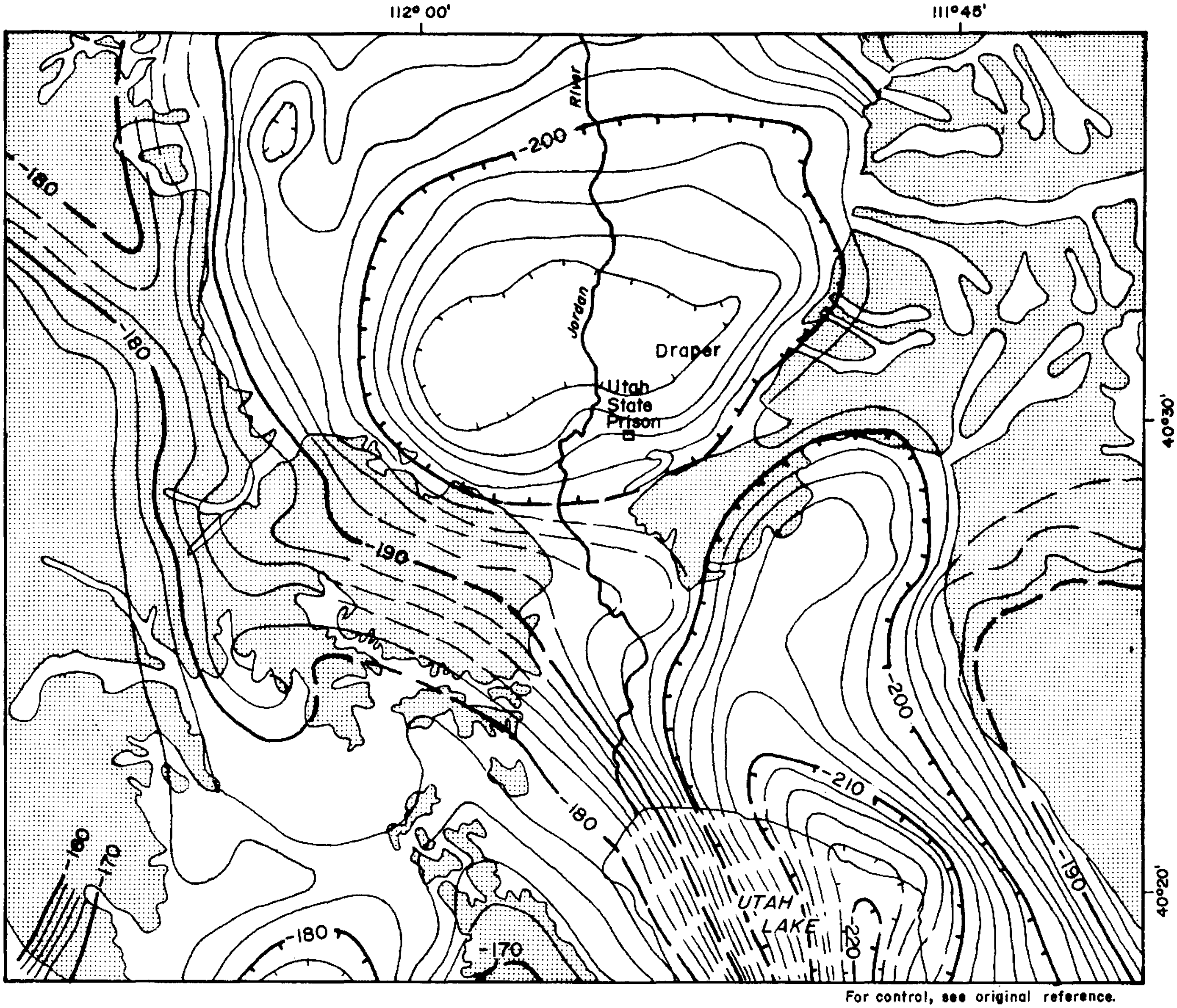

EXPLANATION

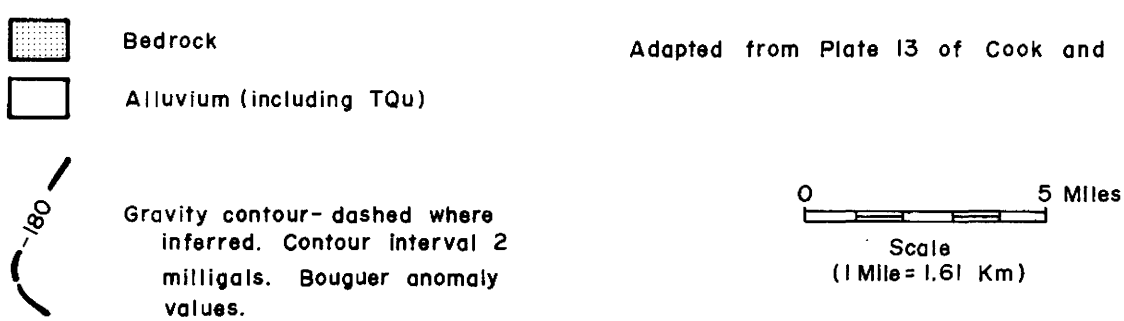

Gravity contour- dashed where inferred. Contour interval 2 milligals. Bouguer anomaly values.

Adapted from Plate 13 of Cook and Berg, 1961

Scale
(1 Mile = 1.61 Km)

Bouguer Gravity Anomaly for the Central Wasatch Front, Utah

Figure 15

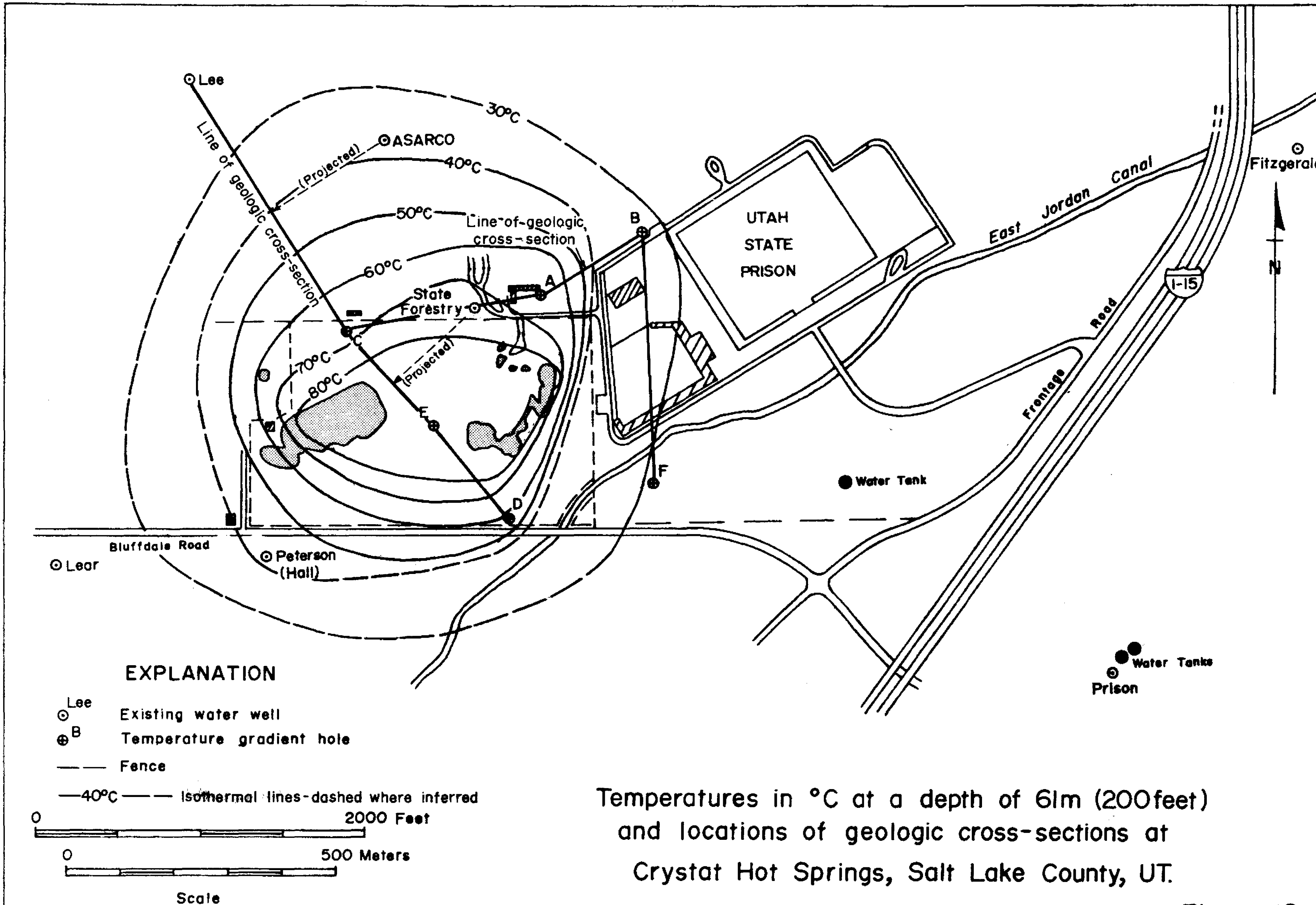

Temperatures in °C at a depth of 61m (200feet) and locations of geologic cross-sections at Crystat Hot Springs, Salt Lake County, UT.

Figure 16

Geology

By using generalized forms of lithologic logs (Appendix A), cross-sections through the area of the springs have been prepared and are presented in figures 17 and 18. Cross-section Lee-D in figure 17 shows a faulted bedrock surface mantled by unconsolidated materials. At the surface, a variable thickness of clay overlies more permiable sands and gravels. The clays are lake clays and contain variable but small amounts of sand. Interbedded in the clays are lenses of sand and sandy gravel with clay that reach a maximum thickness of less than 6 m (20 feet); the clay content appears to decrease with depth in some holes. In the immediate vicinity of the springs (holes D and E) a clean quartzite gravel overlies the fractured quartzite bedrock. Northwest of the springs, the clay content in the quartzite gravels increases, and further west, the gravels are a mixture of sand and well rounded gravel and cobble. Over the downthrown block (figure 17), the Lee and ASARCO holes penetrated additional unconsolidated material consisting of sand and gravel with clay and quartzite boulders in clay.

The bedrock surface in figure 17 was determined by using the drill hole data and the magnetic data discussed above. The main features of the cross-section through the bedrock are: 1) the normal step faulting generally associated with Basin and Range structure, 2) the fractured quartzite on the upthrown side of the southernmost fault, and 3) the andesite porphyry, of high magnetic susceptibility, on the downthrown block of the southernmost fault. Although other interpretations of the data are possible, this cross-section is the simplest cross-section that could be drawn with the available information.

Figure 18 is the cross-section along C-F in figure 16. Beneath the zone of clay at the surface, the unconsolidated materials in holes B and F were significantly different from the unconsolidated materials to the west. The gravels encountered in holes B and F contained significantly more clay and occasional boulders that were not present under the hot springs. The fault indicated in cross-section C-F is based on three lines of evidence: 1) bedrock was not encountered at the depths close to those in holes D and E, 2) the saddle in the aeromagnetic anomaly (figure 14), and 3) the rapid decrease in ground temperatures east of the easternmost lakes (figure 10).

Temperatures

After the gradient holes were completed, they were allowed to equilibrate before temperature gradients were measured. Measurements were made by lowering a thermistor into the one inch pipe and taking readings every 1.5 m (5 feet). The instrument used for the temperature measurements is a thermistor type device (accurate to .05°C) manufactured by Fluid Dynamics Corporation of Golden,

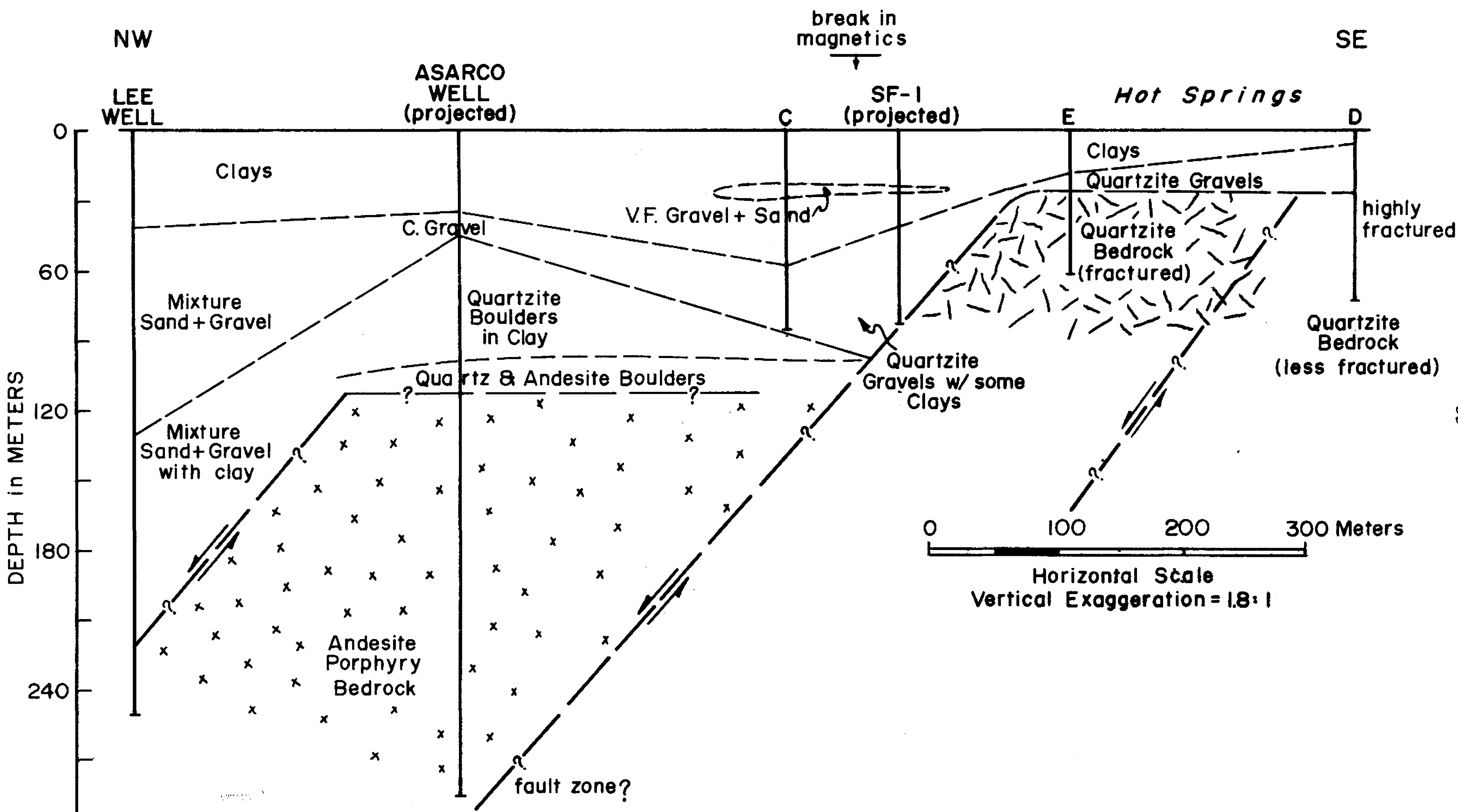

NW-SE Geologic Cross-Section through Crystal Hot Springs
Salt Lake County, Utah

Figure 17

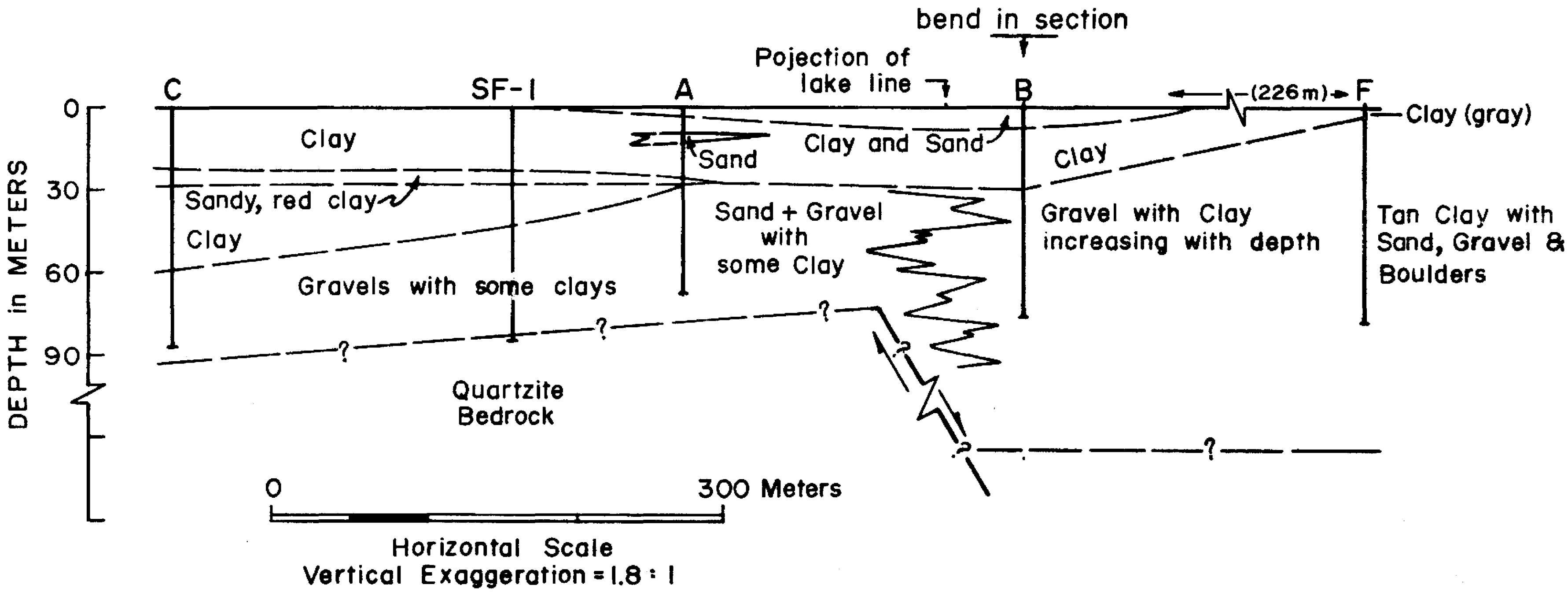

Geologic Cross-Section at Crystal Hot Springs
Salt Lake County, Utah

Figure 18

Colorado. The temperature values obtained from the device are initially read as resistance values which are then converted through a conversion chart to temperature in °C.

The results of the temperature measurements from the gradient holes at Crystal Hot Springs are presented in figure 19. Two sets of curves are shown on this data set. Holes A, C, D, and E all have maximum temperatures greater that 60°C, very steep gradients in the upper 20 m (65 feet), and all the curves are somewhat irregular in shape. Holes F and B have maximum temperatures of 35°C (95°F) or less, and have nearly linear gradients from top to bottom.

In general, the steep gradients in the upper portions of holes A, C, D, and E correlate with the predominantly clay lithologies logged at the top of each hole. Through the clay, a thermal insulator, the temperature increases rapidly with depth to the temperature of water in the underlying relatively permiable material saturated with thermal water. From that point, to the total depth of the hole, each curve is distinctly different.

Hole A. The gradient in the lower portion of hole A is somewhat irregular, but when a straight line is fitted to the curve, a gradient of 254°C/km is obtained. The irregularities in the temperature curve correlate with a complex series of sands and gravels with some clay.

Hole C. The gradient in hole C constantly decreases with depth; the curve is smooth, but an inflection point occurs at approximately 53 m (175 feet). Beyond this point the gradient decreases more slowly and when fitted with a straight line, the lower part of the curve has an approximate gradient of 325°C/km.

Hole D. Temperatures in hole D increase to a maximum of 74.2°C(165°F) at a depth of 20 m (65 feet). From this depth to the total depth of the hole, the gradient in the hole has a steep negative gradient of -459°C/km.

Hole E. The gradient in hole E is approximately 4,300°C/km through the clay at the surface, but then shows a decrease as a straight line through the bottom portion of the curve represents a gradient of 32°C/km. Had this hole continued, it is likely that the temperature gradient may have become isothermal.

Hot geothermal water was not present in holes B and F, and the elevated temperatures in these holes is a result of thermal conduction from below. The gradient in both holes is relatively constant, and the curves generally parallel each other. A straight line through the curve for hole B represents a gradient at 329°C/km, for gradient hole F, the gradient is 325°C/km.

Gradients were also measured in four water wells and the upper portion of the ASARCO ex-

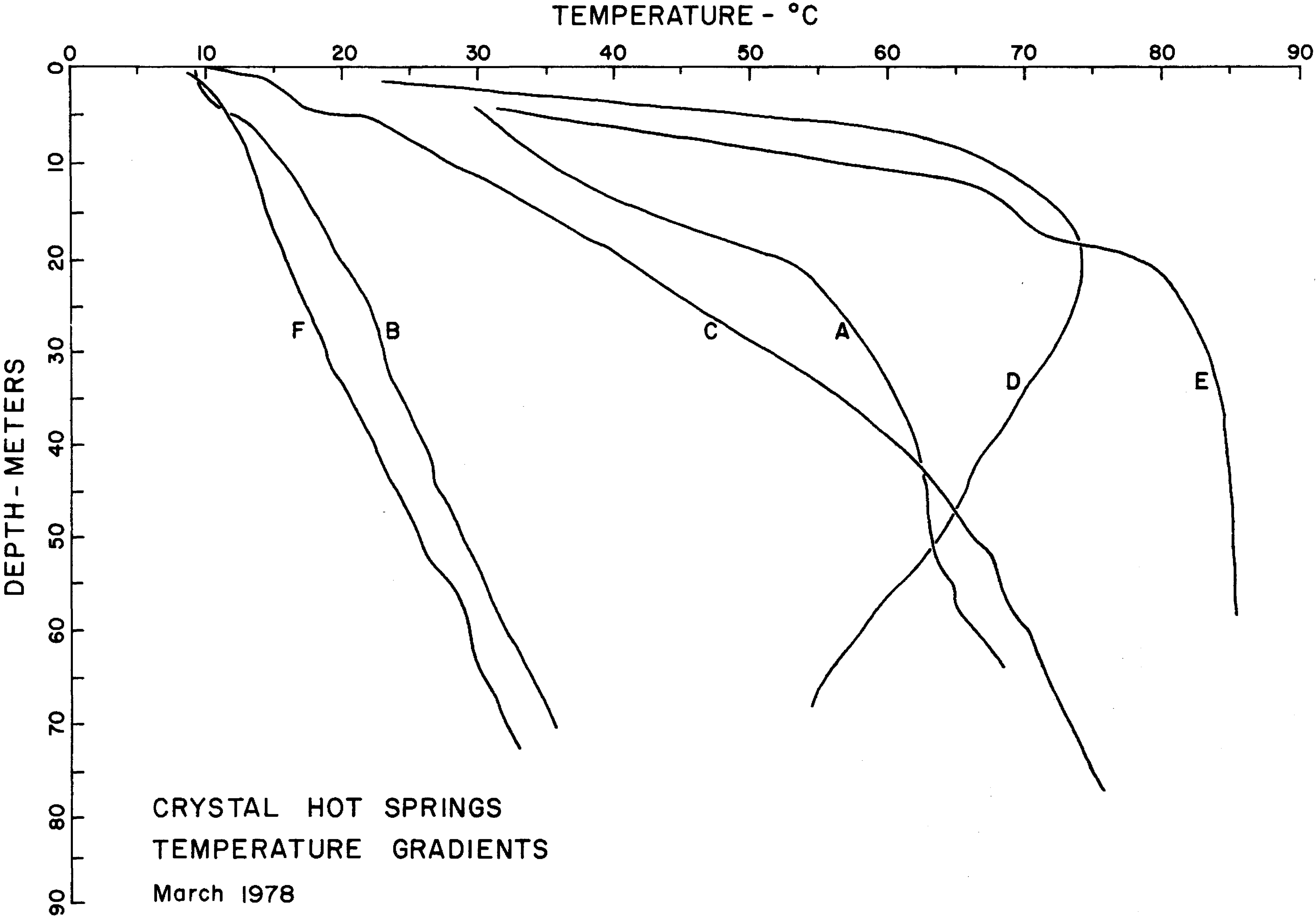
TEMPERATURE - °C
0
10
20
30
40
50
60
70
80
90
DEPTH - METERS
0
10
20
30
40
50
60
70
80
90
F
B
C
A
D
E
CRYSTAL HOT SPRINGS
TEMPERATURE GRADIENTS
March 1978

Figure 19

ploration hole (figure 20). Straight lines fitted through the lower portions of each of the temperature curves yield the following gradients.

C/WW-ASARCO	150°C/km
C/WW-Lee	93°C/km
C/WW-Lear	90°C/km
C/WW-Hall	98°C/km
C/WW-USP	13°C/km

The Lee, Lear, and Hall wells have gradients from 90 to 98°C/km, however, this value is not representative of the regional geothermal gradient. All of the holes mentioned are being influenced by the hot Spring System; possibly by the lateral flow of warm water in aquifers below the depths penitrated by these holes. The USP hole was completed in an artesian cold water aquifer and the thermal gradient is also not representative of the regional geothermal gradient.

The map of temperatures at 61 m (200 feet) in figure 16 illustrates the boundaries presently known to limit the surface repression of the hot spring system. The rapid changes in temperature on the south and east edges of the system are inferred to coincide with the structures discussed previously. The gradual decrease in temperature to the north and west reflects the northwestward flow of warm groundwater in near surface aquifers.

Pump Test of C/WW-SF

On November 7, 1978, a pump test was run on the geothermal test hole drilled by the State Forestry Service in order to obtain data on well yield and aquifer characteristics. Results of the test were modeled by Christian Smith of the University of Utah Research Institute/Earth Science Lab. His discussion of the results is presented in Appendix B. In general, the pump test indicated that the unconsolidated aquifer in which the well is completed is of low transmissivity, and that 30 gpm is the maximum yield to be expected from the well. Pumping the well at 30 gpm over an extended period of time should not have a significant effect upon the natural regime of the springs.

SUMMARY OF THE STRUCTURES IN THE VICINITY OF CRYSTAL HOT SPRINGS AND THE JORDAN NARROWS

Crystal Hot Springs

In previous sections of this report considerable evidence has been presented indicating the structural complexity of the area surrounding Crystal Hot Springs. Using the available evidence, a summary of the structural elements for which the best evidence exists is presented in figure 21. Other structures exist within this area, but confidence in their locations is limited at the present time.

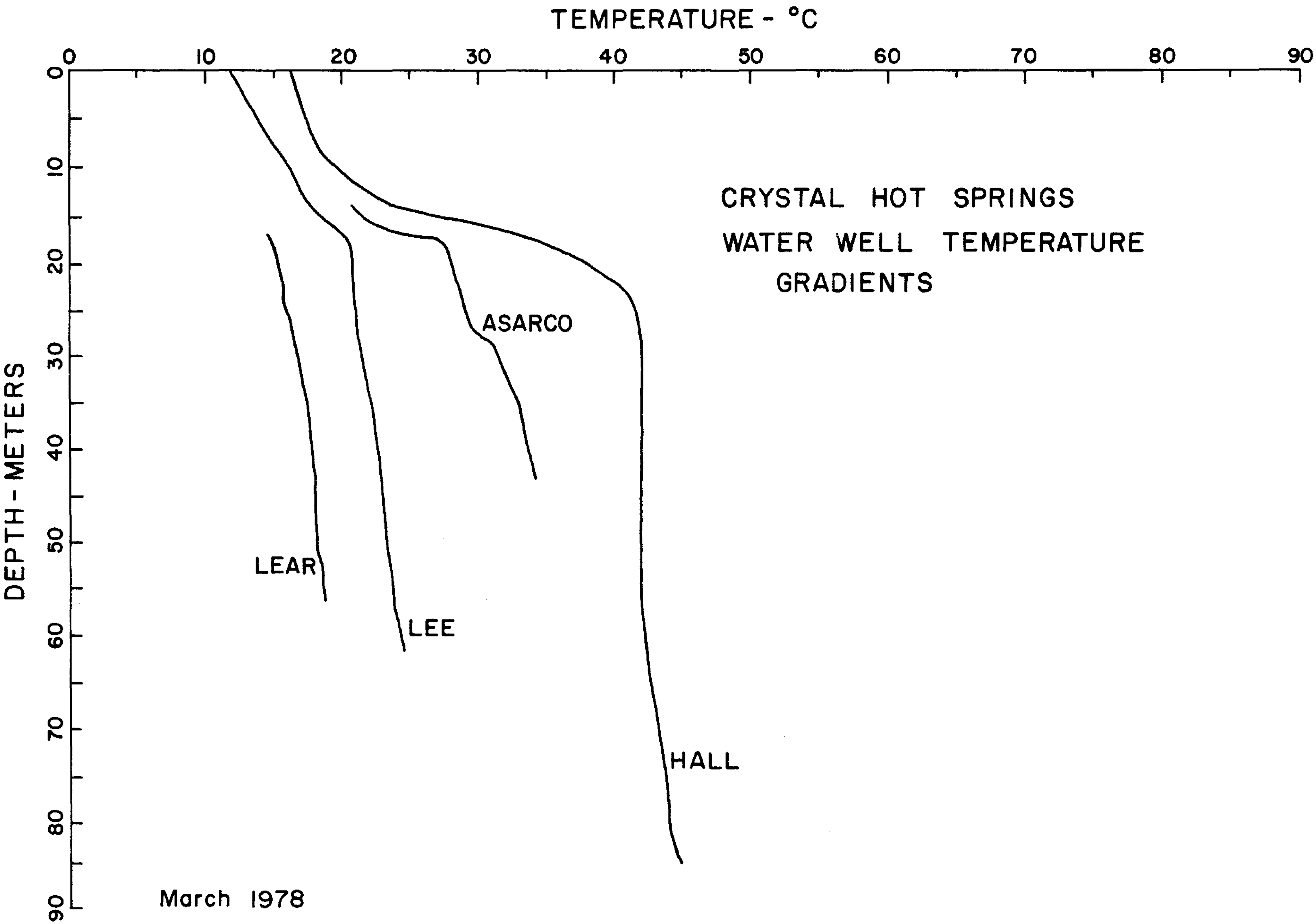
TEMPERATURE - °C
0
10
20
30
40
50
60
70
80
90
DEPTH - METERS
CRYSTAL HOT SPRINGS
WATER WELL TEMPERATURE
GRADIENTS
ASARCO
LEAR
LEE
HALL
March 1978

Figure 20

The following is a brief discussion of the structural elements in figure 21, and the possible resource controlling influences of each of three structual trends: northeast, north-northeast, and northwest.

The most prominent fracture set is a series of normal range front faults that strike northeastward and dip northwestward toward the Jordan Valley graben (figure 21 A). The Steep Mountain fault, and the fault coincident with the Provo shoreline are two of the range front faults that are exposed at the surface. Several other faults trending northeast are present beneath the valley fill. A range front fault having over 90 m (300 feet) of bedrock relief across the fault is present just north of the State Prison. Well data, aeromagnetic data, and a second class lineament, all discussed earlier, define the location of this fault.

The second set of fractures strike north-northeast. This trend was first noticed at the eastern edge of the spring system (figure 10) and repeats itself a number of times on the aeromagnetic surface. Based on the difference in the intensity and shape of the A and B portions (figure 14) of the aeromagnetics anomaly, and the difference in the depth of bedrock, as determined by gradient hole drilling, the movement on the fault coincident with the eastern springs appears to be down to the east-southeast. If the fault is normal, the dip of the fault plane is to the east-southeast. The total displacement on the fault is unknown but the relief on the bedrock surface is estimated to be on the order of 90 to 120 m (300 to 400 feet).

The third set of structures trends roughtly northwest and is best expressed by the fault that bounds the eastern edge of the Jordan Narrows graben (figure 21 B). A second fault with a northwest trend is present near Rideout quarry and displaces the Provo shoreline fault (figure 21 A).

The northeast trending faults in the vicinity of the springs appear to limit the expression of the geothermal resource on both the northwest and southeast and may actually define the limits of the system at depth. The highly fractured quartzite in which the hot water is found in the near surface may be effectively sealed to the northwest by the andesite porphyry faulted against the quartzite and to the southeast by less fractured quartzite. Evidence for the system being bound on the southeast by a fault is present in the temperature gradient taken in hole D (figure 19). The quartzite encountered in hole D was very similar to that encountered in hole E, however, the gradient in hole D reverses, indicating the absence of hot water in the quartzite penetrated by the hole.

Evidence that the fault which bounds the eastern edge of the spring system dips east-southeast, and is the conduit for the movement of hot water to the near surface, is found in the gradients obtained from holes B and F (figure 19). As discussed above, the gradients in B and F indicate conductive heat flow, and the absence of hot water moving through the material penetrated by the holes. The

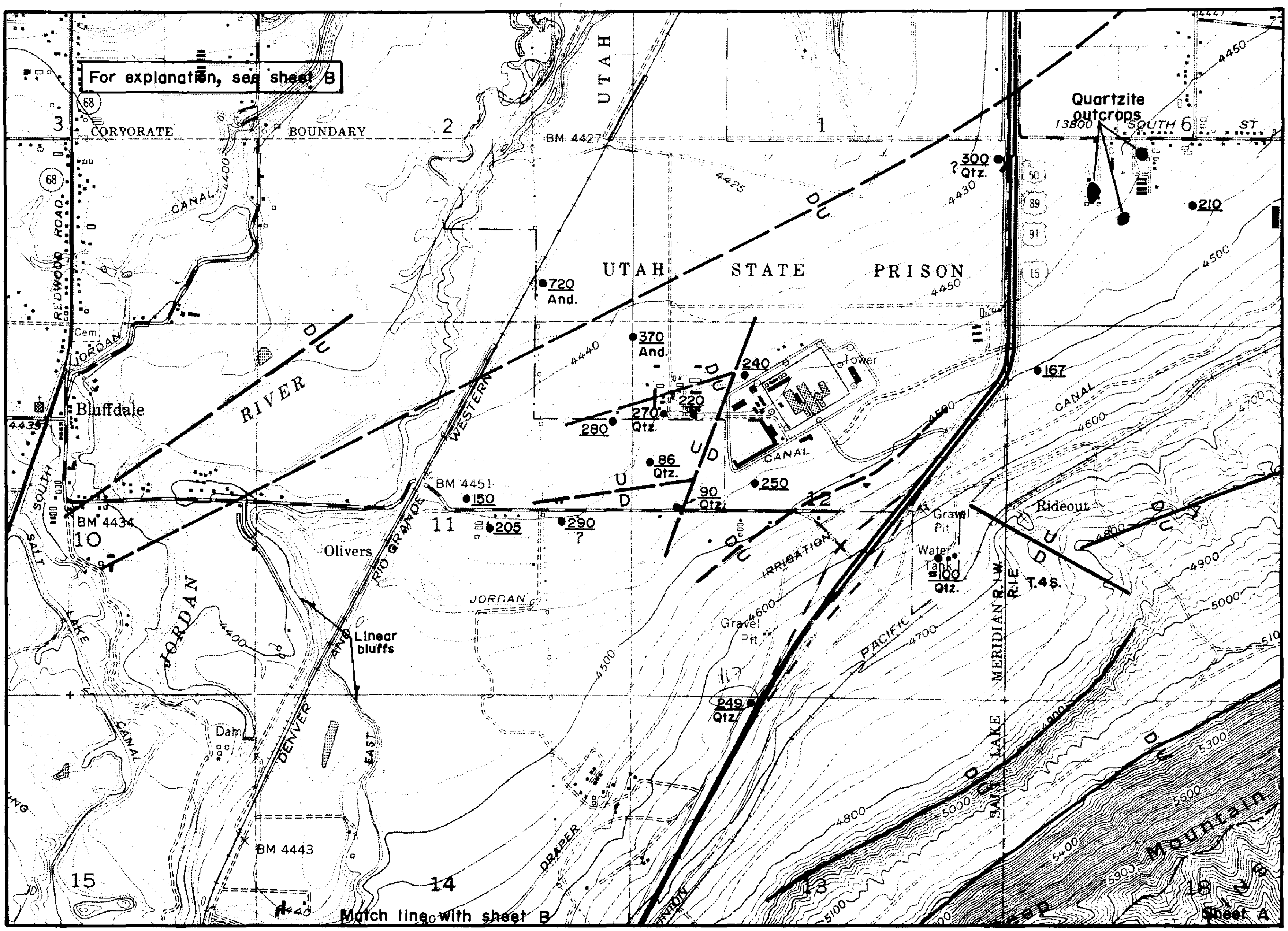

Known and inferred structures in the vicinity of Crystal Hot Springs and the Jordan Narrows, Salt Lake and Utah Counties, Utah

Figure 21a

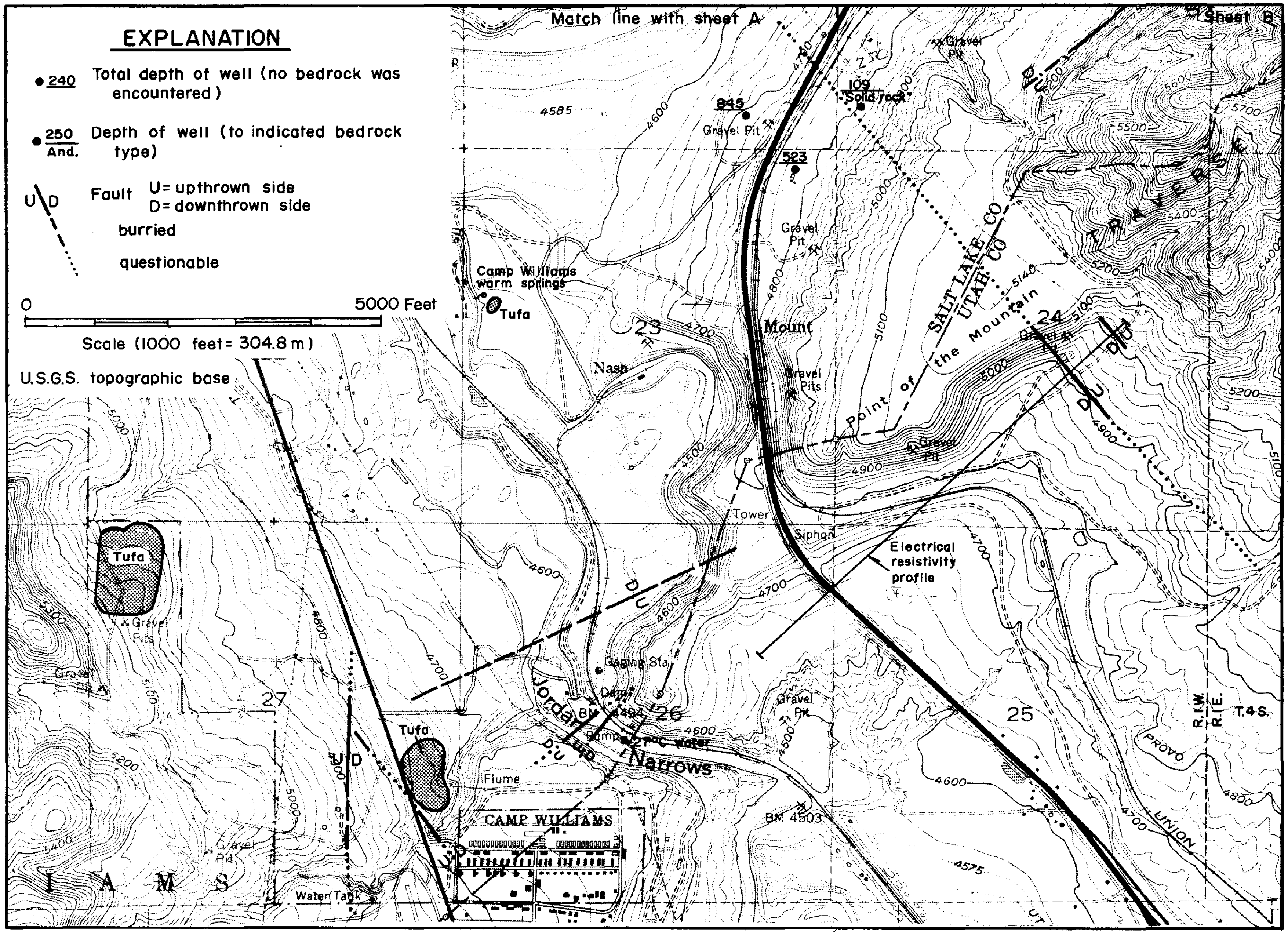

Known and inferred structures in the vicinity of Crystal Hot Springs and the Jordan Narrows, Salt Lake and Utah Counties, Utah

Figure 21b

gradients for the holes are very high, and indicate the presence of abnormally high temperatures at depth. Projection of the gradients observed in holes Band F to the maximum temperature observed at Crystal Hot Springs of 86°C places a possible fault plane transporting hot water, at approximately 245 m (800 feet) beneath the surface in the vicinity of the holes. However, projection of gradient data is very risky, and the observed gradients may be the result of hot water recharging into near surface unconsolidated aquifers at depths much less than 245 m (800 feet). Further investigations planned under the PON awarded to the State of Utah by DOE will provide the data needed to determine the subsurface conditions.

At the present time there is little evidence to indicate that the northwest trending structures have any influence on the expression of the resource. Further investigation will be necessary to determine whether or not these fractures influence the movement of water into the near subsurface.

Jordan Narrows

There does not appear to be any large structural or stratigraphic discontinuity between the East and West Traverse Ranges (Marsell, 1932), but the Jordan Narrows appears to be a structurally complex graben. The graben strikes northwest and is bound on the northeast and west by normal faults. Northeast striking faults cut perpendicular to the graben trend.

Evidence for the faults bounding the Jordan Narrows graben includes:

1) Major pre-pleistocene displacement along the north-south striking fault mapped just west of Camp Williams. Slentz (1955) indicates that the Jordan Narrows unit of the Salt Lake group is faulted down against Paleozoic rocks.

2) Major displacements on the bedrock surface buried beneath the Lake Bonneville spit just east of the Jordan Narrows (figure 21 B). The displacement was detected in an electrical resistivity sounding profile (figure 22) carried out by Zohdy and Jackson (1969). Depth to bedrock in water wells on strike with the westernmost structure indicate the structure may extend northward, possibly as far north as the linear bluff south of Bluffdale road (figure 21 A).

Slentz (1955) mapped a series of northeast trending structures in the Jordan Narrows that he indicates as being branches of the Steep Mountain scarp in the East Traverse Range. In figure 21 B these faults are shown as unconnected sub-parallel faults but they are undoubtedly related to the range front faults in some undetermined manner. These faults displace all the units assigned to the Tertiary Salt Lake group except the Travertine unit.

Although no fault has been indicated in figure 21 B the travertine deposit in the vicinity of the

Camp Williams warm spring, (C-4-1)23bcc, and the large travertine deposit on the west flank of the West Traverse Range, (C-4-1)27bb, are on strike with the fault indicated at an elevation of 4800 feet on the East Traverse Range. The fault may extend across the Jordan River Valley and may have influenced the movement of thermal water during the Tertiary.

THE CRYSTAL HOT SPRING GEOTHERMAL SYSTEM

System Recharge

The water in the Crystal Hot Springs system is meteoric in origin, and the recharge area for the elements carrying the water to depth is undoubtedly the adjacent Wasatch Range. Two elements are likely to be responsible for transporting the water to depth: 1) faults, and fractures or 2) aquifers, or some combination of the two. Since the exposed area of a fault or fault zone may not be extensive enough to provide an adequate recharge area, it can be hypothesized that steeply dipping aquifers in the Wasatch Range are recharged by snow melt and rainfall.

Heat Source

The Crystal Hot Springs geothermal system is a fault controlled, convective system in which meteoric water circulates to depth and is heated by the ambient temperature of the rocks at depth. Within the Basin and Range Province, heat flow is relatively high and the thermal gradient, or change in temperature with depth is normally about 32°C/km. Therefore, water entering the system at the average annual air temperature of 10°C must circulate to depths of approximately 2.5 km (1.55 miles) in order to obtain the maximum observed temperatue of 86°C. If some loss of fluid temperature is assumed to occur by mixing or by conduction to wall rock as the water ascends to the surface, then the water may circulate to greater depths. At depth, the heated water enters zones of high vertical permeability associated with faults and quickly returns to the surface.

The heat source for the water at Crystal Hot Springs is not believed to be the cooling of igneous rock at depth. The Little Cottonwood stock, the youngest dated intrusive body in the region, has been dated at between 24 and 31 million years in age while andesite intrusives of the Traverse Ranges have been dated at 37 million years of age (Crittenden, et. al. 1973). Theoretical cooling models developed by Smith and Shaw (1978) tend to support the theory that even the largest intrusive bodies no longer act as heat sources after 10 million years of the last phase of intrusion.

Springs

The shallow ground temperature survey was one of the first activities undertaken by UGMS at

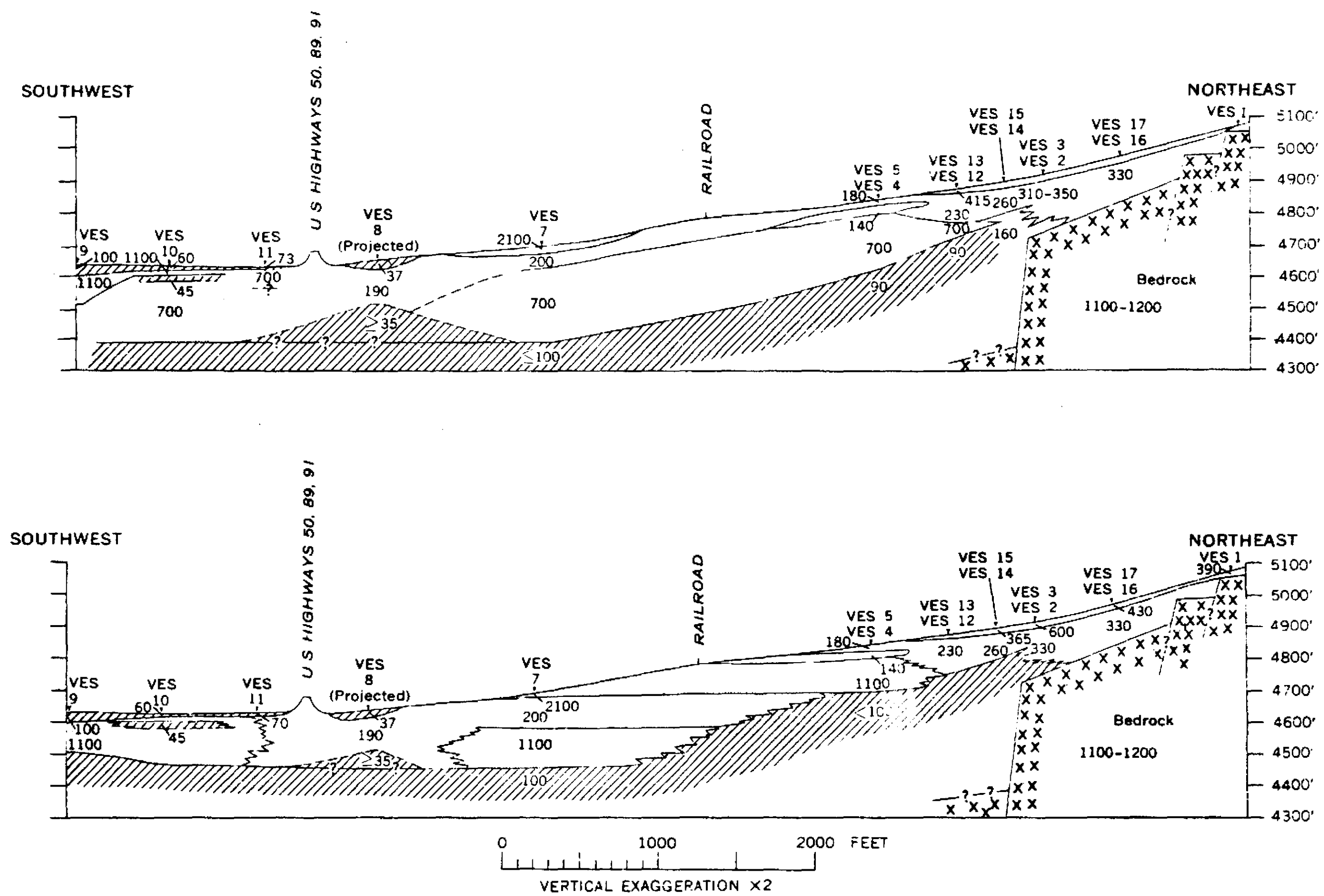

Figure 22. Two equivalent cross sections based on different interpretations of vertical electrical sounding (VES) curves. Numbers designate possible values, in ohm-meters, of true resistivity. Line pattern, low resistivity; stipple, high resistivity. Location of sounding stations shown on figure 1. Profiles shown to illustrate normal faulting in the Jordan Narrows. For explanation of resistivity data see Zohdy and Jackson, 1969.

Crystal Hot Springs. The data from the survey yielded the first indication that structures controlled the resource expression, and was a valuable beginning to the exploration program. The gradient holes that were sited on basis of the results of the shallow temperature survey, and provided information that helped to explain the observed shallow ground temperatures. The following is a description of the near surface portion of the spring system.

As discussed previously, the prominent north-northeast trending zone of high ground temperatures associated with the eastern ponds is coincident with a fault bounding the eastern edge of the spring system. The ground temperatures to the east of the zone decrease rapidly with distance from the ponds, because there is no hot water in the surficial materials to a depth of at least 76 m (250 feet). The low permeability of the surficial materials east of the fault together with the northwestward sloping regional water table surface, prevent the warm water from moving eastward in the near surface. West of the fault, fractured quartzite and quartzite gravels beneath the surface act as a near surface reservoir in which water of approximately 86°C is stored. The reservoir of heated water warms the impermeable, confining, clay or low thermal conductivity by conduction. Together, the variable thickness of clay and the distribution of warm water produce the observed shallow ground temperatures to the west of the fault.

The spring orifices are found along zones of weakness in the clay that confines the near surface reservoir. The zones of weakness in the clay are coincident with the buried fractures described in previous sections of this report. Slight movement on the faults in question after the deposition of the confining clay, would cause the weakness in the clay to develop, and the water flows to the surface under the artesian conditions present in the near surface reservoir.

SUMMARY

The preceding report details research done over the past two years by UGMS at the Crystal Hot Springs system. Emphasis has been placed on reporting results of investigations, and the authors have consciously refrained from drawing definitive conclusions about many detailed aspects of the system. Research efforts either on going or planned (primarily geophysical surveys) may significantly alter the conception of structural geometry presented above. Further reports will be issued as results become available.

In summary, the Crystal Hot Spring geothermal system is a fault controlled convective system in which meteoric water circulates to depth and is warmed in the normal heat flow of the Basin and Range province. A significant portion of the preceding discussion focused on the location of faults in the vicinity of the spring system. The reason for this emphasis is the importance of faults in: a) transporting deep thermal waters to the surface, and b) influencing the near surface expression of the resource. Without an understanding of the systems structural controls, development of the system will be hap-hazard and incomplete. Not all of the faults represented in this report transport thermal waters to the near surface. Therefore, the distribution of thermal waters in the near surface is also important. The use of shallow ground-temperature measurements, and gradient hole drilling have been used to obtain this information. By carefully interpreting the observed distribution of thermal water, the effects of very shallow ground-water systems can be eliminated and the source of the thermal water can be more clearly identified. The rate at which water will be produced from the system will only be determined by additional testing; the only available pump test was a test of a well completed in surficial sands. Similarly, the results of extensive use of the resource will only be determined after an extended period of production pumping.

REFERENCES

ASARCO, 1954, Unpublished contour map of aeromagnetic data flown by the U. S. Geological Survey.

BRAY, R. E., G. Lanier, and E. C. John, 1975, General geology of the open-pit mine, *in* Guidebook to the Bingham mining district: Society of Economic Geologists, p. 49-57.

BULLOCK, R. L., 1958, The geology of Lehi quadrangle: unpublished master's thesis, Brigham Young University.

CLUFF, L. S., G. E. Brogan, and C. E. Glass, 1970, Wasatch Fault (northern portion), earthquake fault investigation and evaluation report to Utah Geological and Mineral Survey, by Woodward-Clyde and Associates.

COOK, K. L., 1971, Earthquakes along the Wasatch Front, Utah – The record and the outlook; *in* Environmental Geology of the Wasatch Front, 1971: Utah Geological Association publication 1.

CRITTENDEN, M. D., Jr., 1964, General geology of Salt Lake County, *in* Geology of Salt Lake County: Utah Geological and Mineral Survey Bulletin 69, p. 11-48.

CRITTENDEN, M. D., Jr., J. S. Stuckless, R. W. Kistler, and T. W. Stern, 1973, Radiometric dating of intrusive rocks in the Cottonwood area, Utah: Journal of Research, U. S. Geological Survey, vol. 1, no. 2, p. 173-178.

DOLAN, W. M., 1957, Location of geologic features by radio ground wave measurements in mountainous terrain: unpublished master's thesis, University of Utah.

GILBERT, G. K., 1890, Lake Bonneville, Monographs of the U. S. Geological Survey, vol. 1, Washington.

GOODE, H. D., 1978, Thermal waters of Utah: Utah Geological and Mineral Survey Report of Investigation 129.

MARSELL, R. E., 1932, Geology of the Jordan Narrows region, Traverse Mountains, Utah: unpublished master's thesis, University of Utah.

MURDOCK, J. N., 1941, Geology of the Alpine-Draper Tunnel: U. S. Department of the Interior, Bureau of Reclamation.

PITCHER, G. G., 1957, The geology of the Jordan Narrows, Utah: unpublished master's thesis, Brigham Young University.

PRESSER, T. S., and I. BARNES, 1974, Special techniques for determining chemical properties of geothermal water. USGS Water-Resource Investigations No. 22-74.

SLEAR, M. L., and M. Barazangi, 1970, Tectonics of the Intermountain Seismic Belt, Western United States, part 1: Earthquake seismicity and composite fault plane solutions (abstract): Geological Society of America Abstracts with Program Circular 2, vol. 2, no. 7, p. 675.

SLENTZ, L. W., 1955, Tertiary Salt Lake Group in the Great Salt Lake Basin, Utah: Ph. D. thesis, University of Utah.

SMITH, C., 1978, Crystal Hot Springs pump test analysis: unpublished UURI/Earth Science Lab technical report, December 15, 1978.

SMITH, R. L., and H. R. Shaw, 1978, Igneous-related geothermal systems, *in* Assessment of Geothermal Resources of the United States, 1978: U. S. Geological Survey Circular 790, p. 12-17.

SMITH, R. B., and M. L. Sbar, 1970, Tectonics of the Intermountain Seismic Belt, Western United States, part 2, focal mechanisms of major earthquakes (abstract): Geological Society of America Abstracts with Programs Circular 2, vol. 2, no. 7, p. 687-688.

TAYLOR, G. H., and R. M. Leggett, 1949, Ground water in the Jordan Valley, Utah: U. S. Geological Survey Water-Supply Paper 1029.

ZIETZ, I., R. Shuey, and J. R. Kirby, Jr., 1976, Aeromagnetic map of Utah: U. S. Geological Survey Geophysical Investigation Map GP-907.

ZOHDY, A. A. R., and D. B. Jackson, 1969, Electrical sounding profile east of the Jordan Narrows, Utah: *in* Geological Survey research, U. S. Geological Survey Professional Paper 650-C, p. C83-C88.

APPENDIX A

WELL - AND SPRING-NUMBERING SYSTEM

THERMAL GRADIENT HOLE LITHOLOGIC LOGS

ABBREVIATIONS

MT = MUD TEMPERATURE

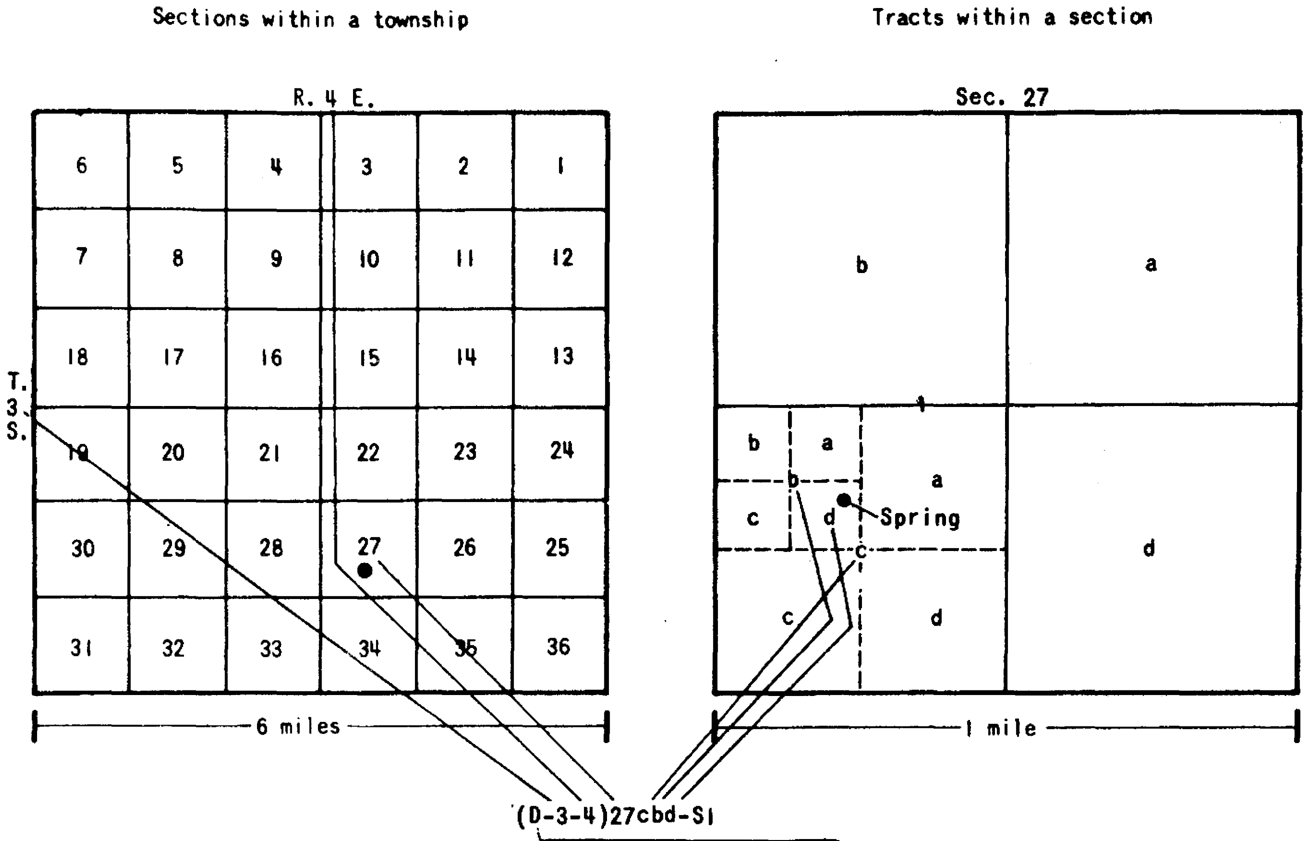

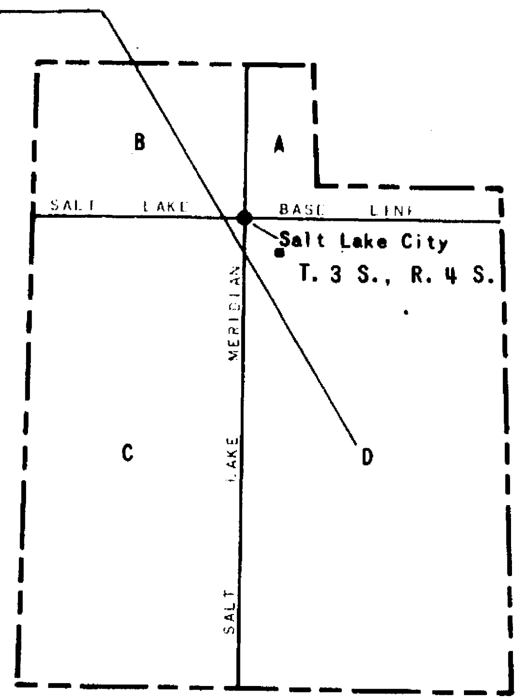

Spring-numbering System

The spring-numbering system used in this report is shown in figure 1 and is based on the U. S. Bureau of Land Management's system of land subdivision. The spring number indicates the location of the spring by quadrant, township, range, section, and position (if known) within the section. Four quadrants are formed by the intersection of the Salt Lake Base Line and the Salt Lake Meridian. The capital letter at the beginning of the location code indicates the quadrant in which the spring is located—A the northeast quadrant, B the northwest, C the southwest and D the southeast. Numbers designating the township and range, respectively, follow the quadrant letter, and the three are enclosed in parentheses. The number after the parentheses designates the section; the lowercase letters, if shown, indicate the location of the spring within the section. The first letter denotes the quarter section (usually 160 acres), the second the quarter-quarter section (40 acres), and the third the quarter-quarter-quarter section (10 acres). The letters are assigned within the section in a counterclockwise direction beginning with "a" in the northeast quarter of the section. Letters are assigned within each quarter section and each quarter-quarter section in the same manner. The capital letter "S" completes the designation of a spring. When two or more springs are within the smallest subdivision, consecutive numbers beginning with 1 are added after the letter "S." For example, (D-3-4)27cbd-S1 indicates a spring in the southeast quarter of the northwest quarter of the southwest quarter of sec. 27, T. 3 S., R. 4 E., and shows that this is the first spring recorded in the quarter-quarter-quarter section. The capital letter D indicates that the township is south of the Salt Lake Base Line and that the range is east of the Salt Lake Meridian.

Page 1

Temperature Gradient Hole Log

Hole C/GH - A　　Location (C - 4 - 1) 12 bbd 1

Surface Elevation 4457'　　Comp. Date 2 - 20 - 78　　T. D. 220'

Comments

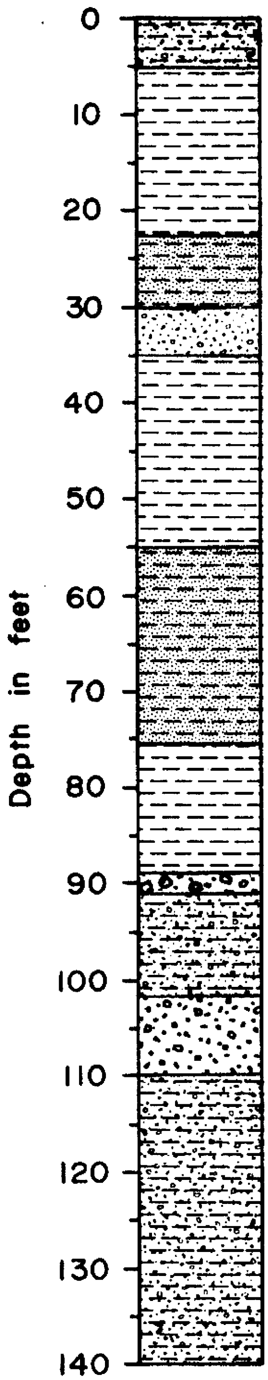

Light brown silt and clay with gravel

MT = 4.3°C
Gray Clay

Sandy clay

Sandy gravel

MT = 4.5°C
Gray clay

MT = 4.6°C

Sandy red clay

MT = 8.5°C

MT = 6.4°C
Clay (color not recorded) with minor gravel

Coarse gravel or a boulder

Sand and gravel with some clay
MT = 7.1°C

Sand, silt, clay and gravel with occasional boulders
MT = 7.1°C

Sand and gravel with clay

MT = 15.7°C

10 feet = 3.048 meters

Page 2

Temperature Gradient Hole Log

Hole C/GH - A (continued)

Comments

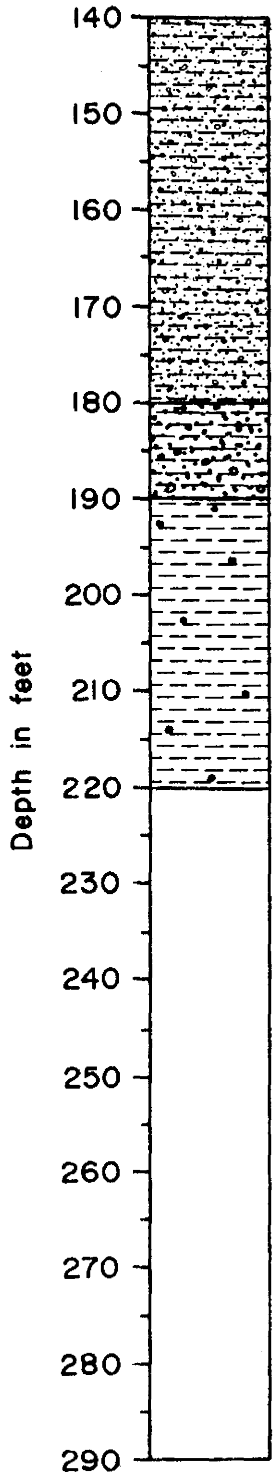

Sand and gravel with clay

MT = 16.5°C

MT = 18.7°C

Red clay and gravel

MT = 20.7°C

MT = 24.3°C

MT = 25.4°C

Stiff green and red clay with small pebbles

Total depth

Page 1

Temperature Gradient Hole Log

Hole C/GH - B Location (C - 4 - 1) 12 bac

Surface Elevation 4450' Comp. Date 2 - 23 - 78 T. D. 245'

Comments

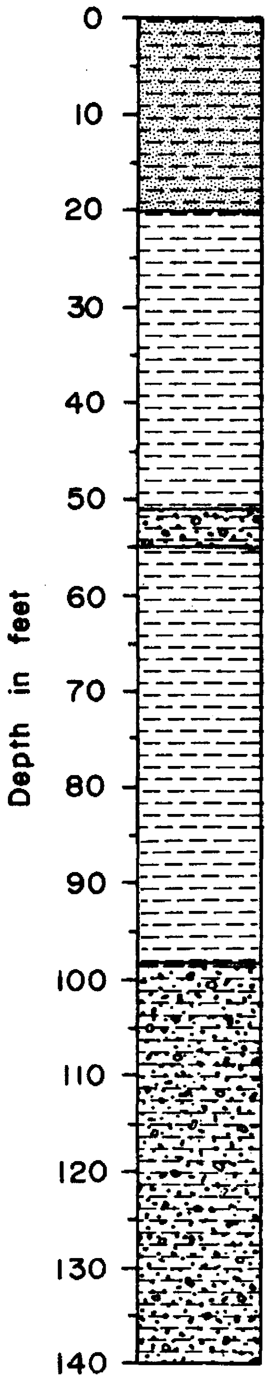

Clay and sand

Gray clay

Quartzite gravel with some clay

Gray clay

Gravel with varying amounts of clay. Gravel is weathered quartz monzonite with occasional quartzite

10 feet = 3.048 meters

Page 2

Temperature Gradient Hole Log

Hole C/GH - B (continued)

Comments

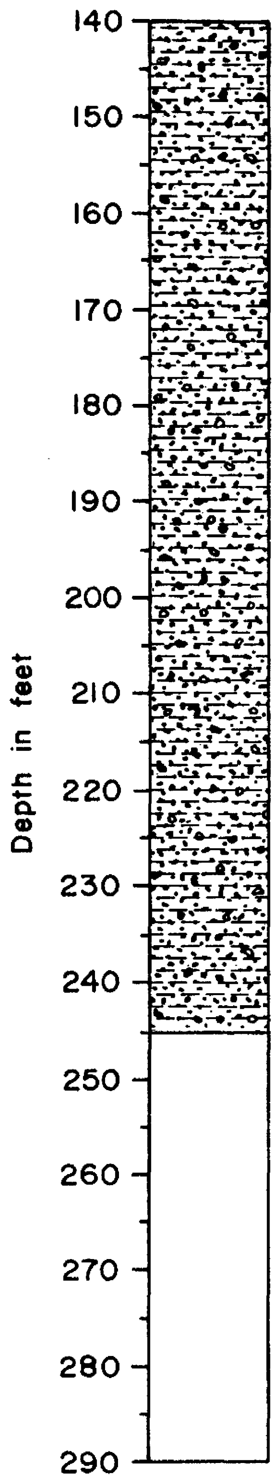

Gravel with varying amounts of clay. Gravel is weathered quartz monzonite with occasional quartzite

Total depth

Page 1

Temperature Gradient Hole Log

Hole C/GH - C Location (C - 4 - 1) 11 add

Surface Elevation 4452' Comp. Date 2 - 24 - 78 T. D. 280'

Comments

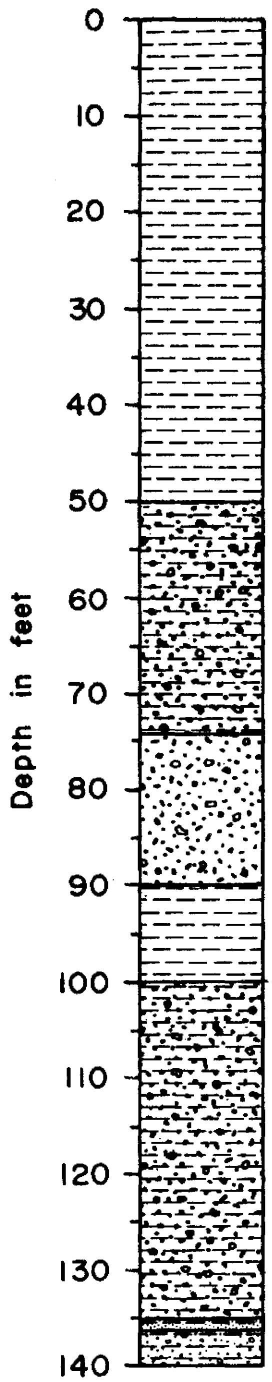

Gray clay

Stiff gray clay with fine gravel

MT = 10°C

Very fine gravel and sand

Brown and gray clay

Gravel in clay

Black clay and sand

Sand and gravel in clay

10 feet = 3.048 meters

Page 2

Temperature Gradient Hole Log

Hole C/GH - C **(continued)**

Comments

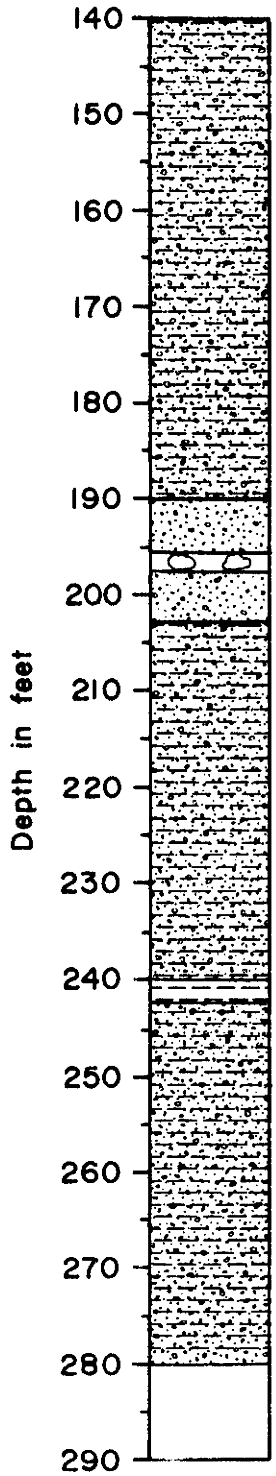

MT = 17°C

Sand and gravel in clay

MT = 19°C

Sand and gravel

Boulder

MT = 22°C

Sand and gravel

MT = 24°C

Sand and gravel in clay

Red clay

MT = 26°C

Sand and gravel in clay

MT = 28°C

Total depth

Page 1

Temperature Gradient Hole Log

Hole C/GH - D Location (C - 4 - 1) 12 bcd

Surface Elevation 4472' Comp. Date 3 - 1 - 78 T. D. 237'

Comments

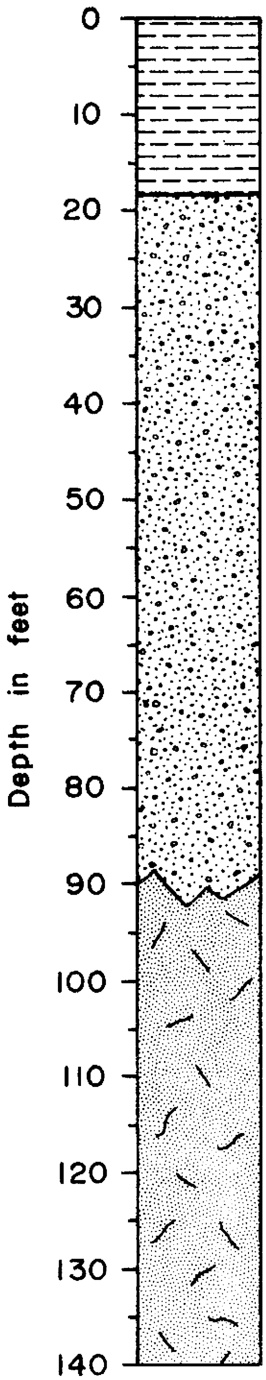

Gray clay

Quartzite sand and gravel

MT = 23°C

Contact uncertain

MT = 27°C

Fractured light gray quartzite

MT = 29°C

10 feet = 3.048 meters

Page 2

Temperature Gradient Hole Log

Hole C/GH - D (continued)

Comments

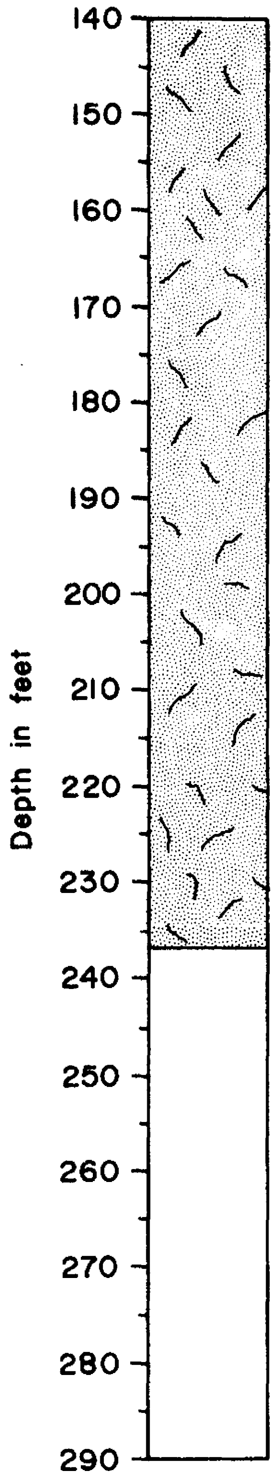

MT = 33°C

Fractured gray quartzite (less fractured and darker than 90'-140')

MT = 29°C

MT = 33°C

Total depth

Page 1

Temperature Gradient Hole Log

Hole C/GH - E Location (C - 4 - 1) 12 bbc

Surface Elevation 4465' Comp. Date 3 - 17 - 78 T. D. 200'

Comments

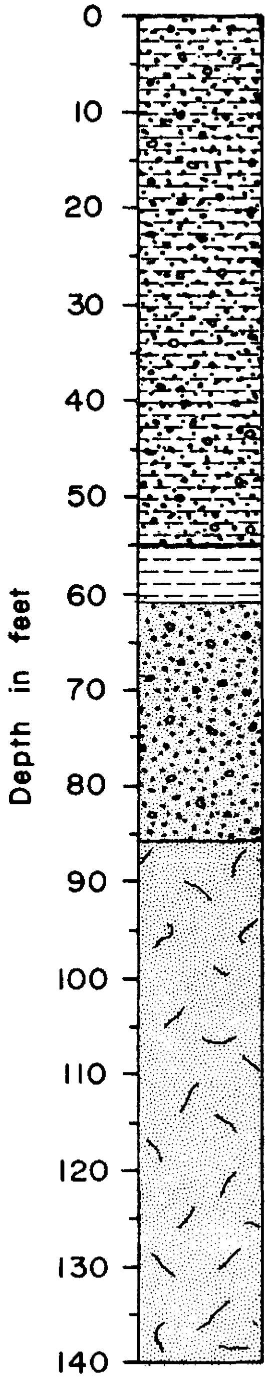

Tan clay with minor fine gravel

Stiff blue clay
MT = 21°C

Quartzite gravel and sand (slow loss of mud in this interval) (hole left over night, flowing next day 5-10 gpm @ 71°C)

MT = 27°C

Fractured light gray quartzite (occasional clay from fractures)

10 feet = 3.048 meters

Page 2

Temperature Gradient Hole Log

Hole C/GH - E (continued)

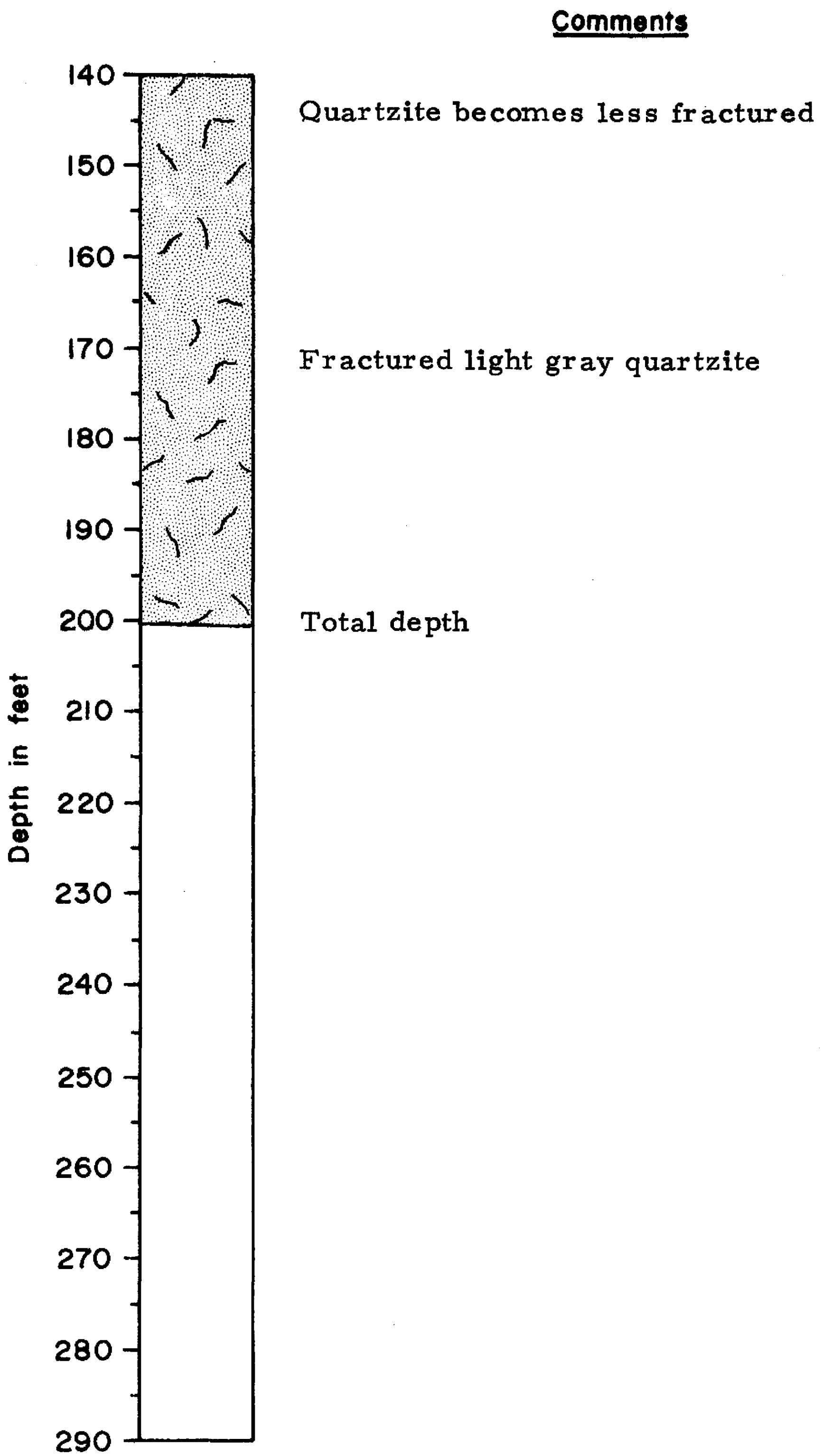

Page 1

Temperature Gradient Hole Log

Hole C/GH - F   Location (C - 4 - 1) 12 bdc

Surface Elevation 4483'   Comp. Date - 21 - 78   T. D. 250'

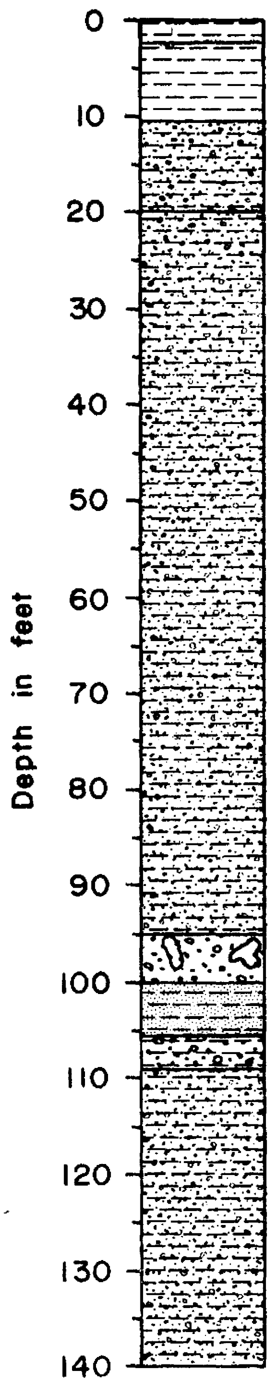

Comments

Tan clay

Gray Clay

Gray clay with sand and gravel

Tan clay with sand and gravel

Andesite gravel and boulders

Sandy tan clay

Gravel in clay

Clay, sand and fine gravel with occasional boulders and gravel layers

10 feet = 3.048 meters

Page 2

Temperature Gradient Hole Log

Hole C/GH - F (continued)

Comments

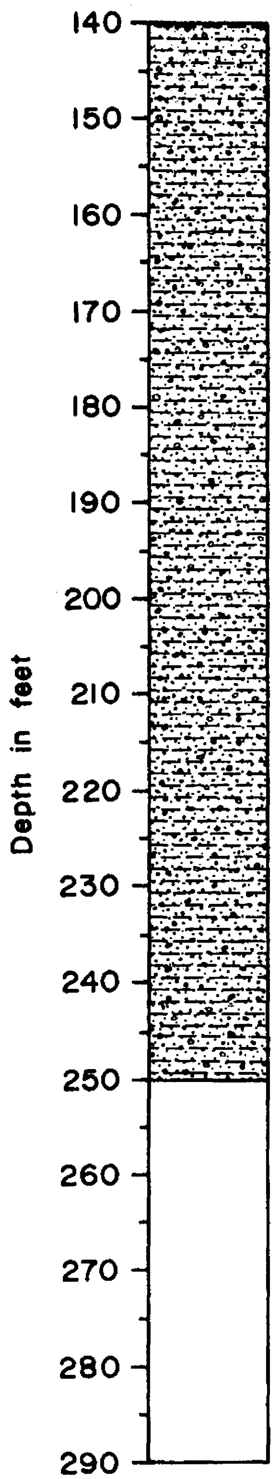

Clay, sand and fine gravel with occasional boulders and gravel layers

Total depth

Page 1

Temperature Gradient Hole Log

Hole C/WW - SF Location (C - 4 - 1) 12 bbd 2

Surface Elevation 4460' Comp. Date 4 - 12 - 78 T. D. 280'

Comments

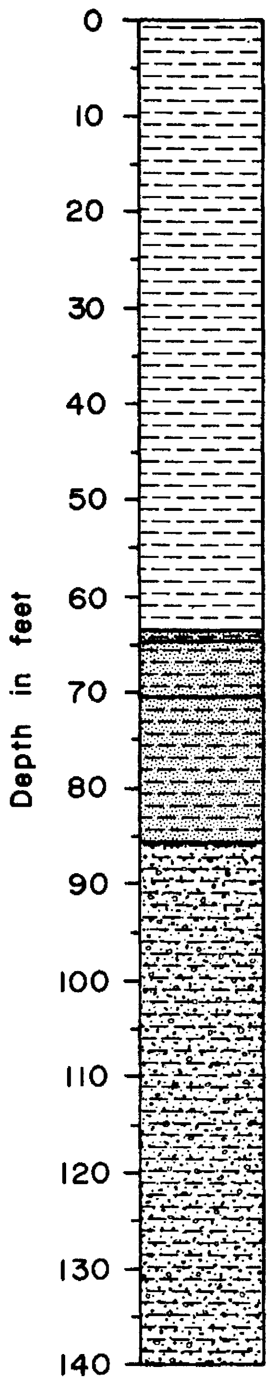

Dark gray clay

Dark brown clay with sand (mud turns brown)

Tan, green and gray clay with sand

Tan and gray sandy clay

Sand and gravel in gray clay

10 feet = 3.048 meters

Page 2

Temperature Gradient Hole Log

Hole C/WW - SF (continued)

Comments

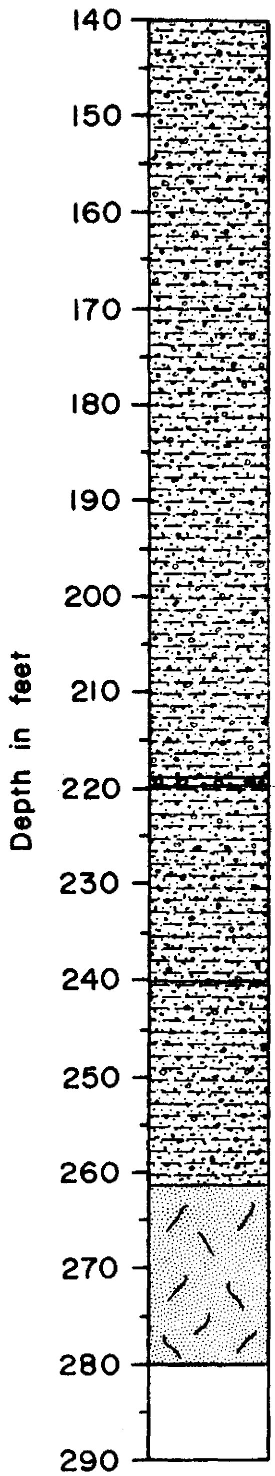

Sand and gravel in gray clay (continued)

White clay in returns

Sand and gravel with some gray clay (slow loss of drilling mud over 170'-218' interval)

Coarse gravel

Sand and gravel with intermittent red clay

Sand and gravel with some clay

Fractured dark gray quartzite

Total depth

Note: casing slotted from 170' to total depth.

Name: Lee
Owner: Utah State Board of Corrections
Location: (C-4-1)2ddb
Driller's Log:

0-3	top soil
3-82	blue clay
82-119	hard pan and sand
119-200	conglomerate
200-205	gray clay
205-248	conglomerate and gravel
248-309	conglomerate
309-340	gravel and a little water
340-397	sand and gravel
397-427	sand and gravel
427-463	gravel and clay
463-503	gumbo clay
503-552	sticky clay
552-582	sand and clay
582-603	sticky clay
603-665	gravel and clay
665-707	sticky clay
707-722	clay and gravel
722-825	bedrock

Name: None
Owner: Karl Dean
Location: (C-4-1)11acc
Driller's Log:

0-45	brown clay
45-90	blue clay
90-110	sand
110-150	sand and gravel

Name: Hall
Owner: Donald W. Hall
Location: (C-4-1)11dad
Driller's Log:

0-76	clay (top soil)
76-127	sandy clay
127-138	sand and gravel (heaved in hole)
138-140	coarse gravel
140-157	clay and gravel
157-174	brown sandy clay
174-182	white rock
182-196	blue shale
196-215	clay and gravel
215-236	gray sandstone
236-262	black sandstone
262-271	bedrock - hard gray
271-290	clay and sand

Name: None
Owner: Evan W. Hanson
Location: (C-4-1)13ccc
Driller's Log:

0-3	silt
3-99	silt, sand, and gravel
99-148	conglomerate
148-195	clay sand and gravel
195-226	sandy clay
226-236	gravel with water
236-241	sand and gravel
241-249	fractured quartzite and water
250-290	solid rock

57-7922

016486

Name: None
Owner: Loran D. Dixon
Location: (C-4-1)13bab
Driller's Log:

0-3	silt and sand
3-9	gravel
9-11	clay
11-30	gravel
30-38	cobbles
38-109	fractured quartzite
109-117	gravel and water
117-121	solid rock
121-140	open hole

Name: None
Owner: Mount Jordan Corporation
Location: (C-4-1)14dcd
Driller's Log: (hole deepened)

438-455	conglomerate
455-466	sand and gravel
466-472	conglomerate
472-490	clay and gravel
490-520	gravel
520-550	clay and gravel
550-555	gravel
555-590	clay and gravel
590-715	clay
715-716	gravel
716-718	clay and gravel
718-758	clay
758-761	sand and clay
761-815	clay
815-821	sand and gravel
821-845	clay

Name:	None
Owner:	Kenneth White
Location:	(C-4-1)23aaa
Driller's Log:	
0-3	topsoil
3-165	dry sand and gravel
165-180	clay and gravel
180-200	dry sand and gravel
200-365	clay and gravel
365-375	conglomerate
375-523	clay and gravel

Name:	None
Owner:	Gene Whendon
Location:	(D-4-1)6caa
Driller's Log:	
0-5	top soil
5-25	bentonite clay
25-27	gravel with water
27-65	clay (bentonite) and sand
65-75	quick sand
75-105	sand and bentonite
105-117	sand and gravel and bentonite
117-125	sand and gravel
125-133	bentonite (sealed off water)
133-143	sand, gravel and bentonite
143-165	sand and gravel with little bentonite
165-170	cobbles
170-178	sand and gravel (bentonite)
178-180	quick sand
180-210	sand, gravel, and little bentonite.

Name:	None
Owner:	Boyd A. Fitzgerald
Location:	(D-4-1)7bbb
Driller's Log:	
0-5	top soil
5-92	clay and gravel
92-94	sand and gravel with water
94-123	clay and gravel
123-125	gravel with water
125-139	clay and gravel
139-167	gravel with water

APPENDIX B

PUMP TEST DATA

AND ANALYSES OF

C/WW - SF

Pump Test Data from C/WW - SF 11/7/78

Time of Day	Water Level	Discharge	Notes
2:32	Above Ground	50 gpm	Engine RPM's set to 1500
2:35	35		
2:37		35 gpm	
2:38	38		
2:40	39		
2:42	43		
2:44	45	25 gpm	
2:47	47	26 gpm	
2:50	47		
2:52	48	28 gpm	
2:56	48		
3:00	47	30 gpm	
3:03	46		
3:09	46	28 gpm	
3:14	46	29	
3:36	47	30	
3:46	47	30	
3:56	48	30	
4:11	48	27	
4:27	43	28	Engine changes RPM's
4:41	48	28	
5:05	47	30	
5:22	48	30	
5:33	43	30	Engine changes RPM's Engine RPM's increased to 1700
5:35	69	37	
5:40	78	32	
5:43	78		
5:51	81	30	
6:00	82	29	
6:15	84	30	
6:32	84	30	
6:46	84	30	
7:00	84	27	
7:17	84	30	
			Engine RPM's increased to 2000
7:20	123	40	
7:23	123	38	
7:28	125	38	
7:36	126	38	
7:45	126	38	

Pump Test Data from C/WW - SF 11/7/78 (continued)

Time of Day	Water Level	Discharge	Notes
8:00	127	35	
8:15	127	35	
8:30	128	38	
8:46	127	38	
8:49	127	38	
8:50	Recovery		Pump turned off
15 secs.	85		
20	75		
32	72		
40	68		
45	66		
60	63		
65	60		
70	57		
80	54		
90	51		
100	48		
110	45		
120	43		
125	41		I seriously question anything above 40 ft. draw down and would not use.
132	39		
140	37		
160	35		
190	33		
210	Flowing at surface		

PETER J. MURPHY
Geologist

UNIVERSITY OF UTAH
RESEARCH INSTITUTE

UURI

EARTH SCIENCE LABORATORY
391 CHIPETA WAY, SUITE A
SALT LAKE CITY, UTAH 84108
801-581-5283

December 15, 1978

Pete Murphy
UGMS
606 Blackhawk Way
Salt Lake City, UT 84108

Dear Pete:

The results of the November 7, 1978 pump test of the flowing geothermal well near Crystal Hot Springs are encouraging. The aquifer can probably support several more low-capacity wells without diminishing the natural discharge to the ponds at Crystal Hot Springs.

The alluvial aquifer is tight, and large diameter wells may not be able to produce more water than smaller, less costly wells. All wells should be completed in bedrock.

I believe that the fractured quartzite is leaking hot water to the overlying alluvial aquifer. An observation well and an additional pump test will be needed to assess this inferred leakage and the accompanying vertical movement of water and delayed yield from storage.

A thin hole within 30 feet of the flowing well, similar to the temperature gradient holes but with perforated PVC casing, would be an adequate observation well that might later be adaptable to production.

Sincerely,

Christian Smith

Christian Smith

CS/smk

encl.

cc: P.M. Wright
D. Foley

CRYSTAL HOT SPRINGS PUMP TEST ANALYSIS

The flowing geothermal well on the grounds of the Utah State Prison near Crystal Hot Springs, Jordan Narrows Quadrangle, Utah was pumped at an average rate of 30 gpm for more than six hours on November 7, 1978. This report summarizes the data and results of this short-term pump test.

Figure 1 is a sketch of the well and the geologic units it penetrates. The well diameter is 6 in, its total depth 285 ft; it is cased to the bottom of the hole. Torch-cut slots in the bottom 110 ft of the casing were used to complete the well. The artesian head is inferred to be 9 ft above ground level; artesian flow is about 8 gpm at 180^{o}F. The 195 ft thick, fine-grained alluvial aquifer is confined above by approximately 90 ft of clay and below by quartzite bedrock. The quartzite is pervasively fractured and locally supplies hot water to the overlying aquifer. While it is not known whether the quartzite yields water directly to the well, it is certain that it does leak hot water to Crystal Hot Springs, a few hundred feet to the south.

The pump test was designed to be, but did not satisfy the strict requirements for, a step-drawdown test and its numerical analysis. Attempts to apply the step-drawdown analysis suggest well-losses are minimal and that the well is efficient. Completion of the well may even have improved the transmissivity of the aquifer within a short distance of the well.

The raw pump test data are plotted in Figure 2. Discharge, Q, in gallons per minute and drawdown (the increasing depth to water), s, in feet are plotted against the logarithm of time. A nearly constant rate of discharge at 30 gpm was sustained for 288 minutes. During this interval the drawdown was also nearly constant (at 57 and 93 feet). Drawdown increased only when discharge exceeded 30 gpm (between 0 and 12 min., and 183 and 188 min.). These observations indicate that there is a source of hot water near the well capable of supplying about 30 gpm instantaneously to the aquifer. The constant drawdown (136 ft) during the final pumping interval indicates that the source of hot water may be capable of supplying as much as 35 gpm.

The source of hot water also fills the ponds at Crystal Hot Springs. It is possible but unlikely that the well is pumping water that would otherwise rise to these ponds. It is also possible that the quartzite is leaking water directly to the well. In either case, pumping 30 gpm should have no observable effect upon the natural regime of the ponds.

Since no observation wells were available, the log-log type curve solution for transmissivity, T, and storage, S, cannot be found. To estimate T, the 'Harrill time', t_H, was used in a conventional straight-line analysis of the recovery data (Fig. 3). This value compensates for the changes in discharge and the nonequal periods of pumping at the different discharges recorded during the test (Harrill, 1970). Two straight-line segments emerged, an 'early' segment and a 'late' segment, from which the corresponding transmissivities T_e and T_l can be computed.

$$T_e = 34.4 \text{ ft}^2/\text{day}$$

$$T_l = 18.7 \text{ ft}^2/\text{day}$$

These values are low but are typical of tight, fine-grained artesian aquifers.

The two estimates of T are sufficiently low to limit the rate at which the aquifer can deliver water to the well. When pumped at a rate less than it can deliver, an aquifer with a low T and a nearby source of water is likely to sustain a constant drawdown. The response in an artesian system may be instantaneous: an increased discharge can cause the water level to drop immediately. If the pumping rate is again dropped to the lower rate, the water level will again remain constant, but at a lower level. This is thought to be what happened during the pump test at Crystal Hot Springs.

Given an estimate of T and the pump-test data, it is possible to estimate the value of storage, S. The well was pumped for 0.26 days at an average discharge of 30 gpm; the total drawdown was 135 ft. The solutions are not strictly valid for reasons discussed below but they are

$$T_e = 34.4 \text{ ft}^2/\text{day} \qquad S = 0.001$$

$$T_1 = 18.7 \text{ ft}^2/\text{day} \qquad S = 0.05$$

Figure 4 is a graph of drawdown as a function of the logarithm of distance from the pumping well for these two solutions. Tables 1 and 2 are the values plotted in Figure 4. Data from an observation well within 30 ft of the pumping well would discriminate between these two solutions. Both values of S are high for artesian systems; the value of S = 0.05 is so high that the T_1 solution is less likely.

The Theis equation has been used to predict the effects of continued pumping on the aquifer (Theis, 1935), and it assumes an infinite isotropic aquifer with no recharge areas near the pumping well, conditions violated at Crystal Hot Springs. Since a recharge area is indicated at Crystal Hot Springs, the Theis equation predicts drawdowns greater than those that will probably be observed. The drawdowns listed in Tables 3a-d and 4a-d and shown in Figures 5 and 6 may be excessive and the values of S too great.

Figures 5 and 6 plot the drawdown as a function of the logarithm of distance from a well pumping 10 gpm for periods of one day, one month, one year, and ten years. It can be seen that continued pumping of the present well is predicted to have little effect on the Crystal Hot Springs area. The aquifer may be able to support several properly spaced small-diameter wells pumping 10 gpm in a well field.

Before production is contemplated, an observation well should be drilled near the present well and a flow test run. The leaky confined aquifer equation of Hantush (1959) could then be used to refine the conclusions presented here.

REFERENCES

Harrill, J. R., 1970, Determining transmissivity from water-level recovery of a step-drawdown test: U.S. Geol. Survey Prof. Paper 700-C, p. C212-C213.

Hantush, M. D., 1959, Nonsteady flow to flowing wells in leaky aquifers: Jour. Geophys. Research, v. 64, no. 8, p. 1043-1052.

Theis, C. V., 1935, The relation between the lowering of the piezometric surface and the rate and duration of discharge of a well using ground-water storage: Amer. Geophys. Union Trans. pt. 2, p. 517-524

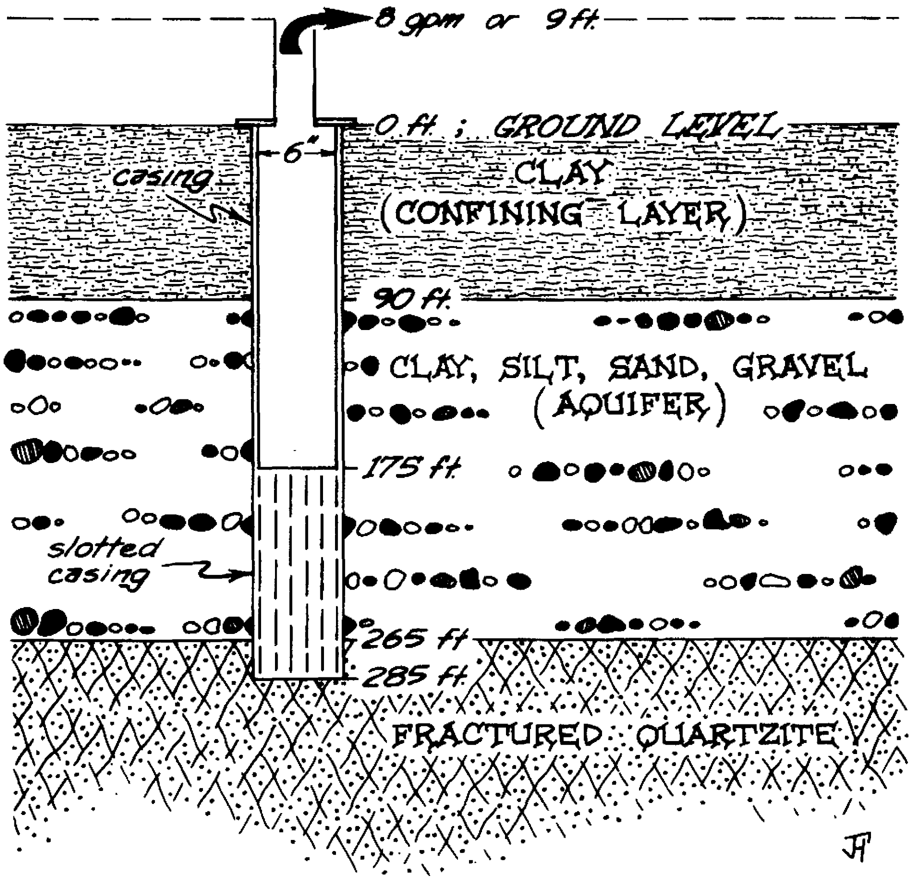

FIGURE 1. DIAGRAMMATIC SKETCH OF CRYSTAL SPRINGS/UTAH STATE PRISON FLOWING GEOTHERMAL WELL

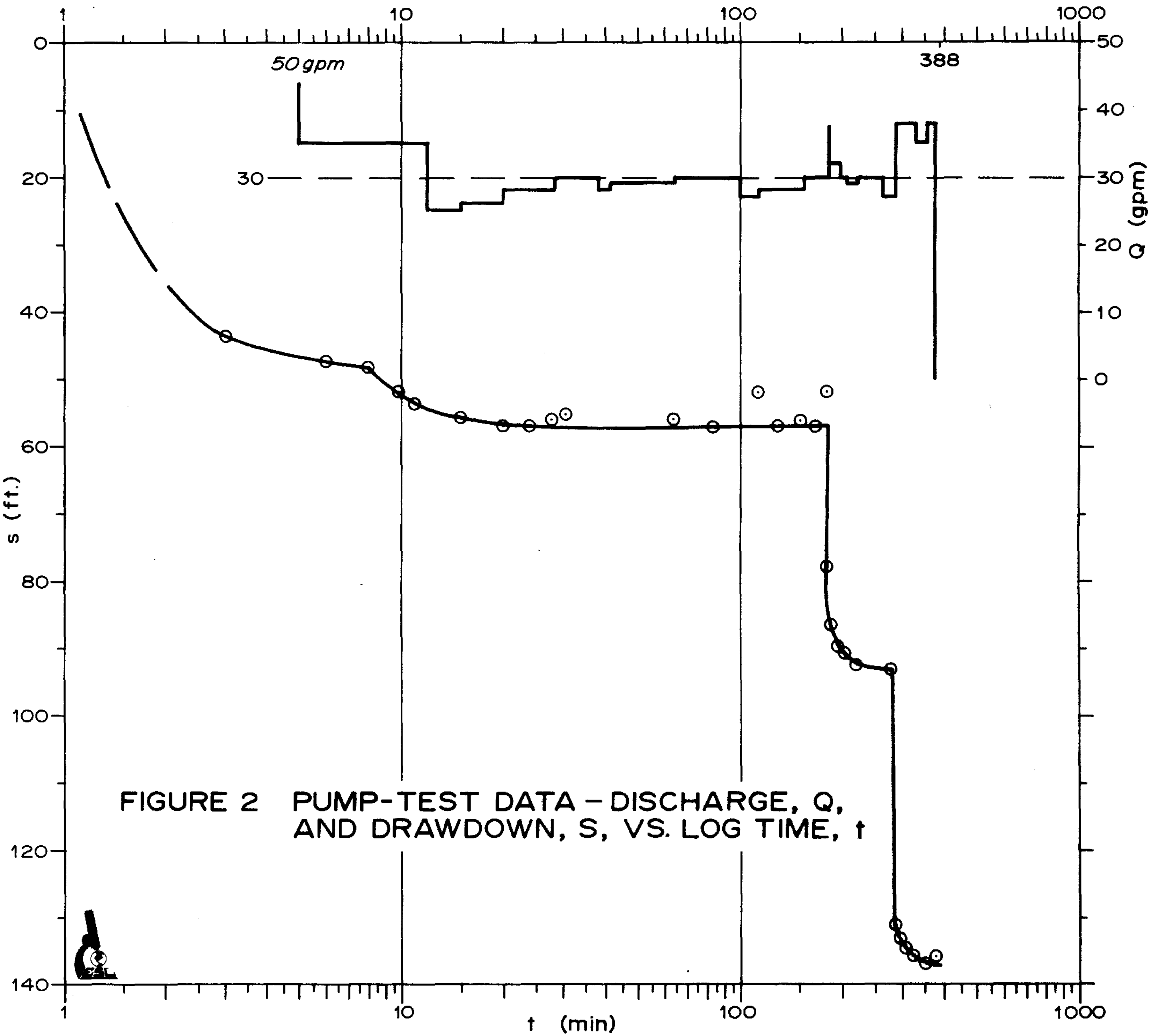

FIGURE 2 PUMP-TEST DATA – DISCHARGE, Q, AND DRAWDOWN, S, VS. LOG TIME, t

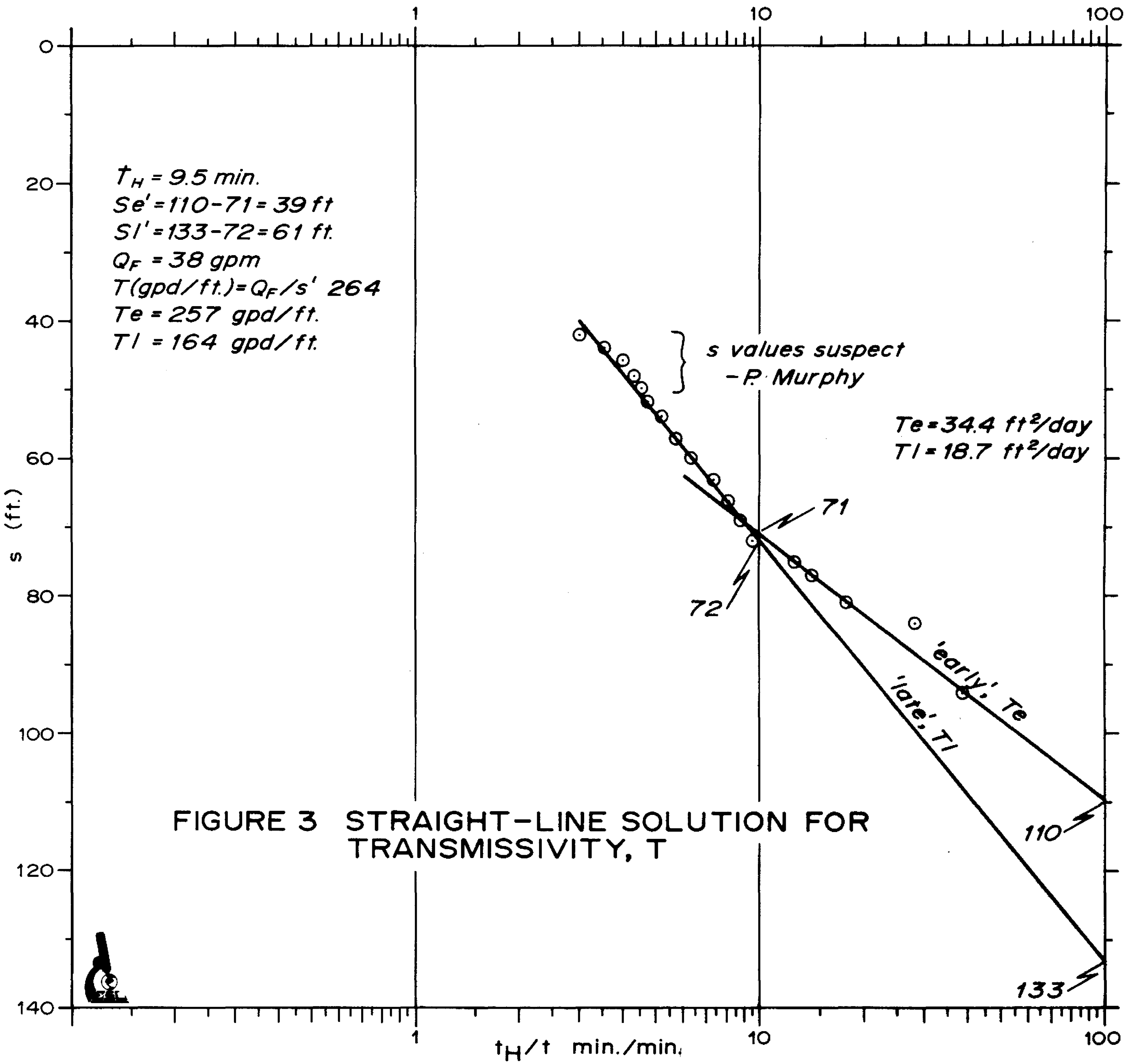

FIGURE 3 STRAIGHT-LINE SOLUTION FOR TRANSMISSIVITY, T

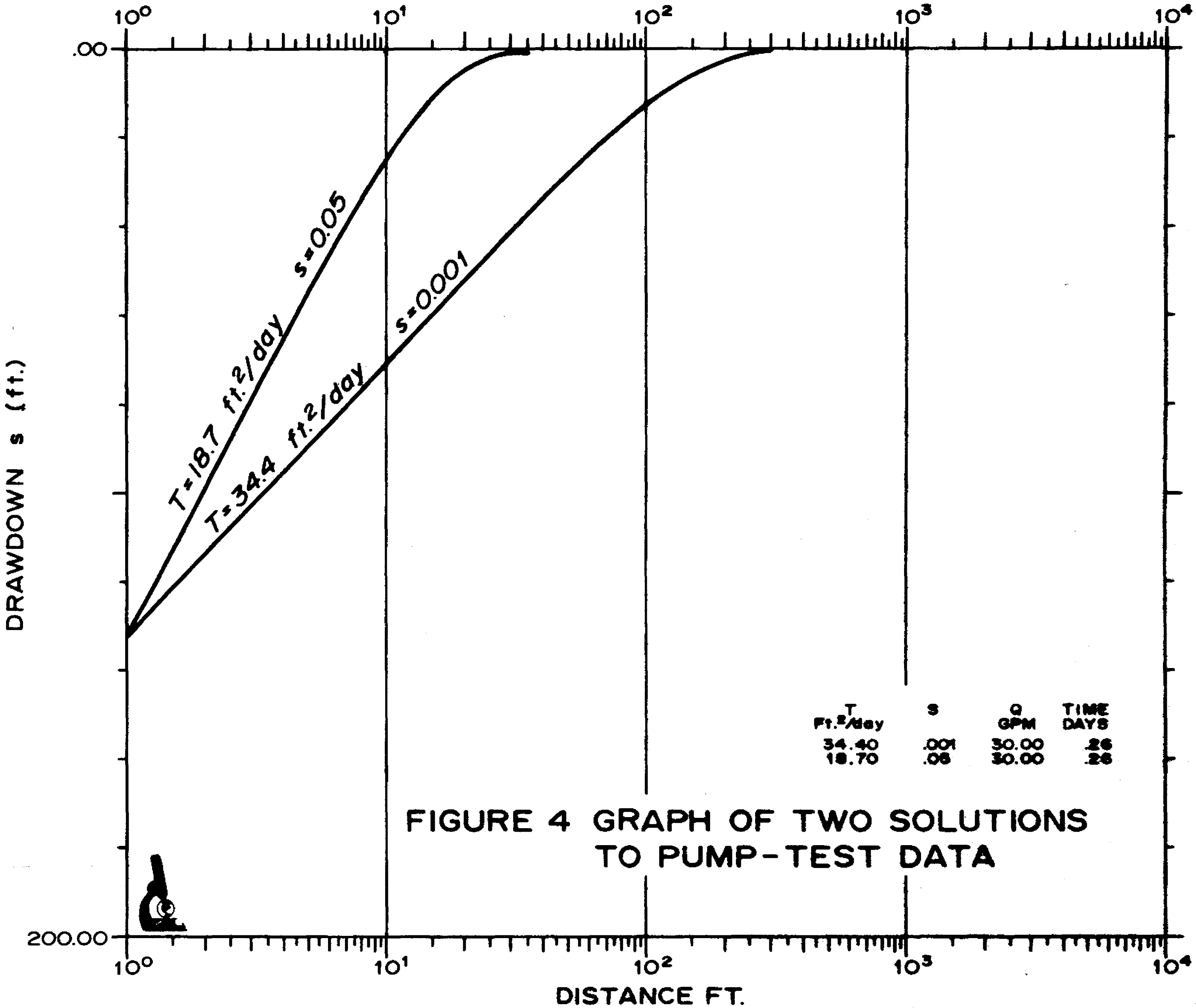

FIGURE 4 GRAPH OF TWO SOLUTIONS TO PUMP-TEST DATA

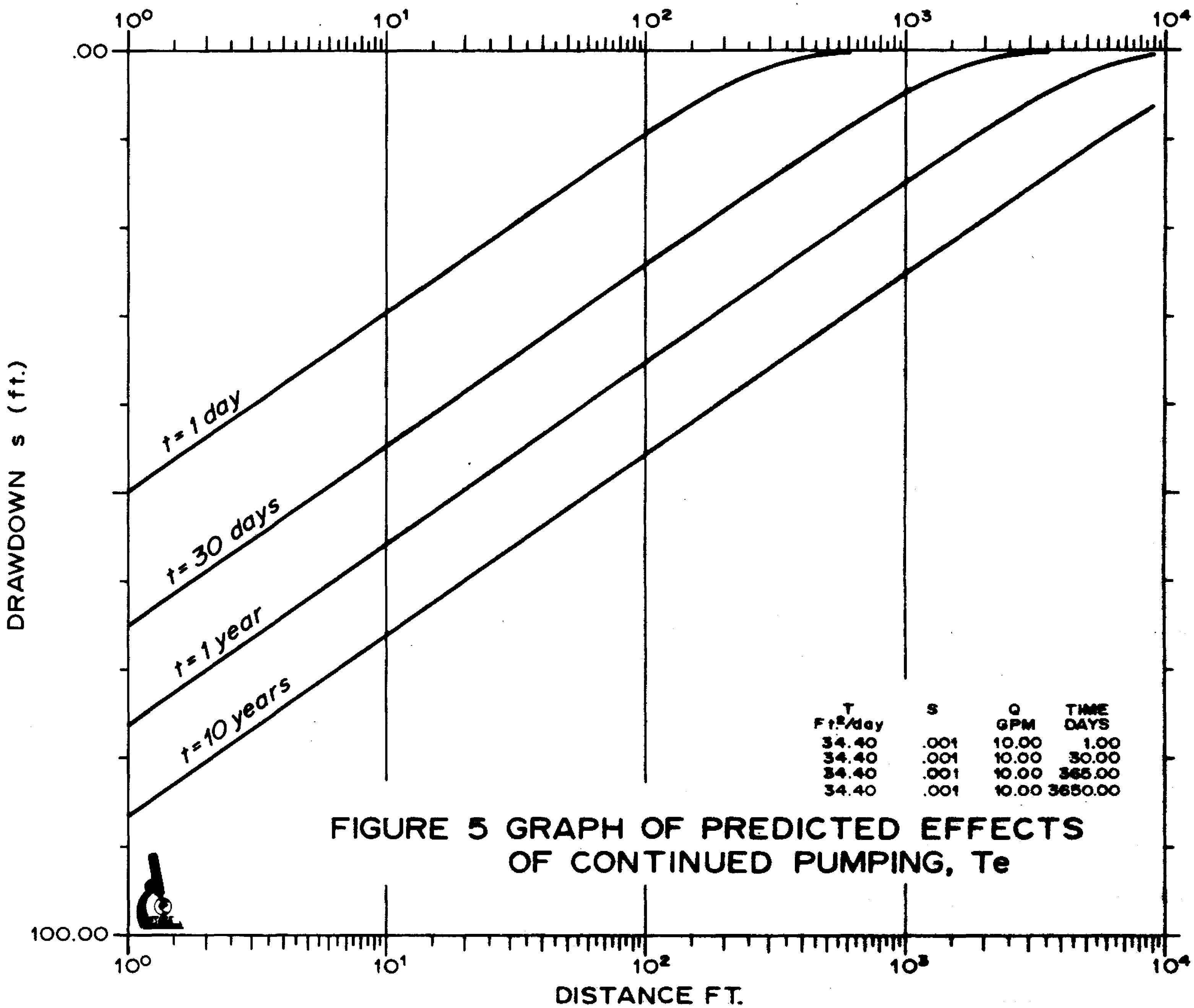

FIGURE 5 GRAPH OF PREDICTED EFFECTS OF CONTINUED PUMPING, Te

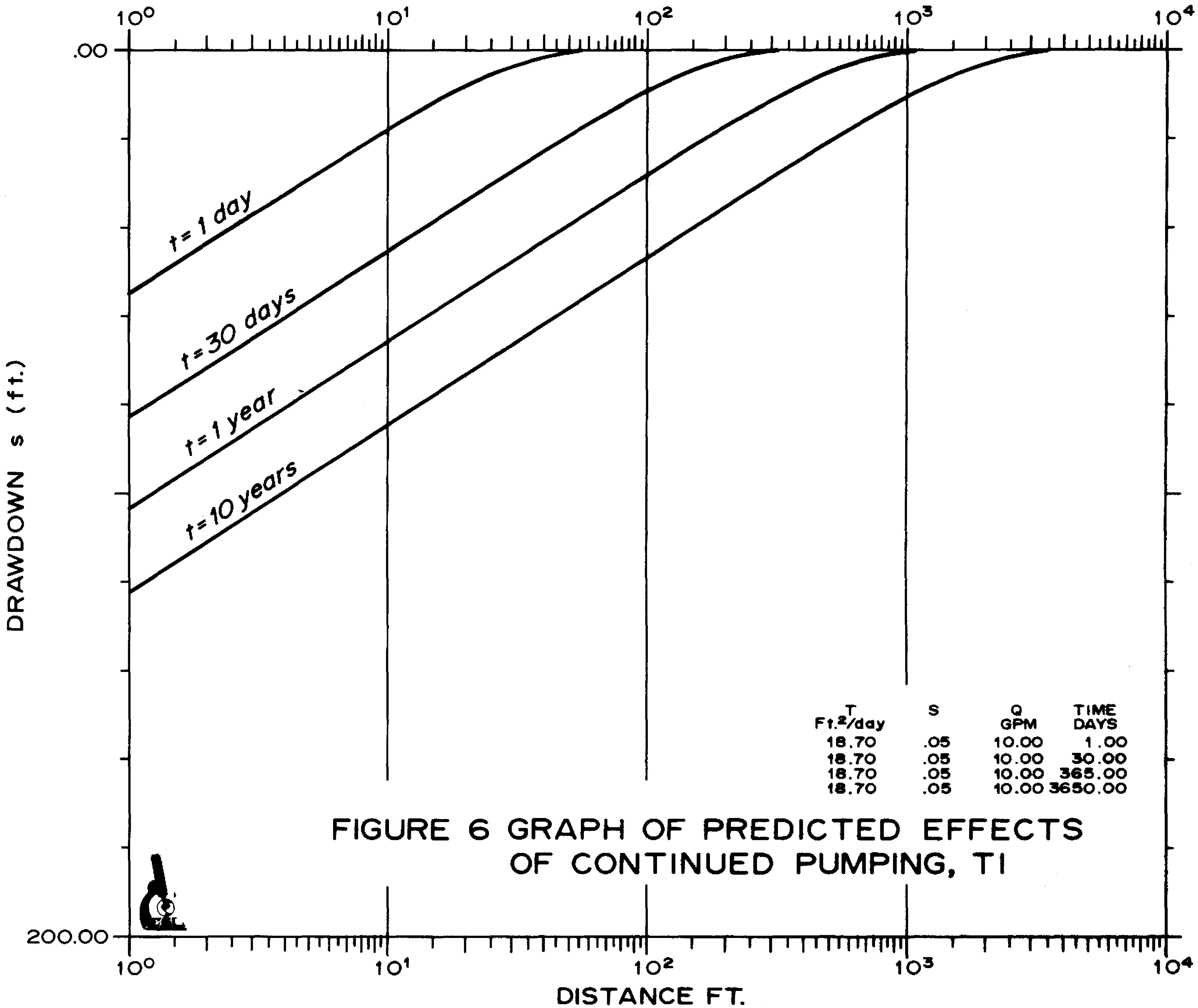

FIGURE 6 GRAPH OF PREDICTED EFFECTS OF CONTINUED PUMPING, TI

Table 1 Solution to pump-test data, Te.

DRAWDOWN # 1

T= 34.4000 S= .0010 Q= 30.0000TIME= .2600

#	DISTANCE	DRAWDOWN
1	1.0000	132.361
2	1.2000	127.490
3	1.4000	123.372
4	1.6000	119.804
5	1.8000	116.657
6	2.0000	113.843
7	2.2000	111.296
8	2.4000	108.972
9	2.6000	106.834
10	2.8000	104.854
11	3.0000	103.011
12	3.5000	98.894
13	4.0000	95.327
14	4.5000	92.182
15	5.0000	89.369
16	5.5000	86.824
17	6.0000	84.501
18	6.5000	82.365
19	7.0000	80.387
20	8.0000	76.825
21	9.0000	73.685
22	10.0000	70.877
23	12.0000	66.022
24	14.0000	61.922
25	16.0000	58.377
26	18.0000	55.255
27	20.0000	52.468
28	22.0000	49.953
29	24.0000	47.662
30	26.0000	45.561
31	28.0000	43.621
32	30.0000	41.820
33	35.0000	37.821
34	40.0000	34.391
35	45.0000	31.398
36	50.0000	28.755
37	55.0000	26.397
38	60.0000	24.277
39	65.0000	22.360
40	70.0000	20.617
41	80.0000	17.567
42	90.0000	14.995
43	100.0000	12.806
44	120.0000	9.327
45	140.0000	6.755
46	160.0000	4.849
47	180.0000	3.442
48	200.0000	2.413
49	220.0000	1.669
50	240.0000	1.138
51	260.0000	.768
52	280.0000	.521
53	300.0000	.379

Table 2 Solution to pump-test data, TI

DRAWDOWN # 2
T= 18.7000 S= .0500 Q= 30.0000TIME= .2600

#	DISTANCE	DRAWDOWN
1	1.0000	132.432
2	1.2000	123.499
3	1.4000	115.955
4	1.6000	109.429
5	1.8000	103.683
6	2.0000	98.552
7	2.2000	93.921
8	2.4000	89.702
9	2.6000	85.830
10	2.8000	82.255
11	3.0000	78.937
12	3.5000	71.563
13	4.0000	65.232
14	4.5000	59.706
15	5.0000	54.819
16	5.5000	50.454
17	6.0000	46.526
18	6.5000	42.967
19	7.0000	39.727
20	8.0000	34.046
21	9.0000	29.237
22	10.0000	25.130
23	12.0000	18.555
24	14.0000	13.641
25	16.0000	9.954
26	18.0000	7.194
27	20.0000	5.142
28	22.0000	3.631
29	24.0000	2.531
30	26.0000	1.743
31	28.0000	1.193
32	30.0000	.835
33	35.0000	.825

DRAWDOWN # 1
T= 34.4000 S= .0010 Q= 10.0000TIME= 1.0000

#	DISTANCE	DRAWDOWN
1	1.0000	50.119
2	1.2000	48.495
3	1.4000	47.122
4	1.6000	45.933
5	1.8000	44.884
6	2.0000	43.946
7	2.2000	43.097
8	2.4000	42.322
9	2.6000	41.609
10	2.8000	40.949
11	3.0000	40.335
12	3.5000	38.962
13	4.0000	37.773
14	4.5000	36.724
15	5.0000	35.786
16	5.5000	34.937
17	6.0000	34.162
18	6.5000	33.450
19	7.0000	32.790
20	8.0000	31.601
21	9.0000	30.553
22	10.0000	29.615
23	12.0000	27.993
24	14.0000	26.621
25	16.0000	25.434
26	18.0000	24.387
27	20.0000	23.451
28	22.0000	22.605
29	24.0000	21.833
30	26.0000	21.124
31	28.0000	20.467
32	30.0000	19.856
33	35.0000	18.494
34	40.0000	17.317
35	45.0000	16.281
36	50.0000	15.358
37	55.0000	14.526
38	60.0000	13.770
39	65.0000	13.077
40	70.0000	12.438
41	80.0000	11.297
42	90.0000	10.301
43	100.0000	9.422
44	120.0000	7.935
45	140.0000	6.720
46	160.0000	5.710
47	180.0000	4.860
48	200.0000	4.137
49	220.0000	3.521
50	240.0000	2.993
51	260.0000	2.540
52	280.0000	2.152
53	300.0000	1.818
54	350.0000	1.178
55	400.0000	.748
56	450.0000	.465
57	500.0000	.283
58	550.0000	.172
59	600.0000	.119

a - 1 day

DRAWDOWN # 2
T= 34.4000 S= .0010 Q= 10.0000TIME= 30.0000

#	DISTANCE	DRAWDOWN
1	1.0000	65.265
2	1.2000	63.641
3	1.4000	62.268
4	1.6000	61.079
5	1.8000	60.030
6	2.0000	59.091
7	2.2000	58.243
8	2.4000	57.468
9	2.6000	56.755
10	2.8000	56.095
11	3.0000	55.480
12	3.5000	54.107
13	4.0000	52.918
14	4.5000	51.869
15	5.0000	50.931
16	5.5000	50.082
17	6.0000	49.307
18	6.5000	48.594
19	7.0000	47.934
20	8.0000	46.745
21	9.0000	45.696
22	10.0000	44.758
23	12.0000	43.134
24	14.0000	41.761
25	16.0000	40.572
26	18.0000	39.523
27	20.0000	38.585
28	22.0000	37.736
29	24.0000	36.961
30	26.0000	36.248
31	28.0000	35.588
32	30.0000	34.974
33	35.0000	33.602
34	40.0000	32.413
35	45.0000	31.364
36	50.0000	30.426
37	55.0000	29.578
38	60.0000	28.804
39	65.0000	28.092
40	70.0000	27.432
41	80.0000	26.245
42	90.0000	25.197
43	100.0000	24.261
44	120.0000	22.642
45	140.0000	21.275
46	160.0000	20.092
47	180.0000	19.050
48	200.0000	18.120
49	220.0000	17.280
50	240.0000	16.515
51	260.0000	15.813
52	280.0000	15.165
53	300.0000	14.562
54	350.0000	13.224
55	400.0000	12.075
56	450.0000	11.071
57	500.0000	10.182
58	550.0000	9.388
59	600.0000	8.673
60	650.0000	8.024
61	700.0000	7.433
62	800.0000	6.395
63	900.0000	5.514
64	1000.0000	4.760
65	1200.0000	3.547
66	1400.0000	2.634
67	1600.0000	1.943
68	1800.0000	1.422
69	2000.0000	1.029
70	2200.0000	.737
71	2400.0000	.521
72	2600.0000	.364
73	2800.0000	.253
74	3000.0000	.176
75	3500.0000	.124

b - 1 month

Table 3 Predicted drawdown, Te

DRAWDOWN # 3
T= 34.4000 S= .0010 Q= 10.0000 TIME= 365.0000

#	DISTANCE	DRAWDOWN
1	1,0000	76.392
2	1,2000	74.768
3	1,4000	73.395
4	1,6000	72.206
5	1,8000	71.157
6	2,0000	70.218
7	2,2000	69.370
8	2,4000	68.595
9	2,6000	67.882
10	2,8000	67.222
11	3,0000	66.607
12	3,5000	65.234
13	4,0000	64.045
14	4,5000	62.996
15	5,0000	62.058
16	5,5000	61.209
17	6,0000	60.434
18	6,5000	59.721
19	7,0000	59.061
20	8,0000	57.872
21	9,0000	56.823
22	10,0000	55.884
23	12,0000	54.261
24	14,0000	52.888
25	16,0000	51.699
26	18,0000	50.650
27	20,0000	49.711
28	22,0000	48.862
29	24,0000	48.087
30	26,0000	47.375
31	28,0000	46.715
32	30,0000	46.100
33	35,0000	44.727
34	40,0000	43.536
35	45,0000	42.489
36	50,0000	41.551
37	55,0000	40.702
38	60,0000	39.927
39	65,0000	39.214
40	70,0000	38.554
41	80,0000	37.365
42	90,0000	36.316
43	100,0000	35.378
44	120,0000	33.755
45	140,0000	32.382
46	160,0000	31.194
47	180,0000	30.145
48	200,0000	29.208
49	220,0000	28.359
50	240,0000	27.585
51	260,0000	26.873
52	280,0000	26.214
53	300,0000	25.601
54	350,0000	24.231
55	400,0000	23.045
56	450,0000	22.000
57	500,0000	21.065
58	550,0000	20.221
59	600,0000	19.451
60	650,0000	18.744
61	700,0000	18.090
62	800,0000	16.914
63	900,0000	15.880
64	1000,0000	14.958
65	1200,0000	13.373
66	1400,0000	12.045
67	1600,0000	10.908
68	1800,0000	9.918
69	2000,0000	9.045
70	2200,0000	8.267
71	2400,0000	7.569
72	2600,0000	6.940
73	2800,0000	6.369
74	3000,0000	5.849
75	3500,0000	4.736
76	4000,0000	3.837
77	4500,0000	3.104
78	5000,0000	2.508
79	5500,0000	2.014
80	6000,0000	1.612
81	6500,0000	1.285
82	7000,0000	1.018
83	8000,0000	.628
84	9000,0000	.378

c – 1 year

DRAWDOWN # 4
T= 34.4000 S= .0010 Q= 10.0000 TIME= 3650.0000

#	DISTANCE	DRAWDOWN
1	1,0000	86.645
2	1,2000	85.021
3	1,4000	83.649
4	1,6000	82.459
5	1,8000	81.410
6	2,0000	80.472
7	2,2000	79.623
8	2,4000	78.848
9	2,6000	78.135
10	2,8000	77.475
11	3,0000	76.861
12	3,5000	75.488
13	4,0000	74.299
14	4,5000	73.250
15	5,0000	72.311
16	5,5000	71.462
17	6,0000	70.688
18	6,5000	69.975
19	7,0000	69.315
20	8,0000	68.125
21	9,0000	67.076
22	10,0000	66.138
23	12,0000	64.514
24	14,0000	63.141
25	16,0000	61.952
26	18,0000	60.903
27	20,0000	59.965
28	22,0000	59.116
29	24,0000	58.341
30	26,0000	57.628
31	28,0000	56.968
32	30,0000	56.354
33	35,0000	54.981
34	40,0000	53.792
35	45,0000	52.743
36	50,0000	51.804
37	55,0000	50.955
38	60,0000	50.180
39	65,0000	49.468
40	70,0000	48.808
41	80,0000	47.618
42	90,0000	46.569
43	100,0000	45.631
44	120,0000	44.007
45	140,0000	42.634
46	160,0000	41.445
47	180,0000	40.396
48	200,0000	39.458
49	220,0000	38.609
50	240,0000	37.834
51	260,0000	37.122
52	280,0000	36.462
53	300,0000	35.847
54	350,0000	34.475
55	400,0000	33.286
56	450,0000	32.237
57	500,0000	31.299
58	550,0000	30.451
59	600,0000	29.676
60	650,0000	28.964
61	700,0000	28.305
62	800,0000	27.117
63	900,0000	26.069
64	1000,0000	25.133
65	1200,0000	23.513
66	1400,0000	22.144
67	1600,0000	20.960
68	1800,0000	19.917
69	2000,0000	18.986
70	2200,0000	18.144
71	2400,0000	17.378
72	2600,0000	16.673
73	2800,0000	16.023
74	3000,0000	15.419
75	3500,0000	14.074
76	4000,0000	12.918
77	4500,0000	11.906
78	5000,0000	11.009
79	5500,0000	10.205
80	6000,0000	9.480
81	6500,0000	8.820
82	7000,0000	8.217
83	8000,0000	7.154
84	9000,0000	6.245

d – 10 years

DRAWDOWN # 1
T= 18.7000 S= .0500 Q= 10.0000TIME= 1.0000

#	DISTANCE	DRAWDOWN
1	1.0000	55.163
2	1.2000	52.179
3	1.4000	49.656
4	1.6000	47.472
5	1.8000	45.546
6	2.0000	43.824
7	2.2000	42.267
8	2.4000	40.846
9	2.6000	39.540
10	2.8000	38.332
11	3.0000	37.208
12	3.5000	34.700
13	4.0000	32.533
14	4.5000	30.626
15	5.0000	28.926
16	5.5000	27.393
17	6.0000	25.998
18	6.5000	24.721
19	7.0000	23.543
20	8.0000	21.436
21	9.0000	19.697
22	10.0000	17.972
23	12.0000	15.216
24	14.0000	12.960
25	16.0000	11.077
26	18.0000	9.486
27	20.0000	8.120
28	22.0000	6.966
29	24.0000	5.965
30	26.0000	5.101
31	28.0000	4.355
32	30.0000	3.710
33	35.0000	2.459
34	40.0000	1.601
35	45.0000	1.022
36	50.0000	.639
37	55.0000	.394
38	60.0000	.254
39	65.0000	.214

a - 1 day

DRAWDOWN # 2
T= 18.7000 S= .0500 Q= 10.0000TIME= 30.0000

#	DISTANCE	DRAWDOWN
1	1.0000	83.020
2	1.2000	80.033
3	1.4000	77.507
4	1.6000	75.320
5	1.8000	73.390
6	2.0000	71.664
7	2.2000	70.103
8	2.4000	68.677
9	2.6000	67.366
10	2.8000	66.152
11	3.0000	65.022
12	3.5000	62.497
13	4.0000	60.310
14	4.5000	58.381
15	5.0000	56.656
16	5.5000	55.095
17	6.0000	53.671
18	6.5000	52.361
19	7.0000	51.148
20	8.0000	48.963
21	9.0000	47.036
22	10.0000	45.313
23	12.0000	42.334
24	14.0000	39.818
25	16.0000	37.642
26	18.0000	35.724
27	20.0000	34.012
28	22.0000	32.466
29	24.0000	31.057
30	26.0000	29.764
31	28.0000	28.569
32	30.0000	27.460
33	35.0000	24.993
34	40.0000	22.872
35	45.0000	21.019
36	50.0000	19.377
37	55.0000	17.908
38	60.0000	16.584
39	65.0000	15.382
40	70.0000	14.285
41	80.0000	12.354
42	90.0000	10.711
43	100.0000	9.299
44	120.0000	7.015
45	140.0000	5.280
46	160.0000	3.953
47	180.0000	2.938
48	200.0000	2.164
49	220.0000	1.578
50	240.0000	1.139
51	260.0000	.812
52	280.0000	.574
53	300.0000	.403
54	350.0000	.213

b - 1 month

Table 4 Predicted drawdown, TI

DRAWDOWN # 3
T= 10.7000 S= .0500 Q= 10.0000TIME= 365.00

#	DISTANCE	DRAWDOWN
1	1.0000	103.486
2	1.2000	100.501
3	1.4000	97.976
4	1.6000	95.708
5	1.8000	93.658
6	2.0000	92.132
7	2.2000	90.571
8	2.4000	89.145
9	2.6000	87.836
10	2.8000	86.620
11	3.0000	85.409
12	3.5000	82.964
13	4.0000	80.776
14	4.5000	78.847
15	5.0000	77.121
16	5.5000	75.559
17	6.0000	74.134
18	6.5000	72.822
19	7.0000	71.608
20	8.0000	69.421
21	9.0000	67.491
22	10.0000	65.765
23	12.0000	62.779
24	14.0000	60.254
25	16.0000	58.068
26	18.0000	56.139
27	20.0000	54.414
28	22.0000	52.854
29	24.0000	51.429
30	26.0000	50.119
31	28.0000	48.907
32	30.0000	47.778
33	35.0000	45.258
34	40.0000	43.076
35	45.0000	41.152
36	50.0000	39.433
37	55.0000	37.880
38	60.0000	36.463
39	65.0000	35.161
40	70.0000	33.956
41	80.0000	31.791
42	90.0000	29.887
43	100.0000	28.189
44	120.0000	25.267
45	140.0000	22.818
46	160.0000	20.719
47	180.0000	18.888
48	200.0000	17.273
49	220.0000	15.832
50	240.0000	14.538
51	260.0000	13.368
52	280.0000	12.306
53	300.0000	11.337
54	350.0000	9.254
55	400.0000	7.562
56	450.0000	6.175
57	500.0000	5.033
58	550.0000	4.089
59	600.0000	3.311
60	650.0000	2.669
61	700.0000	2.141
62	800.0000	1.357
63	900.0000	.840
64	1000.0000	.510
65	1200.0000	.217

c – 1 year

DRAWDOWN # 4
T= 10.7000 S= .0500 Q= 10.0000TIME= 36

#	DISTANCE	DRAWDOWN
1	1.0000	122.351
2	1.2000	119.364
3	1.4000	116.838
4	1.6000	114.650
5	1.8000	112.721
6	2.0000	110.995
7	2.2000	109.433
8	2.4000	108.007
9	2.6000	106.696
10	2.8000	105.482
11	3.0000	104.352
12	3.5000	101.826
13	4.0000	99.638
14	4.5000	97.709
15	5.0000	95.982
16	5.5000	94.421
17	6.0000	92.995
18	6.5000	91.684
19	7.0000	90.470
20	8.0000	88.282
21	9.0000	86.353
22	10.0000	84.626
23	12.0000	81.639
24	14.0000	79.114
25	16.0000	76.926
26	18.0000	74.997
27	20.0000	73.271
28	22.0000	71.709
29	24.0000	70.284
30	26.0000	68.973
31	28.0000	67.759
32	30.0000	66.628
33	35.0000	64.103
34	40.0000	61.916
35	45.0000	59.987
36	50.0000	58.262
37	55.0000	56.701
38	60.0000	55.276
39	65.0000	53.966
40	70.0000	52.753
41	80.0000	50.567
42	90.0000	48.640
43	100.0000	46.917
44	120.0000	43.936
45	140.0000	41.419
46	160.0000	39.240
47	180.0000	37.320
48	200.0000	35.605
49	220.0000	34.056
50	240.0000	32.645
51	260.0000	31.348
52	280.0000	30.150
53	300.0000	29.037
54	350.0000	26.560
55	400.0000	24.428
56	450.0000	22.561
57	500.0000	20.904
58	550.0000	19.420
59	600.0000	18.078
60	650.0000	16.857
61	700.0000	15.740
62	800.0000	13.766
63	900.0000	12.075
64	1000.0000	10.612
65	1200.0000	8.216
66	1400.0000	6.361
67	1600.0000	4.918
68	1800.0000	3.772
69	2000.0000	2.880
70	2200.0000	2.182
71	2400.0000	1.641
72	2600.0000	1.222
73	2800.0000	.902
74	3000.0000	.660
75	3500.0000	.301
76	4000.0000	.223

d – 10 years